International Journal of Biological Macromolecules 165 (2020) 402–435

Contents lists available at ScienceDirect

International Journal of Biological Macromolecules

journal homepage: http://www.elsevier.com/locate/ijbiomac

Review

Performance of chitosan polymer as platform during sensors fabrication and sensing applications

Nabel A. Negm [a,*], Haya A. Abubshait [b], Samar A. Abubshait [c,d], Maram T.H. Abou Kana [e], Eslam A. Mohamed [a], Mohamed M. Betiha [a]

[a] Egyptian Petroleum Research Institute, Nasr City, Cairo, Egypt
[b] Basic Sciences Department, Imam Abdulrahman Bin Faisal University, Dammam, Saudi Arabia
[c] Department of Chemistry, College of Science, Imam Abdulrahman Bin Faisal University, Dammam, Saudi Arabia
[d] Basic & Applied Scientific Research Center, Imam Abdulrahman Bin Faisal University, Dammam, Saudi Arabia
[e] National Institute of Laser Enhanced Sciences (NILES), Cairo University, Egypt

ARTICLE INFO

Article history:
Received 4 May 2020
Received in revised form 8 September 2020
Accepted 15 September 2020
Available online 29 September 2020

Keywords:
Chitosan
Nanochitosan
Biosensor
Immobilization
Limit of detection

ABSTRACT

Chitosan is an important polymer produced from deacetylation of several sea and insects crusts. Due to its environmental fate and biological biocompatibility, it can be used in several biological and environmental applications. Sensing of biological compounds in human bodies and also in serum, blood, and different body fluids has found an important application instead of direct determination of the body fluids using complicated tools. Sensing process of biological compounds during bio-analysis of the biological systems, especially human fluids lack of several parameters including: high sensitivity, repeatability, speed of analysis and biocompatibility of the used analytical methods, especially in-vivo analysis. That was due to the time between sample handling and sample determination can change various components and concentrations of the bio-compounds. The need for in-situ analysis was directed the researchers for biosensors to overcome the upgrading problems of bio-analysis. Biosensors were the future of this issue. Chitosan can reserve as great platform for fabrication of different sensors to determine the elements, compounds and body bioactive compounds. The presence of different terminal amino and hydroxyl groups within chitosan framework facilitates the immobilization of different biomarkers to be used as sensing elements for the determined compounds. The use of chitosan as sensors platform was enhanced by using chitosan in its nanoforms.

Contents

Abbreviations: CH, chitosan; MWCNTS, multiwalled carbon nanotubes; LOD, limit of detection; GO_x, graphene oxide; BPA, bisphenol-A; GCE, glassy carbon electrode.

* Corresponding author.
E-mail address: nabelnegm@hotmail.com (N.A. Negm).

https://doi.org/10.1016/j.ijbiomac.2020.09.130
0141-8130/

1. Introduction

Biological sensors as a fast and low-cost tool in the field of analytical and biochemistry are gaining in relation to traditional tools used in the same area a lot of the curiosity of scientists, and therefore we find that there is a lot of research that is concerned with the development and expansion of the scope of its use at the present time [1–4]. The sensor is a device capable of receiving and responding to the signal and converts the signals falling on it into electrical/magmatic energy that can be recognized after that. Such devices that are used in the biological field are called the biosensors. Such devices that are used in the biological field are called the biosensor. In short, we can say that the biosensor is an analytical device that uses specific biochemical reactions using one of the biological identification tools or elements (e.g., enzymes, DNA, etc.) fixed on the transducer to monitor a very low concentration of specific chemical moieties through some chemical or biochemical change. Therefore, many users of this technology get many advantages, including simplicity of use instead of the ability to adapt, ease of transport, the speed associated with the accuracy of the results, and the ease of reading the results [5–7]. These features formed a strong impetus for researchers to focus on developing these biosensors to have reasonable time and an appropriate economical price for production using the most modern methods, nanotechnology. Considering chitosan as a starting material during preparation of the sensors, its physicochemical properties are changed by changing the molecular weight and the degree of deacetylation. The mechanical properties are decreased by decreasing the molecular weight, while the swelling properties are increased by decreasing the molecular weight as cross-linking and coiling of chitosan segments are decreased. In this review, we presented the principles of sensing using electrochemical and optical measurements, including amperometric, voltammetric, potentiometric, absorption, and emission measurements. Chitosan and modified chitosan polymers were presented and reviewed as sensors for different species, either organic as glucose, uric acid, triglycerides, dopamine and serum enzymes in biological systems, and inorganic species including various gases and metal ions as pollutants in the environment. The review encourages the researchers to create, develop, and improve the sensors' matrices, and to enhance the efficiency of the presented sensors for higher efficiency and accuracy with improved shorter time of detection.

2. Principles of electrochemical biosensors

The Biological sensor devices often contain one of the biological recognition elements (BREs) that include, but are not limited to, proteins, nucleic acids, enzymes, antibodies, cells and receptors that have the ability to instantaneous interact automatically target analyte, producing an electrical signal linked to the intensity of the concentration of the target substance. Depending on the nature of the biological recognition process, electrochemical sensors are divided into two main categories, which are the biocatalytic devices and affinity sensors. The former include fixing tissue slides, cells, or enzymes on an electrode to produce an electrical signal that refers to the material to be recognized, such as glucose, while the latter depends on a selective interaction between one of biological recognition elements (e.g., antibody, nucleic acid, or a receptor) and analyte. Fig. 1 represents the mechanism of BREs in the construction of biosensors during the detection of different compounds in a wide range of applications. Essential requirements in biosensors are fixed, durable, and non-destructive fixation (immobilization) of the BRE onto the various platforms. At this time, the technology of immobilization many biologically active substances such as proteins, plant cells, microorganisms, and some medications on various supports has received particular attention, especially biotechnology and biomedical sciences [8–10].

There are support matrices, the most important of which in the field of biosensors is polymeric membranes, which are distinguished by the diversity of their chemical composition and their ease of preparation. Due to their distinct chemical composition, it is easy to adjust its surface with chemicals such as ligand molecules, which achieve reasonable ease in the immobilization of biological recognition elements on its surface. Among these supports, the acrylonitrile polymer membranes are the most used, because they are distinguished from others in this field by the nature that is resistant to microbial and enzymatic attacks and their reasonable mechanical stability rather than being hydrophilic [11,12].

Also, the optical fiber sensor is one of the preferred biometric sensors due to its biological stability, small size, and energy-saving, and widely accepted technique by researchers who demonstrate outstanding commercial value in chemistry, life sciences, and more. In addition, the optical fiber sensor is broadly used in the sensing of ions contamination, e.g., cadmium (Cd^{2+}) [13], copper (Cu^{2+}) [14], mercury (Hg^{2+}) and chromium (Cr^{3+}) [15], and anions (e.g., nitrate (NO_3^-)) [16], fluoride (F^-) [17].

The electrochemical biosensors are one of the most important model sensor devices that convert chemical events into electrical signals, as the reference electrode is one of the basic components. This reference electrode is used as a support for the immobilization of biomolecules. The further immobilization of nanomaterials on the electrode can enhance the reference electrode's sensitivity and durability, as well as reduce reaction time through enhancing mass transport of reactants. Immobilization of molecular biological recognition elements coupled with nanomaterials on the surface of the supports or electrodes provides better signal translation, which enables adaptability, rapid response, the ability to more precisely detect and quantify the target material by converting heat, light, mass, or impedance, potential changes, and redox to a measurable electrical identity. The key benefits of the biosensor are high sensitivity, durability, adaptability and portability and ease of use [18–21].

3. Chitosan in biosensing

Chitosan is one of the polymers that are abundant in nature and can be considered environmentally friendly polymers due to its low toxicity. One of the advantages of CH is that its surface can be modified chemically by many functional groups. Also, it has bacterial inhibiting properties, biodegradable, high permeable to water, good gel-forming, and adhesive characteristics due to the high hydrophilicity. These characteristics were reflected in many applications, especially in the fields of medicine and engineering, where it was indicated that CH is one of the most promising materials in the field of biological sensing after modifying a surface with BREs to sense some chemical and biological molecules. Therefore, CH-based biometric sensors have gained tremendous success as an effective analytical device consisting of BREs (e.g., DNA, proteins, enzymes, antibodies, etc.) connected to transducer surface to translate the signal to a detector as an electrical signal, and this signal can be quantitatively measured [22–26]. The type of BRE immobilized on CH-based nanocomposites determines the signal types such as intensity, color, etc. and also played a key role in the fabrication of biosensors (conductimetric, amperometric, and potentiometric sensors). Given the reported characteristics of CH, CH was considered one of the most important and most popular polymers, the materials used in biological sensors, as it was successfully used in many detections, as will come later [21].

One of the advantages of CH, being an environmentally friendly polymer, is that it is suitable for modifying the surface of the transducer through its ability to immobilized biological recognition elements

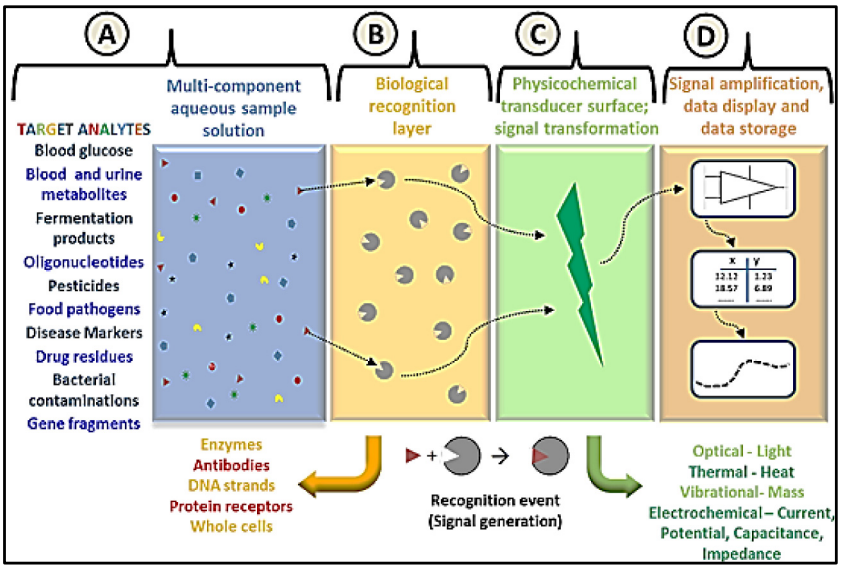

Fig. 1. Presentation of biosensors design: (A) compounds in the tested solutions, (B) immobilization layer for biological detecting elements, (C) physicochemical platform produces measurable signal based on interaction of biological compounds with substrate, (D) module for quantitatively or qualitatively recognition.

(BREs) on its surface. CH shares some other polymers that have an effect on the modification of transducer surfaces, such as polyglutamate ($(C_5H_7NO_3)_n$), poly-lysine ($(C_6H_{12}N_2O)_n$) and polyarginine as well as alginic acid ($(C_6H_8O_6)_n$) and hyaluronic acid ($C_{14}H_{21}NO_{11})_n$ [24]. Despite the success of the previous modifiers in developing the sensor, CH has shown more attractive features, the most important of which are non-toxicity, reasonable cost, and good water solubility, especially at pH 6.3, as solubility in neutral medium ensures proper immobilization of BREs without denaturation. Moreover, CH also has the ability to form electrodeposition thin films on the negatively charged electrode [21,24]. Due to the multiplicity of the nanometric materials that can be immobilized on the surface of CH, CH-based nanoparticles play a diversified pivot role in developing sensors by integrating BREs with varied types of transducers, such as optical, conductimetric, potentiometric, and piezoelectric biosensors, etc. [8,9]. This following section presents a comprehensive discussion on the usage of CH in biosensor fabrication, incorporating the first two types of transducers exclusively.

4. Chitosan modified EC-enzyme biosensors

The newly recognized proposed structures for biosensors are complex systems consisting of many components that integrated with each other as modified and unmodified CH composition. CH modifiers include immobilization of a specific enzyme in addition to some nanomaterials such as graphene (GO_x) (Fig. 2), clays, nano-carbon (carbon nanotube, CNTs), oxides of minerals and ionic liquids to recognize the analyte molecule [8,9]. The mentioned materials that have been immobilized individually or coupled nanomaterial with the enzyme on the surface of the electrode to generate cycles of oxidation and reduction of sites associated with the enzyme and thus increases the conductivity of immobilization materials. The properties of the immobilized enzyme are affected by the type of supports, nanomaterials, and enzymes [8,9,24,27].

Hence, it is taken into consideration that the selection of such substances is very accurate, not to mention that many substances are not suitable as a support for any enzyme. The support must fulfill some specifications in order to be a good support, including high hydrophilicity, good mechanical stability, low cost, and the most important characteristics are the high affinity to protein and low diffusion limitation to ease reach to the active sites as well as non-toxic, especially, if the sensors are intended for use in medicine, pharmacy and agriculture applications.

It should be noted that there are a lot of organic and inorganic supports as well as natural ones that have been exploited in the processes of immobilization of different enzymes on their surface, but as it provides advantages of CH, it is one of the promising materials to immobilize many enzymes on its surface, as it enhances the diffusion of a cofactor to the immobilized enzyme.

So far, two methods may be used to immobilize the enzymes on the support. The first is the physical entrapment, and the second is the covalent binding of the enzymes to the chemical groups (poly-cationic chains) on the surface of CH. However, the covalent binding mothed is the most used and most interested of researchers. In such a method,

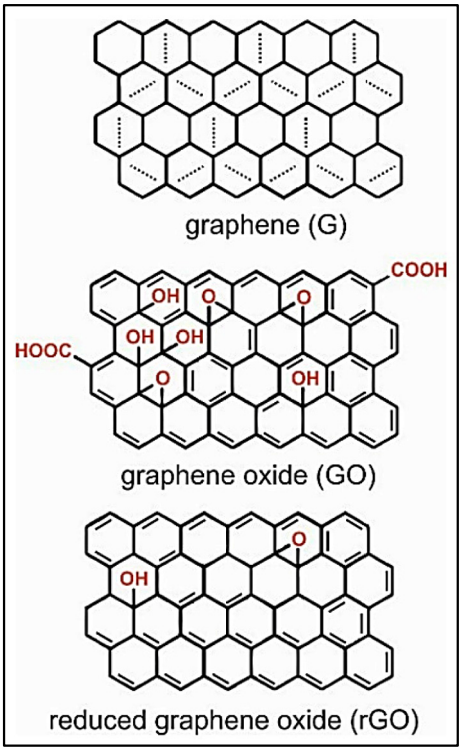

Fig. 2. Different structures of graphene.

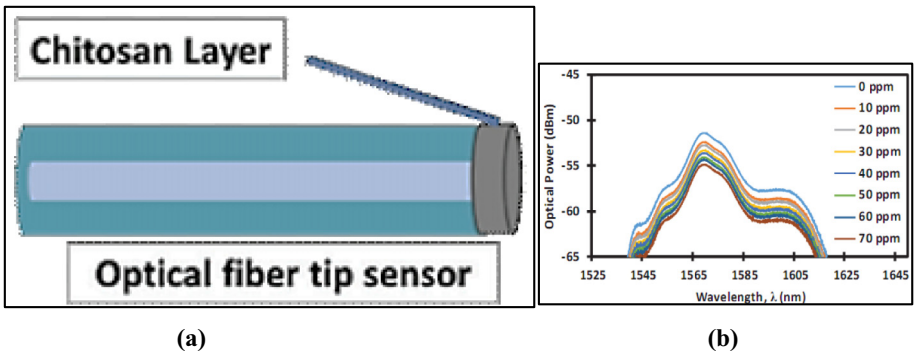

Fig. 3. (a) Fabrication of chitosan coated optical sensor, (b) variation of optical density output by variation of Pb^{2+} metal ions concentration.

crosslinking agents such as glyoxal ($C_2H_2O_2$), carbodiimides (RN=C=NR), epichlorohydrin (C_3H_5ClO), glutaraldehyde ($C_5H_8O_2$), N-hydroxy succinimide ($C_4H_5NO_3$), and cyanuric chloride ($C_3Cl_3N_3$) have been used [28]. The physical entrapment is the most favorable technique than the covalently bonded enzymes to the sensors due to the reported toxicity of the used cross-linkers in the binding process of enzymes. That was prompted researchers to pay attention to the physical entrapment approach, as it does not require a significant chemical modification for the enzymes [29,30]. That may depends on the enzyme deposition or entrapment of enzyme on the CH networks by the electrostatic attraction between amino-groups or protonated amino-groups of CH and enzyme.

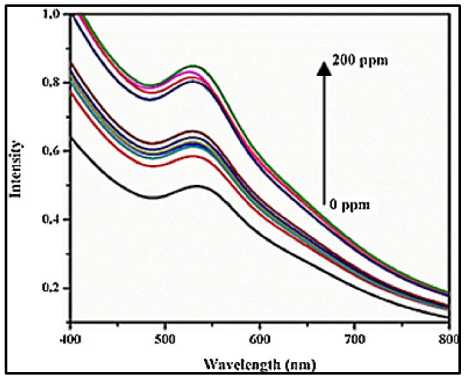

Fig. 4. UV–Vis spectra response of CH/Ag-Au nanocomposite at different concentrations of Hg-ions.

5. Chitosan biosensors in metal ions sensing

One of the contemporary problems that threaten human health and living organisms, which is one of the global challenges, is the problem of water contamination with heavy elements. The seriousness of heavy metals is that they pollute not only surface water but also groundwater. Pollution of water with heavy elements results from untreated industrial and municipal wastewater [31]. It is frightening that heavy metals are not biodegradable and thus accumulate in living cells, causing serious diseases and disorders of living tissue. Often, researchers found that wastes that contain heavy elements are from chemical industries such as mining operations, metal coating, and painting and finishing facilities. So, there needed to be protocols to detect these elements. Among the most toxic elements, lead, mercury, and copper are the most effective metal ions on human health, and there are many methods have taken to get rid of them such as precipitation, filtration (reverse osmosis, nano-filtration, etc.), adsorption, electrolytic reduction, and ion exchange [32]. In order to know the type and percentage of heavy elements in the water or other media, the sensors were used to determine their concentration as well as to identify the type of heavy-element and among these sensors is CH-modified biosensors.

5.1. Sensing of metal ions in different environment

Razali et al. [33] synthesized an optical sensor to detect lead ions consisting of optical fibers coated with CH and compared the synthesized sensor to an optical fiber (Fig. 3a), where the sensor encapsulated with CH showed a sensitivity of seven times that of non-CH-coated optical fibers. The authors explained the result they reached with a high CH affinity to adsorb lead ions from the medium, and this sensor

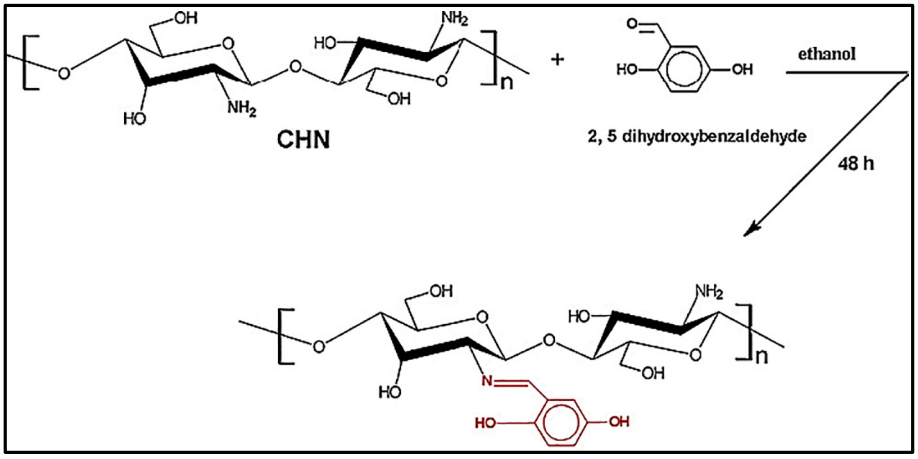

Scheme 1. Synthesis of nano-chitosan Schiff base ligand.

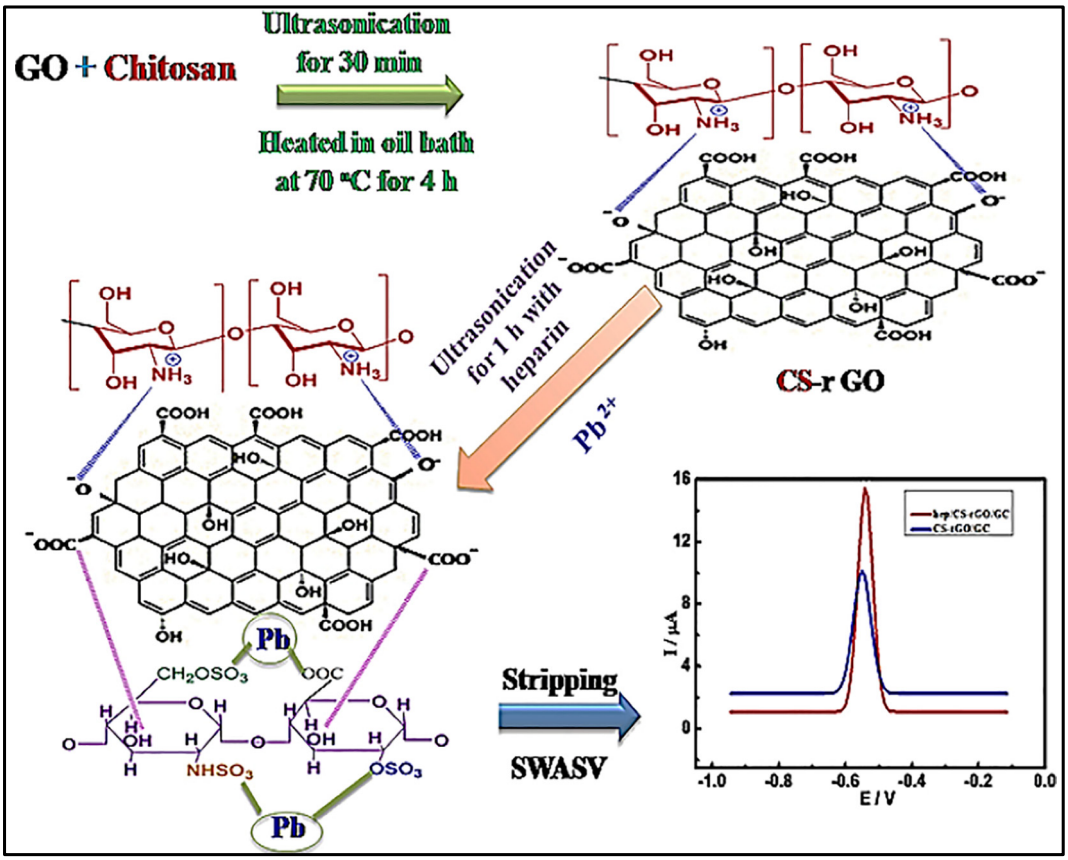

Scheme 2. Development of hep/CS-rGO/CG electrode.

showed a potential industrial application to monitor industrial and environmental installations. Moreover, the synthesized CH-coated optical fiber's sensor showed optical intensity output is proportional to the concentration of lead ions (Fig. 3b).

A biosensor was fabricated with an innovative and effective method from chemically modified carbon paste biosensor with a Schiff base modified nano-CH (34 nm) to detect lead ions [34]. A nano-CH-Schiff base was obtained by the reaction of CH amine groups with 2,5-dihydroxy benzaldehyde (Scheme 1). The biosensor was identified using the scanning electron microscopy and cyclic voltammetry. The fabricated electrode showed one peak in the anodic region at 0.34 V (vs. Ag/AgCl) for the oxidation of Pb^{2+}.

Nivethaa et al. [35] fabricated a CS/Ag-Au (CH/silver-gold) sensor using a chemical reducer method. 5-Fluorouracil has also been prepared and encapsulated the nanocomposite in order to study cellular toxicity towards breast cancer cell lines. The optical properties of the nanocomposite enabled it to be used in cellular imaging as it was used as a nanoscale sensor to identify the mercury element and found that the LOD is 5.0×10^{-8} M (14 ppm) (Fig. 4).

To identify the lead element's determinants in environmental samples, a sensor composed of CH and immobilized heparin on reduced graphene (rGO_x) was fabricated to modify the glassy electrode [36]. The advanced electrode (Scheme 2) application was used to detect lead ion in the presence of many other elements such as Zn^{2+}, Cd^{2+}, and Cu^{2+} using square wave anodic stripping voltammetry (SWASV). The electrode (hep/CS-rGO/GC) has demonstrated low LOD (0.03 $\mu g \cdot L^{-1}$ and 1.34 µA/mM) as well as good re-usability. Fig. 5 represents the SWASV response of the metal cations in acidic electrolytes using the hep/CH-rGO/GC developed electrode. The sharp peak current was observed for Pb^{2+} metal cations in the presence of Zn^{2+}, Cd^{2+}, and Cu^{2+} metal cations in a concentration of 10.25–15.25 $g \cdot L^{-1}$.

Kucukkolbasi et al. [37] prepared a fabricated electrode from a modified carbon paste with modified CH nanoparticles with a Schiff base functional group to detect lead ions in wastewater using differential pulse anodic stripping voltammetry (DPASV). The surface of CH was modified by the interaction of peripheral amine groups with 2,4-dihydroxy benzaldehyde (Scheme 3). The electrochemical properties of the fabricated electrode were studied, and the influencing factors such as pH, concentration, reduction potential, and time required to detect the ion were studied in addition to studying the percentage of elements involved in electrode fabrication. They concluded that the modified electrode showed only one oxidation peak in the anodic scan at −0.35 V (vs. Ag/AgCl) for Pb(II). The premium combination of 73.7% carbon powder, 5.3% CH, 21% paraffin oil, 0.2 $mol \cdot L^{-1}$ sodium acetate solution at pH 6 as supporting electrolyte, pre-concentration time of 600 s, a reduction potential (−0.1 V), and reduction time (10 s) provided the best voltammetric response (Fig. 6).

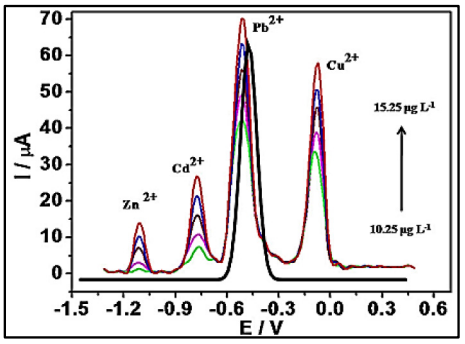

Fig. 5. SWASV response of the metal ions in acidic electrolyte using hep/CH-rGO/GC developed electrode.

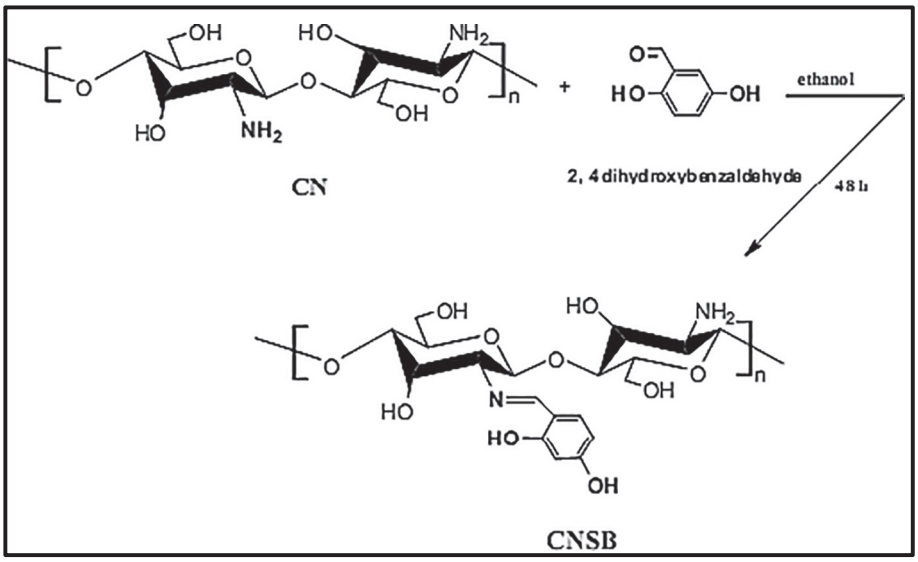

Scheme 3. The schematic representation of the synthesis of chitosan nanoparticle Schiff base (CNSB).

The electrode response was excellent for lead ion, which had a LOD of 7.24×10^{-7} mol·L^{-1}, and showed a linear response in the range of 1×10^{-6} to 1×10^{-4} mol·L^{-1}. However, as the cadmium and copper ion concentration increases, the peak of lead ion decreases as a result of competition between the ions of cadmium and copper to active complexing sites.

Abdi et al. [38] provided a sensor based on surface plasmon resonance (SPR) to detect lead and mercury ions of small quantities in their solutions. Polypyrrole-CH (conducting polymer) modified the gold surface by electrodeposition technique. The sensor showed a high amount of resonance angle unite for the polypyrrole-CH film due to the high affinity of lead and mercury ions towards the CH functional group; however, the sensor showed high sensitivity towards lead ion than mercury ion and the LOD was in the range of 0.03 to 0.07 ppm.

Junior et al. [39] introduced the electrical chemical application of a modified carbon paste-CH with a different percent of carbon to determine the detection of mercury ions, Hg^{2+}, in water using anodic stripping voltammetry. The optimized composition that provided best voltammetric response was of 60%-graphite powder, 20%-CH and 20%-mineral oil with $NaNO_3$ (0.1 mol·L^{-1}) solution at pH 6.3 as supporting electrolyte, a pre-concentration potential (20.2 V), pre-concentration time (270 s) and a scan rate of 25 mV/s (Fig. 7). Voltmeter signals of the proposed sensor were linearly dependent on the mercury (II) concentration in a range of 9.99×10^{-7} to 3.85×10^{-5} mol·L^{-1} with a LOD of 6.28×10^{-7} mol·L^{-1}. When the sensor was tested for solutions containing mercury and known concentrations of other salts, a noticeable effect was observed only for copper (10^{-7} mol·L^{-1}). It was also observed that approximately 100 times the excess of alkali and 10 times the Cd(II), Pb(II), Co(II), Ni(II) and Cr(III) have an effect not exceeding 5.0% when determining mercury concentration of 1×10^{-6} mol·L^{-1}.

Chen et al. [40,41] presented a colorimetric sensor that acts as a signaling probe composed of CH functionalized gold nanoparticles for assaying mercuric ions. The complexation of Hg(II) and CH functionalized gold nanoparticles leads to decreasing the absorbance of gold nanoparticles, and the color is changed from red to blue with a LOD lower than 1.35 μM (Fig. 8). This system showed advanced detection for mercuric ions in drinking water (30 μM) as defined by WHO, in addition, the method of preparation is inexpensive and does not require the addition of other reagents in order to improve sensitivity.

Cuprous oxide and nano-chitosan composites (Cu_2O@NCH) were fabricated by a one-step reduction method, and thymine-rich (T) DNA was immobilized on the surface of the Cu_2O@NCH electrode [42]. The electrode (Cu_2O@NCH/DNA) was used as a highly sensitive electrochemical DNA sensor for Hg^{2+} ions in water (Scheme 4). The output of the electrochemical impedance device was used for sensing Hg^{2+} ions, which showed single-stranded. From the results, it was found that the Cu_2O@NCH/DNA sensor has a sensitivity to detecting mercury ions exceeds the sensitivity of Cu_2O@NCH sensor (Fig. 9a). That sensitivity leads to a high difference in charge-transfer resistance during Hg^{2+} detection at different concentrations of Hg^{2+} (Fig. 9b). Moreover, the sensitivity of the Cu_2O@NCH/DNA sensor towards Hg^{2+} ion was tested

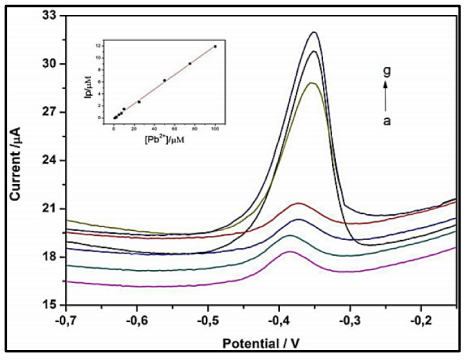

Fig. 6. DPSAV curves of different concentration of Pb(II) (a–g: 1–100 μM) at CNSB-CPE in 0.20 mol·L^{-1} NaAc, reduction potential, −1.0 V.

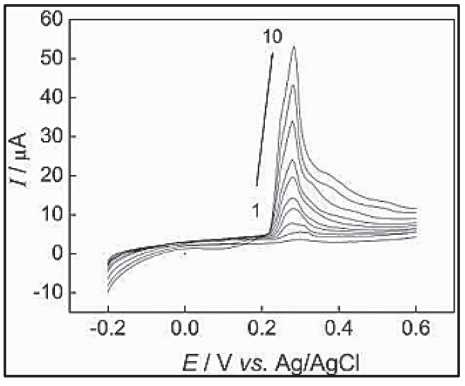

Fig. 7. Anodic stripping voltammograms of Hg(II) at different concentrations in 0.1 mol·L^{-1} $NaNO_3$ solution.

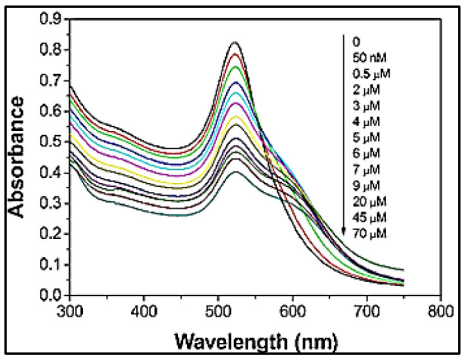

Fig. 8. UV–Vis absorbance spectra of AuNPs in 0.1 mg·mL^{-1} CH in 20 mM Tris-HCl buffer solution (pH 7.4) in different concentrations of Hg^{2+} (50–70 μM).

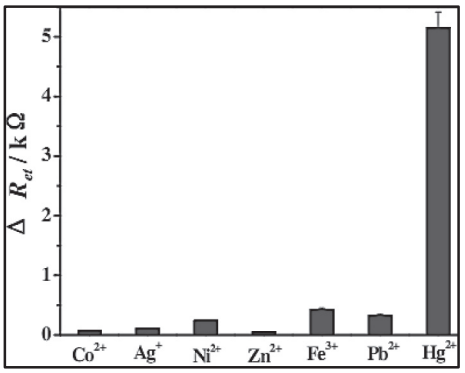

Fig. 10. The selectivity of Cu_2O@NCs/DNA sensor in the presence of Co^{2+}, Ag^{1+}, Ni^{2+}, Zn^{2+}, Fe^{3+}, and Pb^{2+} ions.

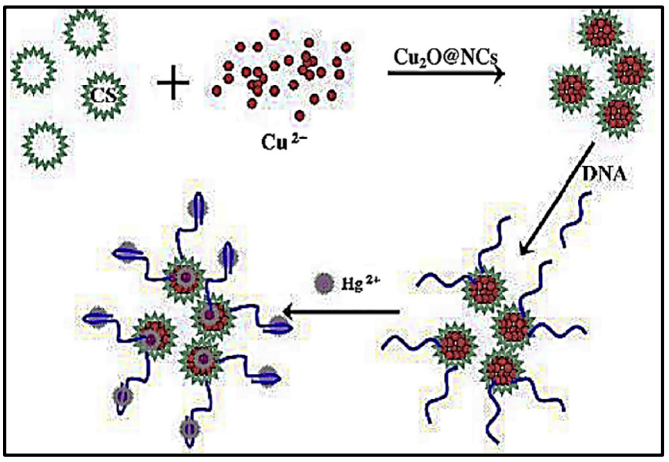

Scheme 4. Preparation of cuprous oxide and nano-chitosan composites (Cu_2O@NCs).

in the presence of different metal cations such as Co^{2+}, Ag^{1+}, Ni^{2+}, Zn^{2+}, Fe^{3+}, and Pb^{2+} (Fig. 10); however, the sensitivity of the sensor is decreased due to the interference of metal cations with Hg^{2+} ion.

Janegitz et al. [43] introduced the preparation of glutaraldehyde-CH composite to obtain a network model of CH chains bound together through the Schiff base groups (Scheme 5) and the use of the resulting composite (CNPE-CTS-GA) to modify a CNTs paste electrode to detect the elemental mercury and lead traces using linear anodic stripping voltammetry (Fig. 11A, B). the authors reported that at Cd(II) concentration of 5.9×10^{-8} to 1.5×10^{-5} mol·L^{-1}, the peak current was linear. The fabricate electrode, CNPE-CTS-GA, showed considerable selectivity towards Cd(II) and Hg(II) ions that present urine, water, and industrial wastewater.

Low-molecular-weight CH oligomers were reacted by fluorescein isothiocyanate (FITC) to obtain a modified CH probe (CH/FITC) (Scheme 6) for determination of Cu^{2+} metal ion in the medium [44]. The prepared probe showed enhanced fluorescent properties due to the presence of the $NHCOO^{-}$ moieties (carbamato anion) as a fluorophore. Under visual and UV detection, the CH oligomer-FITC composite showed significant color variation related to the types of metals in the medium (Fig. 12a, b). The CH/FITC material showed high selectivity towards copper ion, and the LOD was 60 μM (LOD) (Fig. 13). As Cu^{2+} adsorbed on FITC, the electron transferee from FITC and Cu^{2+} causing fluorescent quenching of the CH/FITC. This behavior greatly enabled the CH/FITC material to be used as a promising colorimetric sensor to detect Cu^{2+}.

An electrochemical Cu^{2+} ion sensor was developed by grafted chitin (CH) and polyaniline (PANI), CH-g-PANI (Scheme 7), coated on indium-tin-oxide (ITO) glass electrode and a laboratory designed potentiometric cell were reported [45]. The prepared sensor was applied in potentiometric detection of copper ion for natural and artificial samples under optimized conditions. The mechanism of Cu^{2+} sensing using CH-g-PANI was suggested to be the complexation between the polymeric framework and the metal ions, as indicated by FTIR spectra. The complexation mechanism was proved due to the appearance of an additional peak at 577 cm^{-1} due to associative interaction between copper ions and $-NHCOCH_3$ group of Chit molecules. Furthermore, the peak at 1075 cm^{-1} in CH-g-PANI becomes sharper due to the interaction of copper and rearrangement of the CH-g-PANI matrix. The ion-induced interaction between Cu^{2+} and the sensor supports the electronic conduction and basis for the ion to electron conversion in the electrode. The electrochemical sensing response showed linearity to Cu^{2+} concentrations

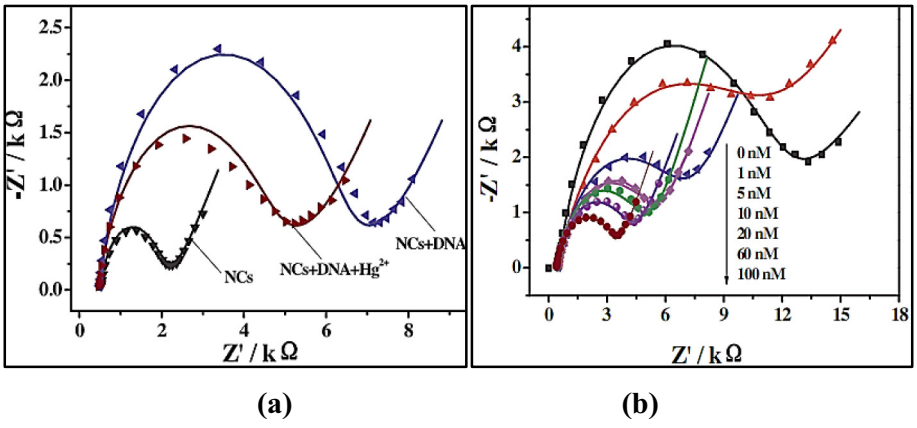

Fig. 9. (a) EIS Nyquist of NCs, NCs + DNA, NCs + DNA + Hg^{2+}, (b) EIS Nyquist of DNA-immobilized on modified Au electrode in different concentrations of Hg^{2+} (0–100 nmol·L^{-1}).

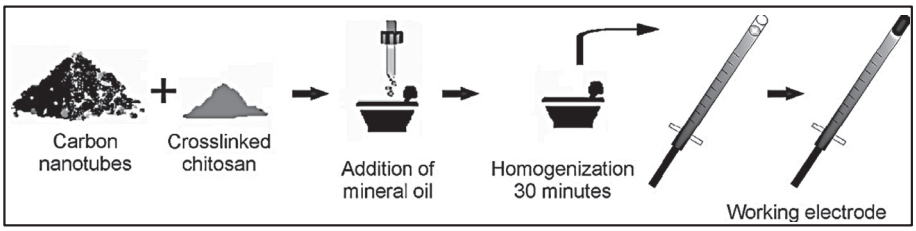

Scheme 5. Schematic construction of CNPE-CTS-GA electrode.

range of 1–1000 ppm with sensitivity 2.55 $mV \cdot ppm^{-1} \cdot cm^{-2}$, the response time of 240 s, and long-term stability due to formation of interactive sites and chemical responsiveness due to grafting of CH and PANI.

6. Sensing of gases

Ammonia is one of the pillars of tremendous cultural progress in the present time, and as a result of its frequent use in industry, the quantities that are in the air and other means of disposal of waste may be large enough to the extent that it harms humans and other beings. Therefore, it was necessary to find highly sensitive sensors to detect it. Sensors of ammonia are useful to a large degree in many areas, including air quality monitoring, as well as in the field of medicine, where the level of ammonia is monitored in biological and clinical samples [46,47].

El-Sherbiny et al. [48] prepared hyperbranched nano-chitosan (HBCH-NPs) by using nanospray dryer and functionalized the surface of HBCH-NPs by dendritic polyamidoamine (PAMAM) to fabricate amino-group-end-capped-hyperbranched CH nanoparticles (HBCH-NH_2) NPs. The author used HBCH-NH_2 as support of silver nanoparticles (AgNPs). The deposition of silver on HBCs-NH_2 is carried out using different amounts of $NaBH_4$ (60–300 μL), and the resultant average particle size of silver nanoparticles was of 20–50 nm (Scheme 8). The HBCH-NH_2-NPs-AgNPs sensor has demonstrated good potential as an optical sensor to detect low concentrations of ammonia, as the SRP of the sensor is greatly changed. Both position and absorption intensity of SPR of HBCH-NH_2-NPs-AgNPs is affected by the change in the concentration of ammonia (Fig. 14). Linear relationships associated with the regression coefficient (R^2) of 0.9811 has resulted from HBCH-NH_2-NPs-AgNPs at ammonia concentration of 10–50 ppm.

The application of anthocyanins of black carrots (ABC) (Fig. 15) immobilized on the CH-cellulose matrix has been studied as a colorimetric pH indicator to monitor the spoilage in pasteurized milk (change of pH during the decomposition of pasteurized milk) by Tirtashi et al. [49]. The basic catalyzed sol-gel route was followed to prepare a colorimetric pH indicator. In brief, 0.007 g ZnO, and 1 mL ammonia was used to synthesize CH solution followed by addition of 500 μL tetraethylorthosilicate (as a silica source), 200 μL tris(hydroxymethyl) aminomethane and polycyclic antibacterial peptide, and finally, the obtained film is impregnated with a cellulosic paper by the dip-coating procedure. The immobilization of ABC on the cellulose-CH matrix had no noticeable effect on the chemical structure of the matrix. The pH sensor showed a clear difference in colors from pink to khaki according to the change in the pH from 2 to 11 (Fig. 16). Moreover, the sensor showed excellent stability for one-month storage at 20 °C.

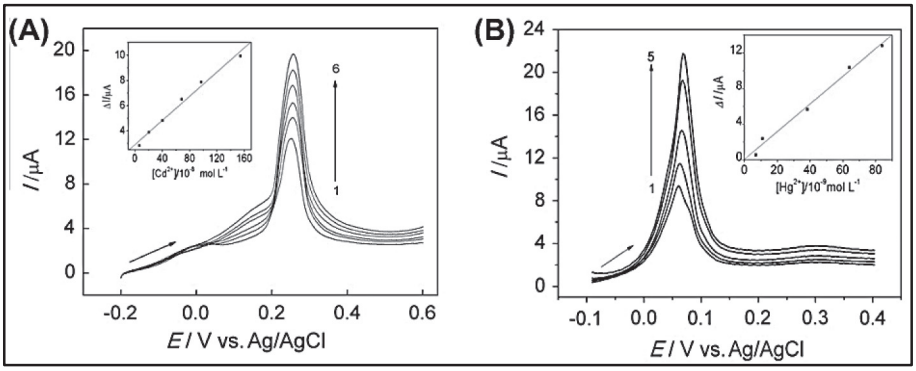

Fig. 11. Voltammograms and calibration curve obtained with CNPE-CTS-GA at different concentrations of: (A) Cd(II), and (B) Hg(II).

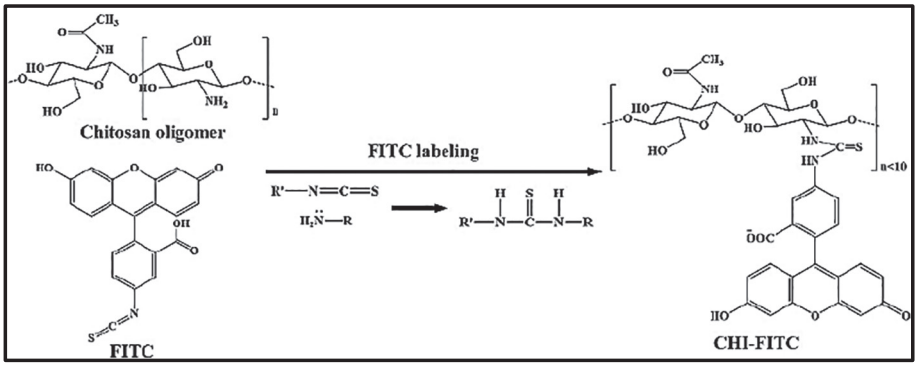

Scheme 6. Reaction of fluorescein isothiocyanate (FITC) and low molecular weight chitosan (CHI) to obtain modified chitosan probe (CHI/FITC)

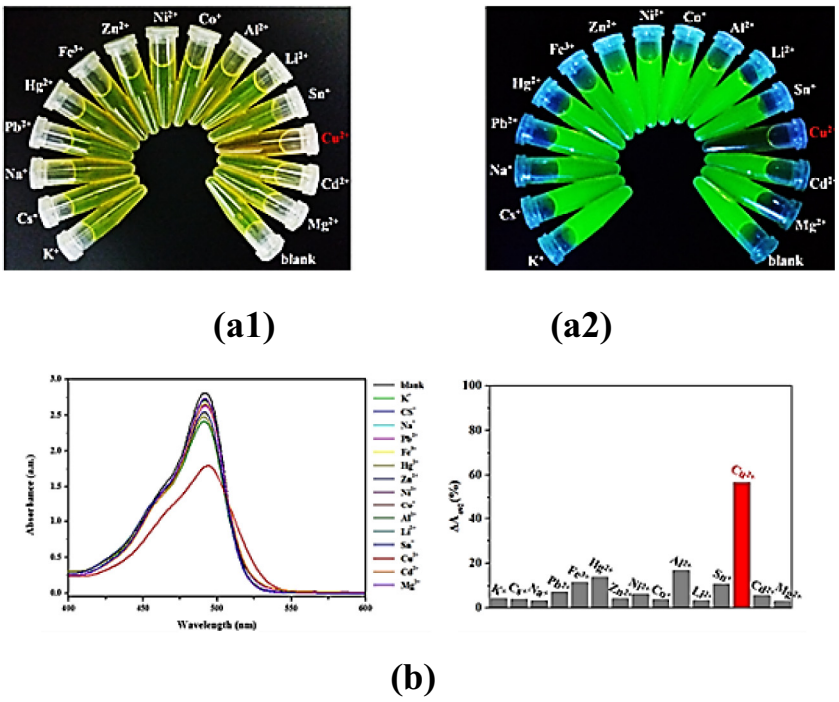

Fig. 12. (a) Visible detection of different metal ions under visible (1), and UV light (2); (b) UV-detection of the different metal ions using CH/FITC probe.

Another application of CH is the detection of the proportion of carbon dioxide in the air as Abou Hammad et al. [50] introduced a new sensor made of Al_2O_3NPs/CH/CAS nanocomposite (CAS: calcium aluminosilicate). The nanocomposite prepared via a sol-gel process, and the percent of Al_2O_3NPs was calculated as 3, 5, 7 mol%. 5%-Al_2O_3NPs/CH/CAS nanocomposite material showed an excellent tendency to capture carbon dioxide, and also, the sensor showed an excellent sensing response to the gas with good reproducibility and reliability. Al_2O_3NPs/CH/CAS nanocomposite sensor has the ability to operate at a minimal concentration in which the capacity for CO_2 is increased linearly as a function of the gas concentration, however at the linearity is lost for the high concentration of CO_2 gas due to limited sites that adsorb the gas (Fig. 17a, b).

A biosensor based on immobilized Cyt-c (cytochrome-c) at CH-MPA-AuNPs (chitosan-mercaptopropionic acid-gold nanoparticle) and Nafion nanocomposite was fabricated for nitric oxide detection [51]. UV–Vis absorption spectra analysis indicates that the Cyt-c molecules kept their original structures at the CH-MPA-AuNPs nanocomposite, and CH-MPA-AuNPs improved electron transfer between Cyt-c and CH-MPA-AuNPs. The reversible redox peaks are well defined for Nafion/Cyt-c/CH-MPA-AuNPs/SAMs-Au electrode in 0.1 M phosphate buffer solution (pH 7). The anodic and cathodic peak potentials of Cyt-c/CH-MPA-AuNPs/SAMs-Au electrode were at 0.006 and −0.043 V (vs. Ag/AgCl), respectively. Moreover, the developed Cyt-c/CH-MPA-AuNPs/SAMs-Au biosensor showed good sensitivity, selectivity, and stability. A special electrical activity was shown by Cyt-c/CH-MPA-AuNPs for NO-reduction. There is a linear relationship between peak current and concentration of NO gas in the range of 10–215 μM with a LOD of 4.5 μM and a response time of 5 s (Fig. 18).

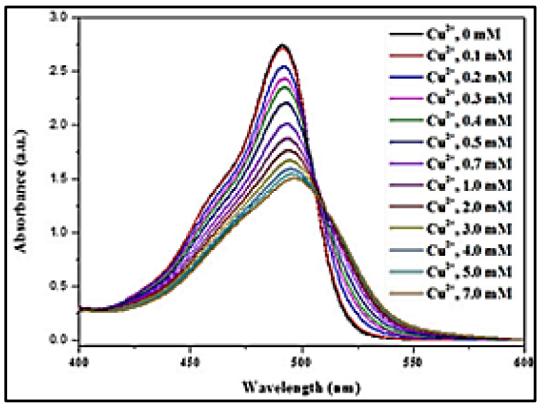

Fig. 13. Quantitative determination of Cu^{2+} metal ions in the medium using CH/FITC probe.

Sisman et al. [52] used CH to functionalize SnO_2 nanowires and apply it as a sensor to measure moisture at room temperatures. SnO_2 nanowire (NW) was prepared using a seed-layer-assisted vapor-liquid-solid (VLS) method, and CH was deposited on the SnO_2 NW by spin coating technique to achieve CH@SnO_2 hybrid NW sensor. The sensor exhibited excellent behavior towards humidity at different concentrations (25%, 50%, 75%) during electrical conductivity in the dark and under UV-light irradiation. The best sensor response was obtained at a humidity of 75%, resulting in 1.1 and 2.5 in the dark and UV-irradiation, respectively. Based on the conductometric profile of the humidity sensing (Fig. 19a), the suggested mechanism is explained by the proton-conduction mechanism [53,54]. The water vapors (humidity) is adsorbed on the CH@SnO_2 hybrid NW sensor surface, causing neutralization of basic amino-group of the CH network, as suggested by the following equation [54]:

$$R\cdots NH_3^+ \rightarrow R\cdots NH_2 + H^+$$

Through Fig. 19b, the first region suggests a sudden increase in the conductivity value as soon as water vapor is injected. The electrical conductivity of the nanostructures dominated by the protonic conduction, as protonic conduction reduces the CH layer resistance and, consequently, hybrid system equivalent resistance also decreased. Through the second region (Fig. 19b), the conductance began to decline after reaching the peak point during the continuous flow of water vapor. It could be the possible explanation is that the valence electrons for SnO_2 involved in the surface reaction and the mechanism of sense. Likewise, the proton conduction of CH may create electrical potential at the interface of CH/SnO_2. The attracted valance electrons of SnO_2 by H^+ on

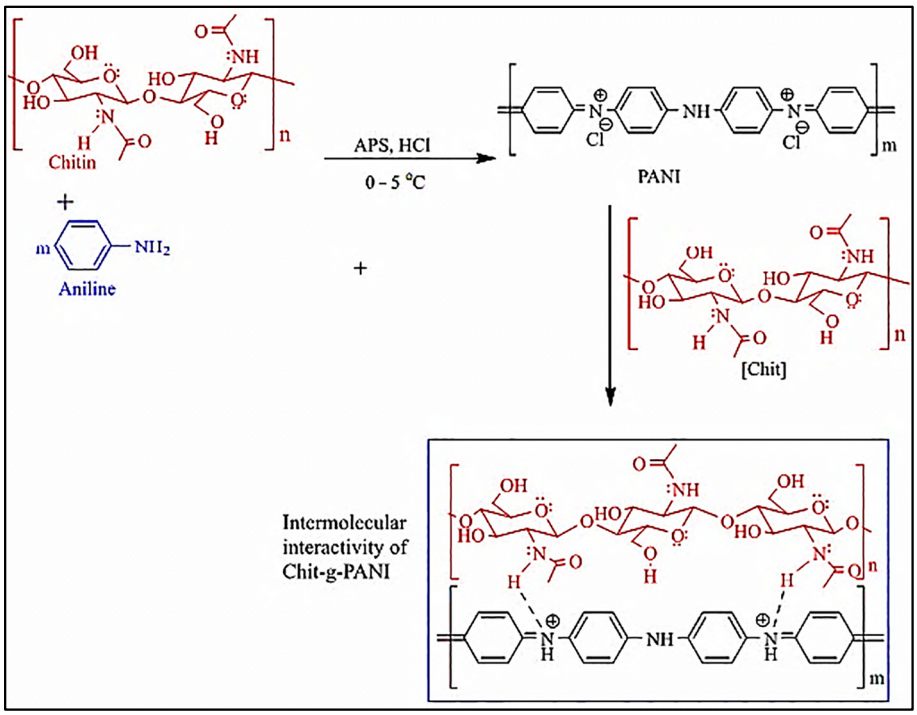

Scheme 7. Preparation of Chit-g-PANI biosensor for Cu^{2+} detection.

the surface of CH@SnO_2 hybrid NW causes an increase in equivalent resistance (Fig. 20) and thus neutralized the agglomerated H-protonic conduction.

7. Sensing of organic compounds

Gabrovska et al. [55] constructed a new amperometric biosensor for urea detection using a newly prepared enzyme membrane as support. New support based on enzyme immobilization of urease and (5%) rhodium nanoparticles loading on activated charcoal followed by chemical bonding by CH-acrylonitrile copolymer at different concentrations of modified CH (0.15–5%) to form the biosensor membrane (Scheme 9). The high sensitivity of the assembled biosensor (3.19 $\mu A \cdot mM^{-1} \cdot cm^{-2}$) was ascribed to the presence of CH and the rhodium nanoparticles in the polymer membrane. That was due to the high immobilization of urease, biocompatibility, and effective catalysis of the ammonia oxidation. Two advantages were provided by this sensor, and the first is the enzyme membrane can be replaced when its activity is decreased; the second is the asymmetry of the size and geometry of the pores of acrylonitrile copolymer membrane retains its selectivity at one selective side. The immobilized enzyme molecules at the non-selective side are protected and cannot be leached due to any electrochemical interference existing in the medium.

Mulyasuryani et al. [56] developed potentiometric urea biosensor fabricated from [H_3O^+] electrode as a transducer and glutaraldehyde-CH membrane as a urease immobilization material (Fig. 21). As the

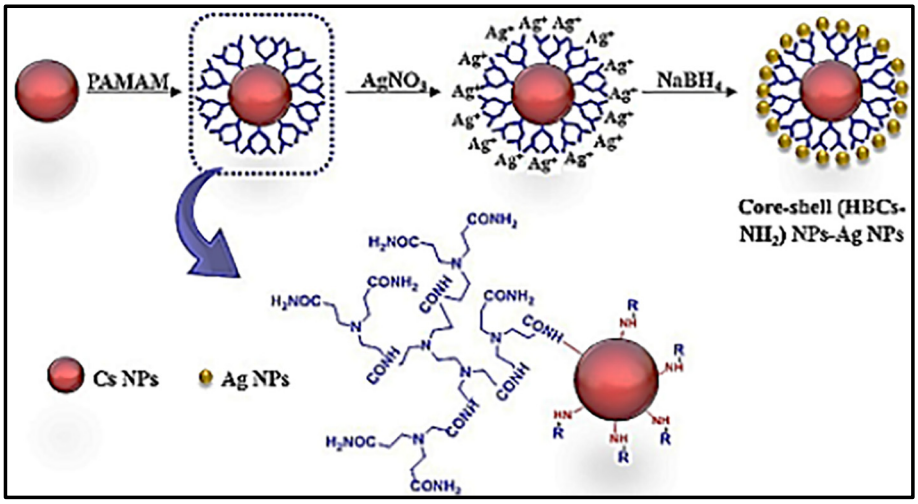

Scheme 8. Preparation of core-shell amino-terminated hyperbranched chitosan nanoparticles (HBCs-NH_2) NPs-AgNPs.

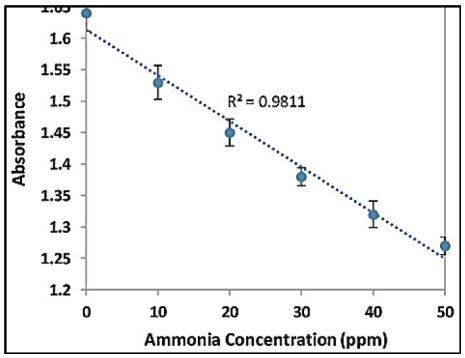

Fig. 14. The changes in the absorption intensity of SPR of (HBCs-NH_2) NPs-AgNPs at different concentrations of ammonia.

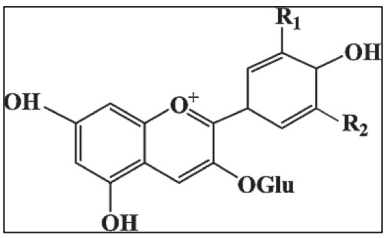

Fig. 15. Chemical structure of anthocyanin.

immobilized urease on the glutaraldehyde-CH membrane is released, the CO_2 diffusion rate increases. The CO_2 at the transducer was higher than the similar urea concentration in second-time measurements. A third time, the Nernstian factor is decreased due to a decrease in urease quantity. The high performance of the biosensor was obtained at a thickness of 0.21 mm and a pH of 7.3. The Nernstian factor of the biosensor was of 28.40 mV/decade, and the concentration of urea was ranged from 0.1 to 6.0 ppm with a LOD of 0.073 ppm. The urea sensor biological response time is 280 s, and the sensor is capable of measuring 32 samples with accurate accuracy of 94–99%.

Chitosan functionalized magnetic GO_x nanocomposite (Fe_3O_4@SiO_2@CH/GO_x) was developed [57] using a facile amide reaction between CH and GO_x (Scheme 10). A novel extraction method using Fe_3O_4@SiO_2@CH/GO as nano-adsorbent was developed and applied to the efficient determination of several alkaloids from their complex matrix. The adsorption of alkaloids occurred via π-π electron-donor-acceptor interaction, cation-π interaction, and hydrogen bonding. At the optimized conditions, the LOD was 0.016–0.092 $\mu g \cdot kg^{-1}$.

Sharma et al. [58] reported a green synthesis of nanocomposite hydrogel of chemically modified CH and sodium alginate (Na-Ala) incorporated with carbon quantum dots (CQDs) (Na-Ala/CH-polyAAm/CQDs) (Scheme 11) for picric acid sensing in the industrial wastewater. The nanocomposite precursor was derived from the CH-sodium alginate hybrid backbone and acrylamide monomer through the formation of the semi-IPN matrix (Na-Ala/CH-polyAAm). The developed hydrogel nanocomposite displayed 99% quenching efficiency for the selective detection of picric acid.

Bakhsh et al. [59] were designed a biosensor made of copper nanoparticles embedded in the CH polymer backbone. The designed biosensor has the tendency to simultaneous recognition and reduction of 4-nitroaniline. The active biosensor material (CuNPs-CH) was coated on the carbon electrode to obtain an efficient electrochemical sensor for 4-nitroaniline. The efficiency of the CuNPs-CH sensor towards 4-nitroaniline was evaluated using amperometry (Fig. 22a) and cyclic voltammetry (Fig. 22b) measurements at potential of −0.76 V and pH 7. The sensitivity of CuNPs-CH sensor was $-8.166\ \mu A \cdot mM^{-1} \cdot cm^{-2}$, with a LOD of 0.37 μM.

Among the most important dyes in the textile field are methylene orange (MO) and methylene blue (MB), which have been classified as one of the most important dangerous pollutants for of certain industrial effluents [60], as they are one of the highly toxic to aerobic and aquatic life as well as causes cancer and mutation [61,62], and neurotoxicity [63]. Different layers from polypyrrole-chitosan-calcium ferrite (PPy-CH-$CaFe_2O_4$) with a thickness of 2.8–59.5 nm were prepared by electrodeposition technique [64]. The refractive index of layered was in the range of 1.66131 + 0.156i to 1.62734 + 0.167i. The sensor has been applied in identification MO and MB in a solution containing 0.01, 0.1, 0.5, 1, 10, and 20 ppm by recording the resonance angle variation with time and concentrations (Fig. 23a–c). The thin layer PPy-CH-$CaFe_2O_4$ has the capability to detect both cationic and anionic dye with high selectivity to cationic dye as the dye interacts with the PPy-CH-$CaFe_2O_4$ sensor.

Chakraborty and Ilagan [2] fabricated medium-molecular-weight CH film and used it as a support for curcumin. The curcumin was immobilized on CH film in methanol or n-butanol as a solvent; however, the amount of immobilizing curcumin in the case of methanol was more than that in case of butanol as a solvent. The highest percent that achieved from the immobilization curcumin on CH was 2.3%-Cur-CH. Fluorescence intensity of Cur-CH films got quenched when contacted with the solution of o-nitrophenol (ONP) and sodium fluoride (NaF) with different extents in each compound (Fig. 24), and also on their concentrations. The intensity was highly pronounced when the concentration of ONP and fluoride (FL) was as low as 2.0×10^{-6} M and 2.5×10^{-5} M.

Mironenko et al. [65] fabricated fluorescent optical sensor from a thin membrane of high molecular weight CH doped with europium dibenzoylmethanate ($Eu(dbm)_3$) and then bromothymol blue (BTB) (Scheme 12). At a wavelength of 350–400 nm, the excitation of Eu $(dbm)_3$ with dibenzoylmethane ($(C_6H_5CO)_2CH_2$) showed a typical lanthanide emission (618 nm). The luminescent spectra of the Eu

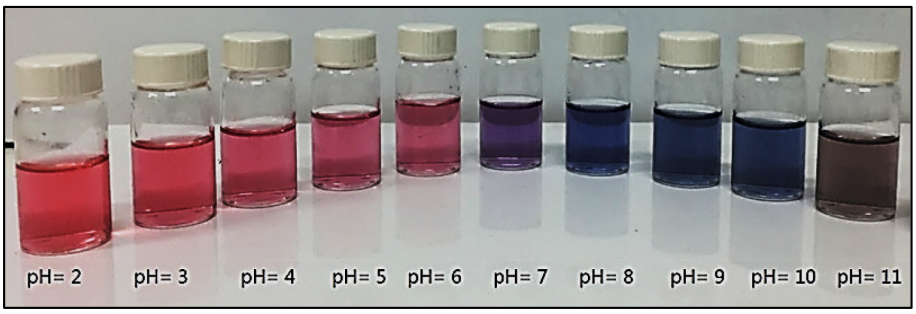

Fig. 16. Anthocyanin modified sensor response at the wide pH range.

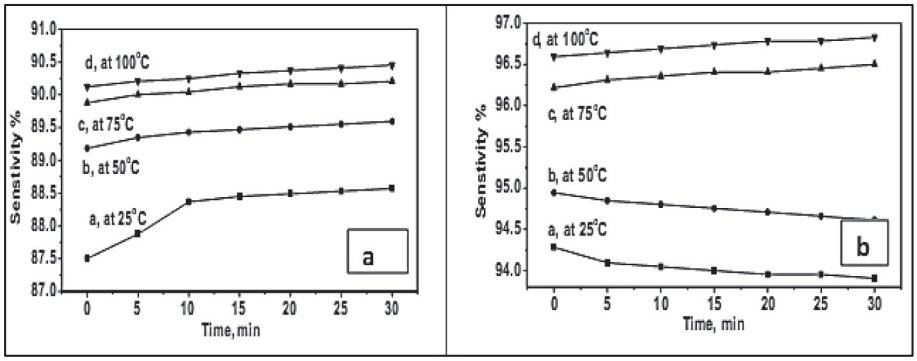

Fig. 17. a) Variations of sensitivity with time for CH/CAS nanocomposite at different temperature, b) variations of sensitivity with time for CH/CAS nanocomposite co-doped with 5% of Al_2O_3-NPs, at different temperature.

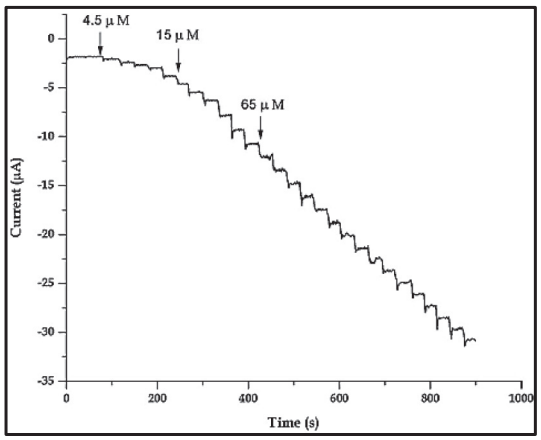

Fig. 18. Amperometric response of the Nafion/Cyt-c/MPA-AuNPs-CH/SAMs-Au electrode at different concentrations of NO.

$(dbm)_3$ is insensitive to the presence of methylamine gas. Therefore, bromothymol blue, which has an absorbance maximum closed the Eu^{3+} emission band to the film to provide a non-fluorescent reversible response to different concentrations of methylamine, and thus the Eu^{3+} emission can be measured (Fig. 25).

Two CH derivatives containing thiourea group (as chromophoric moiety) were synthesized by the reaction of CH with 1-isothiocyanato-4-nitrobenzene (derivative 1), and 2-(4-isothiocyanatophenyl)-1-(4-nitrophenyl)diazene (derivative 2) (Scheme 13) [66]. The two CH derivatives were used to determine different organic anions such as acetate, hexanoate and butylate, and inorganic anions such as phosphate and chloride. Using diffuse reflectance ultraviolet-visible spectroscopy (190–800 nm), the sensing of inorganic anions and carboxylate was performed. The analysis showed red-shift as a result of the formation of a hydrogen bond between thiourea and anions. The CH derivatives showed anion selectivity in order acetate > phosphate > chloride like thiourea anion chromophore, and anion sensitivity was better in dimethyl sulfoxide than acetonitrile. In addition, chitosan derivatives exhibited selectivity to carboxylate in the current order hexanoate, butylate, and acetate. The CH derivative 1 showed superior anion sensing than CH derivative 2 (Fig. 26a, b).

A simple electrochemical sensor was developed to detect catechol using molecularly imprinted polymers (MIP) electrochemical sensor [3]. MIP film was synthesized, using electro-deposition of CH through

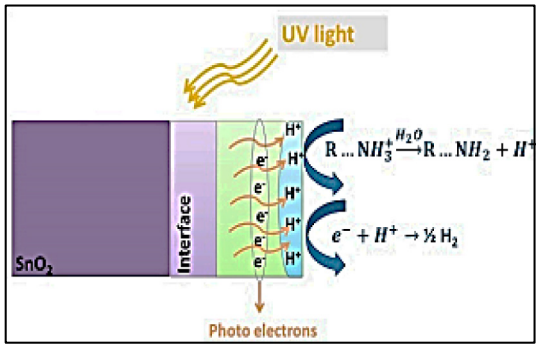

Fig. 20. Sensing mechanism of hybrid CH@SnO_2.

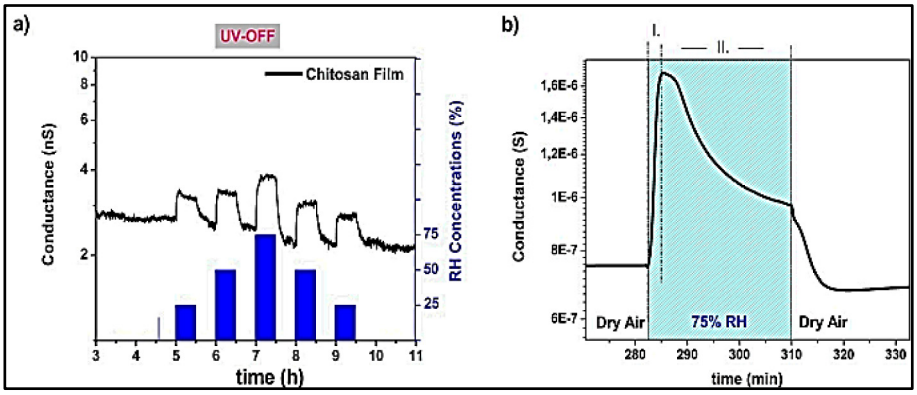

Fig. 19. (a) Humidity measurement profile of CH film, (b) zoomed conductance profile of CH@SnO_2 nanowires hybrid in dark condition towards 75% RH injection.

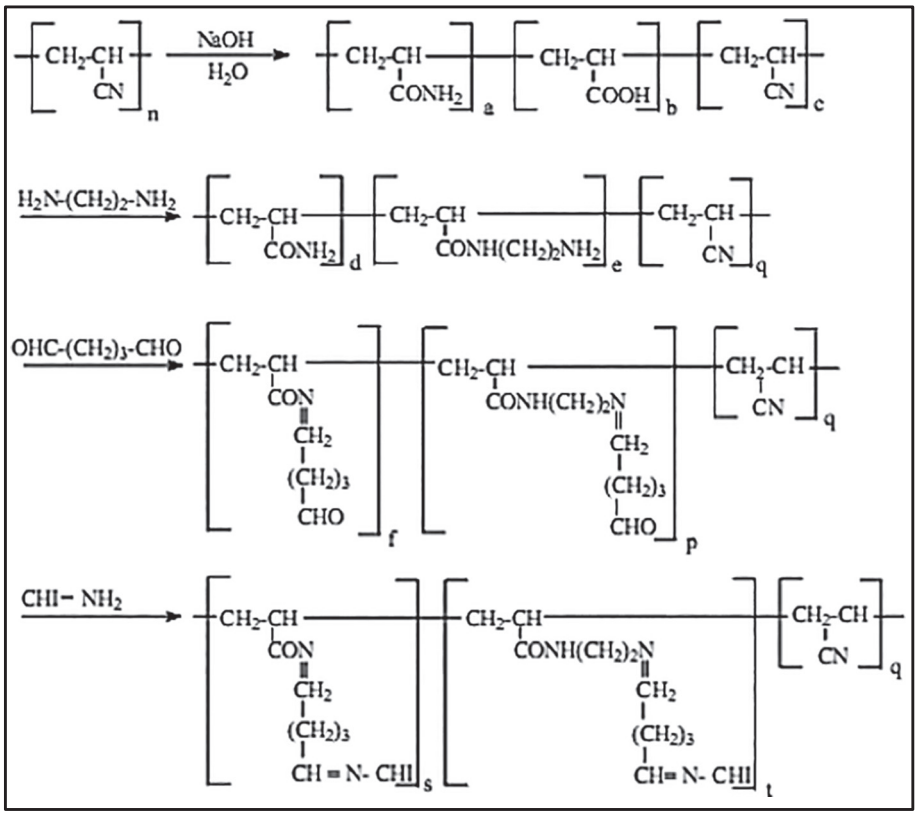

Scheme 9. Preparation of modified chitosan-acrylonitrile membrane.

chronoamperometry, on the surface of conducting boron-doped diamond electrode (BDD) in the presence of catechol as a template. The catechol compound was detected using a MIP-based electrode by measuring the cyclic voltages (CV) and comparing the resulting electrochemical signal with signals of non-molecular imprinted polymers electrode. The effect of the presence of various nesting phenolic compounds with a concentration of 10^{-4} M (e.g., 4-aminothiophenol, BPA, 2-nitrophenol, 4-tert-butyl catechol, and 4-nitrophenol) was studied during the detection of the catechol compound to determine the selectivity of the completed sensor at a concentration of 10^{-4} M catechol dissolved in 0.1 M PBS solution and pH 7.4. The results demonstrated high selectivity of the sensor to detect catechol; however, the signal increases by 18% in the case of BPA or 4-tert-butyl catechol due to the adsorption of both of them molecules adsorb on the MIP surface (Fig. 27).

A simple sensor from CMK-3 (ordered mesoporous carbon) modified nano-carbon ionic liquid paste electrode (CMK-3/nano-CILPE) is fabricated with the aim of sensing BPA [67]. The CMK-3/nano-CILPE sensor exhibited good electroactivity towards BPA using linear sweep voltammetry (LSV). Applying optimal conditions, there was a steady proportion between the oxidation peak current and the BPA concentration in the range from 0.2 to 15 μM, with a low LOD of 0.05 μM (Fig. 28). The CMK-3/nano-CILPE sensor presented low resistance, ease of modification, and renewability.

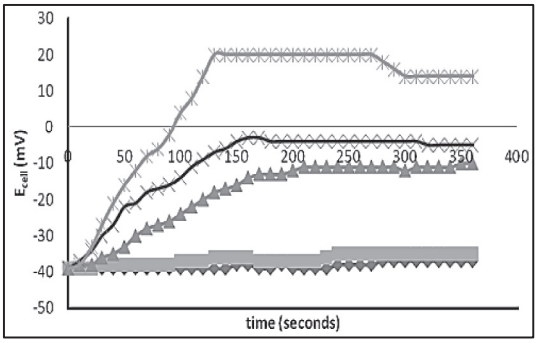

Fig. 21. Potentiometric urea biosensor response at different urea concentrations.

A sensitive electrochemical sensor was fabricated with the purpose of sensing BPA using AuPd nanoparticles-loaded graphene nanosheets (GNs) electrode (AuPdNPs/GNs) by the spontaneous redox reaction between bimetallic precursors and GNs (Scheme 14) [68]. The synergistic effect of Au and Pd with GNs exhibited high electrochemical activity with well-defined BPA-oxidation voltammetric peaks lower overpotential compared to noble metals alone deposited on the GNs. Under optimized conditions, differential pulse voltammetry (DPV) (Fig. 29) showed a linear response at BPA-concentration of 0.05–10 μM with a LOD of 8 nM, which enabled AuPdNPs/GNs sensor to be used for detection of BPA-molecule in the food field.

Jing et al. [69] reported low-cost graphene–IL modified GCE as a BPA electrochemical sensor. The type of ionic liquid molecule is 1-butyl-3-methylimidazolium hexafluoro-phosphate ($BmimPF_6$), and the electrode material is glassy carbon electrode. The authors reported the electrochemical behaviors of BPA on the graphene–IL modified GCE, which is an adsorption controlled irreversible oxidation process. The fabricated graphene–IL modified GCE electrode showed superiority than both graphene-modified and bare electrodes like the ease of manufacture and operation, and the possibility of re-preparation with the same specifications, as well as accuracy and reasonable economic cost. The concentration obtained for the linear range was from 20 μM to 2 μM with a LOD of 8 nM. The graphene–IL modified GCE was applied successfully for an estimate of milk and soda spiked BPA.

[70] reported a biochemical sensor to detect BPA building from flower-like MoS_2 (molybdenum disulfide, MoS_2), CH-AuNP composites modified electrode (AuNPs/MoS_2/GCE). Flower-like MoS_2 is synthesized by a simple hydrothermal method, while AuNPs are synthesized using tri-sodium citrated as capping agent and sodium born anhydride as a reducing agent. The AuNPs/MoS_2/GCE electrode showed good

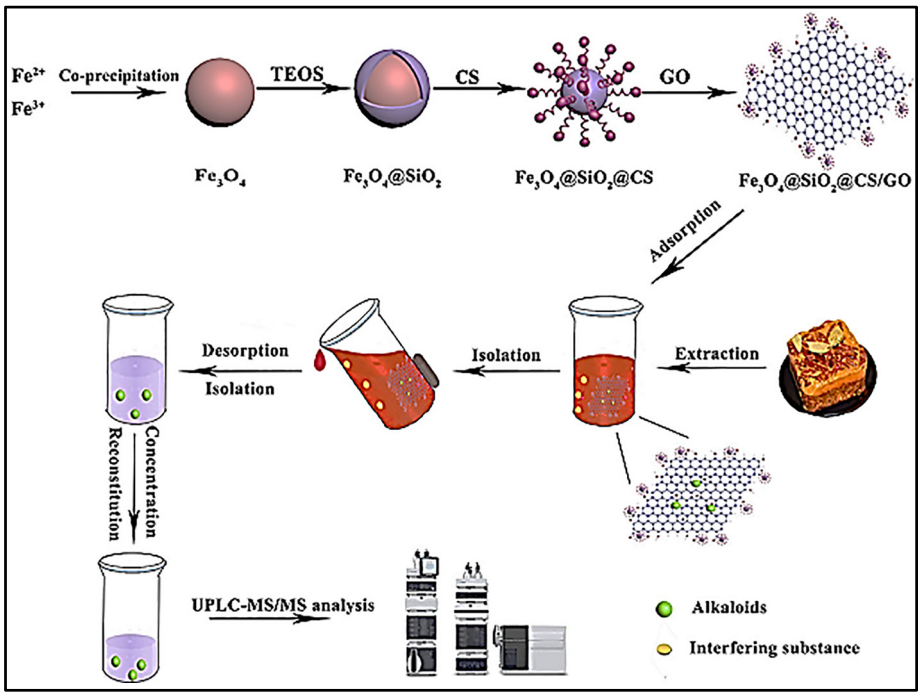

Scheme 10. Preparation of chitosan functionalized magnetic graphene oxide nanocomposite (Fe_3O_4@SiO_2@CS/GO).

electrocatalytic behavior towards PBA oxidation, and excellent long-term stability, as well as demonstrated good analytical performance, with a LOD of 5×10^{-9} M. Furthermore, a significant improvement in the electron transport kinetics of BPA has been observed on the surface of the AuNPs/MoS2/GCE electrode by significantly reducing oxidation overpotential and increasing the oxidation peak current.

8. Sensing of biological molecules in bio-systems

The average level of uric acid in serum was estimated to be between 0.13 mM and 0.46 mM [71]. Increased serum uric acid levels may lead to diseases, including gout, arthritis [72], cardiovascular disease [73], and neurological diseases [74]. Consequently, working to determine uric

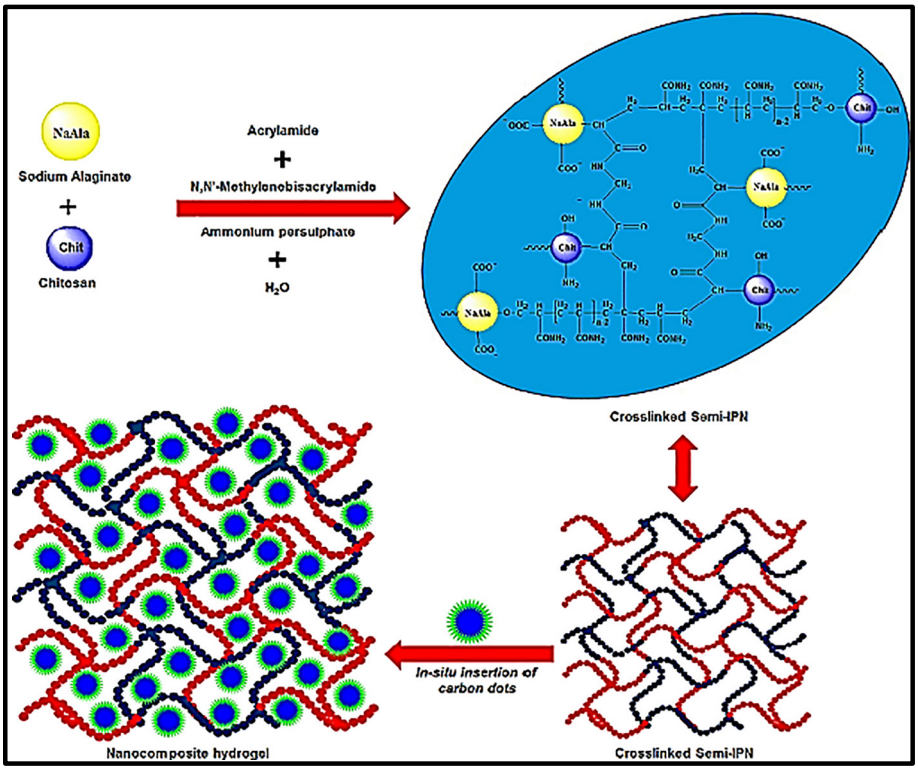

Scheme 11. Fabrication of Na-Ala/Ch-polyAAm/CQDs picric acid sensor.

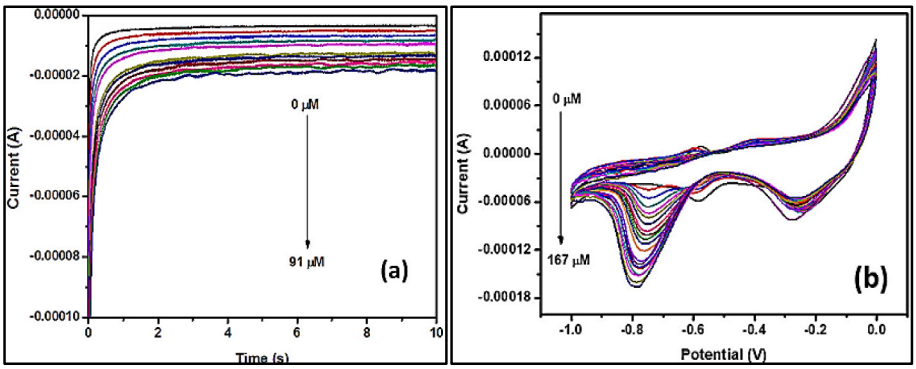

Fig. 22. Sensing the concentration of 4-nitroaniline, (a) amperometrically, (b) cyclic voltametrically at −0.76 V and pH 7.

acid is one of the most important matters in the diagnosis and management of diseases that result from purine metabolism. In this manner, a uric acid biosensor was prepared by crosslinking immobilization of the uricase enzyme-modified CH-glutaraldehyde polymer onto Prussian blue nanoparticles (PBNPs) absorbed onto MWCNT and polyaniline (PANI) assembled by electrochemically deposited on Au electrode (Scheme 15). The prepared amperometric uric acid biosensor was fabricated and worked as a working electrode. Ag/AgCl and Pt electrodes were used as standard and auxiliary electrodes in the potentiostat during the amperometric measurements. The prepared biosensor exhibited a LOD of 0.005–0.8 mM and fast response after 4 s at pH 7.5 when operated at 0.4 V vs. Ag/AgCl.

Glutathione (GSH, Fig. 30) is a tripeptide distributed in living systems and participated in many important processes in cells. It plays a major role in maintaining red blood cells and the metabolism of endogenous substances and drugs [75]. It is the primary component of antioxidant defense systems, and it plays an important role in protecting cells against infections [76]. The ratio GSH to glutathione disulfide compound (GSSG) is applied as an indicator of oxidative stress [77]. Therefore, it is important to find a permanent and reliable approach to the measurement of GSH and GSSG to determine the ratio of GSH to GSSG, and hence the ease of investigating oxidative stress and the toxicity mechanism. This ratio has gained special attention due to the vital biological functions that it plays, such as enzyme activity conservation, bioreductive reactions, and protection against oxidative stress and detoxification [78]. Also, there is a direct correlation between the reduced amount of GSH in intracellular fluids and the aging of life [79].

In this context, Chauhan et al. [80] reported an amperometric biosensor capable of measuring and determining glutathione (GSH) by forming a covalent bond between the immobilized glutathione oxidase ($GSHO_x$) on Au coated magnetic nanoparticles (Fe@AuNPs)-modified a platinum electrode by CH to insert organic amine groups onto the surface of Fe@AuNPs (Scheme 16a). The covalent bond enables a high percent of the enzyme as well as shelf life with the maximum response time at 4 s at the condition of polarization (+0.4 V), pH (7), and 25 °C. The addition of 1 mmol·L^{-1} of GSH increased both the reducing and oxidation currents as a reflection of the catalytic oxidation properties of the modified electrode (Scheme 16b).

Triglycerides (TG) are produced from a chemical reaction (esterification reaction) between the hydroxyl groups of glycerol with three times the molar fatty acid. The safe percentage of TG in the blood serum represents between 40 and 190 mg/L [81], and exceeding this safe range is one of the most important factors of atherosclerosis associated with vascular diseases, the most important of which coronary heart disease (CHD) [82]. One of the most important and useful methods for determining TG is electrochemical sensing because of its advantages over other methods such as simplicity, speed, and sensitivity, as well as the low requirements for sample preparation. Narang et al. [83] has provided a TG bio-sensor for triglycerides, where they have prepared NiONPs–CH/ZnO–ZnHCF hybrid film as an amperometric sensor. The authors used nickel oxide nanoparticles–CH as support of lipase enzyme, glycerol kinase (GK, phosphotransferase enzyme) and glycerol-3-phosphate oxidase (GPO) and the hybrid material is adsorbed on the zinc oxide/zinc hexacyanoferrate (ZnO–ZnHCF) electrodeposited on the Au-electrode surface (Fig. 31).

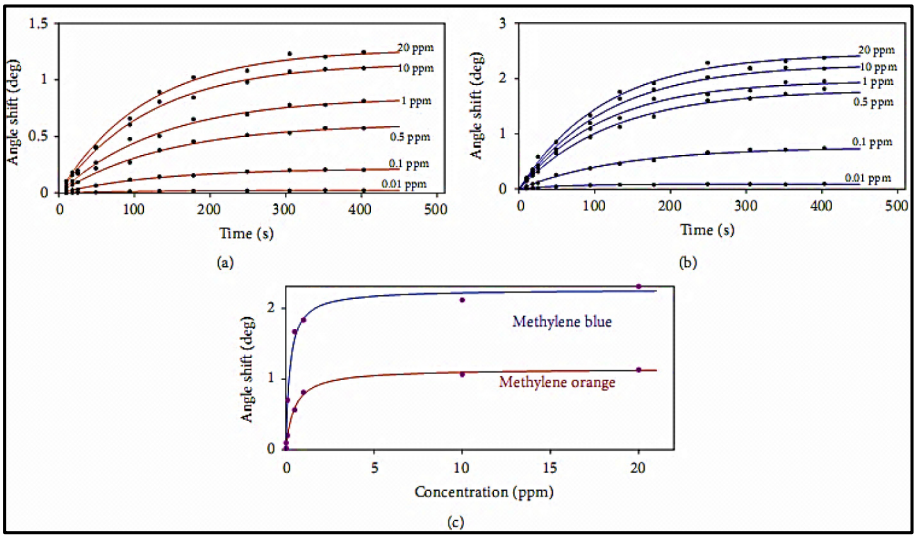

Fig. 23. Variation of the resonance angle shift with time for: (a) MO, (b) MB, and (c) with different concentrations of MO and MB.

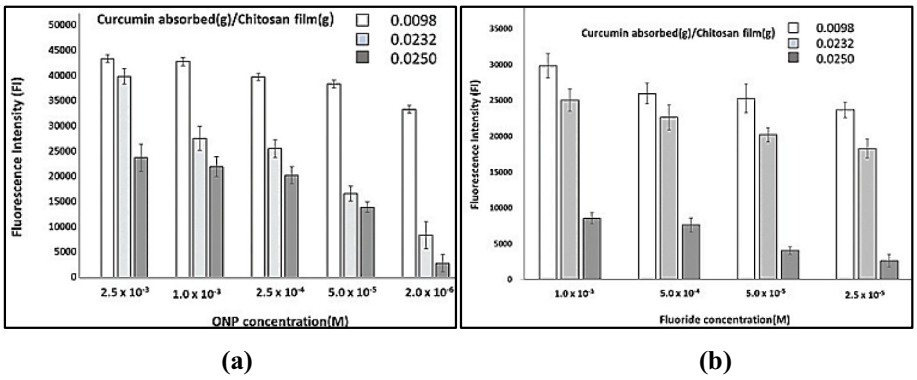

Fig. 24. The variation in fluorescence intensity of Cur-CH films in the presence of (a) ONP, (b) FL.

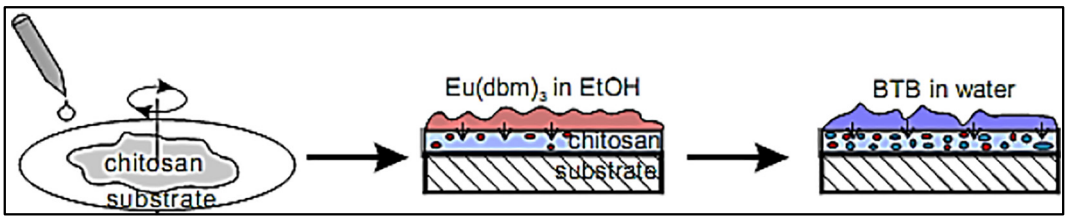

Scheme 12. Fabrication of chitosan thin film co-doped with Eu^{3+} and bromothymol blue, and mechanism of methyl amine sensing.

The NiONPs–CH/ZnO–ZnHCF biosensor showed the optimum response when polarized at +0.4 V vs. Ag/AgCl at 35 °C, pH 6 within 4 s, with a LOD of 10 mg/L. It was found a linear relationship between the concentration of triolein in the range of 50–700 mg/dL and the sensor response, and the sensitivity was 0.05 μA/mg/dL. After re-using the NiONPs–CH/ZnO–ZnHCF biosensor 100 times, it lost nearly 50% efficiency over 180 days when stored at 4 °C.

Dopamine (DA) (Fig. 32) is a chemical that belongs to the catecholamine and phenethylamine families and is one of the excitatory neurotransmitters that have a vital role in the functioning of the central nervous system, cardiovascular system, kidneys, and hormones [84]. An increase or deficiency of dopamine may result in brain disorders, neuroendocrine disorder, and Parkinson's disease [85]. The main problem with the determination of dopamine electrochemically is the interference between dopamine and ascorbic acid (AsA) since the two compounds have closed oxidation potential. Also, the ascorbic acid being anionic and dopamine is cationic, which results in the strong interaction, so this relationship affects the determination of the ratio of dopamine in the presence of ascorbic acid [86]. This problem attracted the curiosity of many researchers towards finding or developing different electrodes to identify or selectively detect dopamine in the presence of ascorbic acid [87,88].

Pandiselvi and Thambidurai [89] reported glassy carbon electrode (GCE) was modified with CH–ZnO/polyaniline film. The inorganic (ZnO)-organic (CH)/polyaniline (PANI) was prepared by chemical coprecipitation technique of CS–ZnO and then polymerization of aniline monomer with the precipitated CH–ZnO by ammonium persulfate initiator. The final nanocomposite ($CH_{0.12}$-$ZC_{2.5}$/PANI) was modified GCE electrode for the purpose of identifying dopamine (DA) in the presence of ascorbic acid in 0.2 M phosphate buffer solution (pH 7). The ascorbic acid and dopamine electrochemical signals are well identified with a potential separation of 303 mV (Fig. 33). The signal separation is sufficient enough to know any of them in the presence of the other. At dopamine concentration of 2×10^{-4} to 1.8×10^{-3} M, a linear response is obtained LOD of 0.21 μM and sensitivity of 0.013 $A \cdot M^{-1}$.

Norfloxacin (Fig. 34) (1-ethyl-6-fluoro-1,4-dihydro-4-oxo-7-(1-piperazinyl)-3-quinoline carboxylic acid, NF) is a member of fluoroquinolone (FQ) antibiotics of the third generation. It is used to treat various

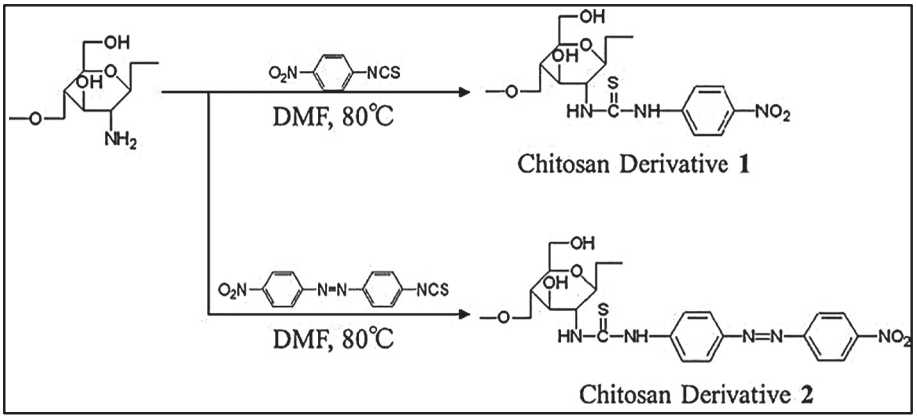

Scheme 13. Synthesis of chitosan derivatives 1 and 2.

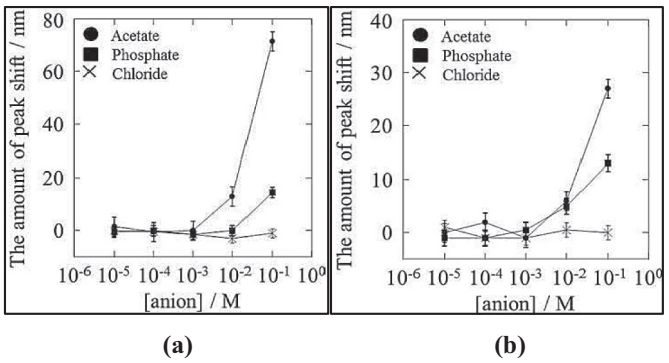

Fig. 26. Variation in peak wavelength shift of the derivative spectra of: (a) CH derivative 1, (b) derivative 2, as a function of anion concentration in dimethyl sulfoxide.

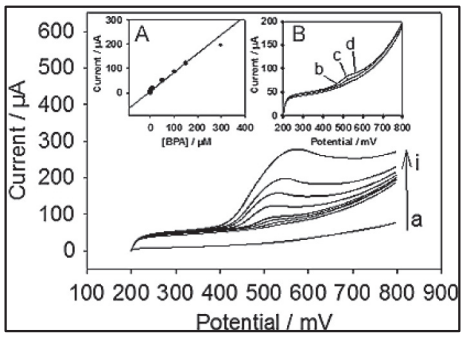

Fig. 28. LSVs for different concentrations of BPA (from a–i: 0–300 μM BPA). (A): relation between the oxidation peak current and the concentration of BPA; (B): LSVs of low concentrations of BPA (b, 0.2 μM; c, 1 μM; d, 5 μM).

infectious caused by *E. coli*, *Campylobacter*, *Salmonella Shigella*, and *V. cholera*. Detection of NF in clinical and biological samples is of supreme importance because of its toxic effects. NF has been detected by sequential analytical methods like fluorometry [90], spectrophotometry [91], and high-performance liquid chromatography (HPLC) [92]. HPLC is extensively used owing to its selectivity, susceptibility, and capability to diminish interferences, but it is time-taking, requires wide solvent-usage and high-class devices, with a high maintenance cost, which limits its usage.

In order to use simple, time, and expensive chemicals non-consuming method to detect NF trace-level in human urine samples, a new biosensing platform has been reported using the electrochemical technique. Nanostructured yttrium oxide (nY_2O_3) was synthesized [93] at low-temperature, using a one-step hydrothermal process. A biosensing platform based on nY_2O_3 modified with chitosan (CH) was fabricated for the detection of NF (Scheme 17). Fluoroquinolone antibodies (anti-FQ) were immobilized on the CH-Y_2O_3/ITO electrode via covalent interaction. Non-specific sites were deactivated using bovine serum albumin (BSA). The response study of BSA/anti-FQ/CH-Y_2O_3/ITO electrode (Fig. 35) revealed a wide range (1 pM–10 μM) with a lower LOD of 3.87 pM using differential pulse voltammetry (DPV) with a fast response time of ~10 min.

A superior modified new and sorely selective electrochemical nano-hydrogel was created as a sensing platform for the determination of 5-fluorouracil (5-FU, Fig. 36) [94]. The platform made of CH (CH)-based hybrid semi-interpenetrating nano-hydrogel prepared during reductant-free gold nanoparticles (AuNPs) synthesis in CS-poly (methacrylic acid) (Au@CS-PMAA) framework (Scheme 18). The covalently cross-linked Au@CS-PMAA nano-hydrogel with CS chains semi-interpenetrating in PMAA cross-linked network show superior H-bonding interaction between the -OH and -COOH groups of CS and PMAA segments with 5-FU. AuNPs showed remarkable features as a superior electrochemical response (Scheme 19), better solubility, large surface area, and plentiful binding sites for improved absorption of the 5-FU. That offers good efficiency during the determination of 5-FU with a wide linear range from 0.1–497 μM and low LOD of 0.03 μM.

One of the major challenges to human health is the diagnosing of invasive Aspergillosis (IA), which is caused by *Aspergillus fumigatus*. Bhatnagar et al. [95] reported the fabrication of sensitive electrochemical nano-biosensor through detecting glip-T. The sensor includes 1,6-hexanedithiol ($HS(CH_2)_6SH$) and CH stabilized gold nanoparticle self-assembly of glip probes (glip-P) on the gold electrode (Scheme 20). The biosensor showed LOD in buffer sample by $0.32 \pm 0.01 \times 10^{-14}$ M and in the real sample by $0.81 \pm 0.01 \times 10^{-14}$ M. The sensor can be used 7th times, which made this sensor a potential candidate for conversion into a glip-T-miniaturized hand-held device for Invasive Aspergillosis-patients.

Baraketi et al. [1] has been developed a new approach that allows simultaneous enrichment as well as rapid and accurate detection of *Escherichia coli* disease by indirect enzyme-linked immunosorbent assay (ELISA) using an enhanced support film based on CH, cellulose nanocrystals (CNCs), and glycerol. The combination of pathogen capture and enrichment steps for microbial growth resulted in a high detection signal at a low fertilization level without cross-reaction with Pseudomonas and Salmonella strains. The detection was made at different incubation periods and multiple levels of inoculations for a bacterial culture of *E. coli*. The authors obtained much higher signal detection for samples incubated with the CH-based support reinforced with CNCs than free CNCs material. The CH/cellulose nanocrystals/glycerol (CCG) with 0.6% showed an improvement of the signal of *E. coli* by 25% compared to control (Table 1). The entire bacterial culture also showed

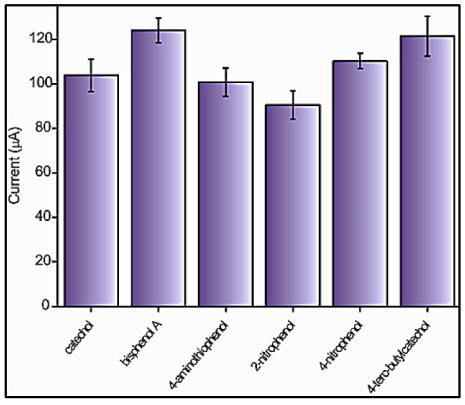

Fig. 27. Cyclic voltammetry (CV) anodic peak maximum obtained by CH-MIP/BDD sensor during the detection of catechol in the presence of different phenolic compounds at pH 7.4.

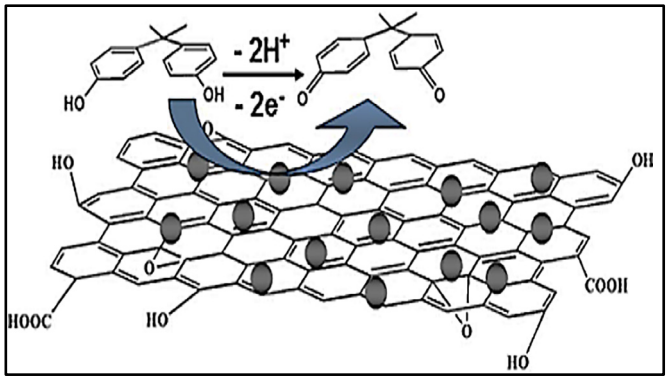

Scheme 14. Surfactant-free AuPd nanoparticles-loaded graphene nano-sheets (AuPdNPs/GNs).

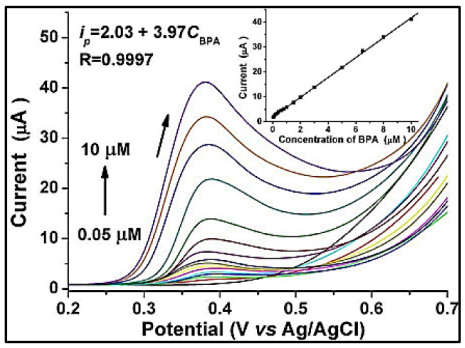

Fig. 29. DPVs at AuPdNPs/GNs-GCE in 0.1 M phosphate buffer solution (pH = 7.5) containing different concentrations of BPA.

higher immobilization signals than the un-filtered and cell-free supernatant. Compared to conventional methods, the spider-web-trap-approach (SWTA) detects *E. coli* after 4 h of enrichment, which is a good result as traditional methods gave detection after 24 h. This modification enables to reduce the risk of cross-contamination, and thus food product recalls easily by detection of foodborne pathogens samples.

Cell inhibition drugs (cytostatic drugs) are a wide range of chemotherapy compounds that are mainly used in the treatment of tumors, skin diseases, and the treatment of infections. Flutamide (FLU, 2-methyl-N-[4-nitro-3-(trifluoromethyl)phenyl]propanamide) (Fig. 37) is an anti-androgen drug. It is an effective non-steroidal anti-androgen drug for the treatment of advanced prostate cancer.

FLU blocks male natural hormone, testosterone, that stimulates the growth and spread of prostate cancer cells [96]. After oral administration, FLU is mainly extracted in the urine, as an unchanging drug and hydroxyl metabolites, especially 2-hydroxy-flutamide and 3- trifluoromethyl-4-nitro aniline. This drug also reduces the metabolism of C-19 steroids by the cytochrome P-450 system in target cells in secondary sexual organs [97]. In addition, it can also be used to treat excess anti-androgen levels in women, specifically women with polycystic ovary syndrome (PCOS) [98]. As a result of this importance, the vision requires the development of an analytical tool with high sensitivity and selective towards flutamide.

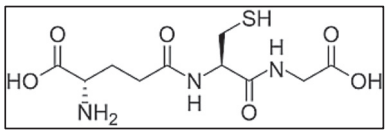

Fig. 30. Chemical structure of glutathione.

Mutharani et al. [99] reported an innovation in the routine anti-androgen drug flutamide (FLU) monitoring in real samples. The author performed electropolymerized of bromophenol blue (BPB) on the CS-Au CG surface-modified glassy carbon electrode (GCE) to get CS-Au CG/PBPB modified GCE. The author uses a one-step green method to prepare CS-Au CG using low molecular weight CH as a reducing and stabilizing agent as well as a suitable support for PBPB electrodeposition with the aim of detection of FLU in human urine and human blood serum (Scheme 21). The prepared CS-Au CG/PBPB modified GCE electrochemical sensor showed linearity in the FLU concentration of 0.01–1245 μM along with good sensitivity (0.63 $\mu A \cdot \mu M^{-1} \cdot cm^{-2}$) with a LOD of 4.8 nM.

The concentration of Mucin glycoprotein (CA125) in human serum and correlates with developing ovarian cancer risk and indicates a response to treatment in patients who have been diagnosed. Careful detection of CA125 in vital fluids is of great clinical importance. Hasanzadeh et al. [100–102] were innovative immunoassay for the detection of CA125 using signal amplification strategy. Horseradish peroxidase (anti-CA 125) was immobilized onto a nanocomposite containing conductive matrix (polycetyltrimethyl ammonium bromide (PCTAB), CH and signal amplification element (AgNPs)). The immunometric sensor tested using CV and DPVs techniques. The immunometric sensor exhibited linearity of CA125 at 00.01–400 U/mL along with low LOD (0.001 U/mL).

Malondialdehyde (MDA, $CH_2(CHO)_2$) is the main reactive aldehyde compound, which is caused by oxidation of the cell membrane, and it is usually used as a biomarker for manifestations of tissue damage [103]. MDA has been extensively studied as a peroxide product [104,105].

MDA interacted with the functional groups of various cellular structures, including NH_2 and SH groups in sulfhydryl compounds, and

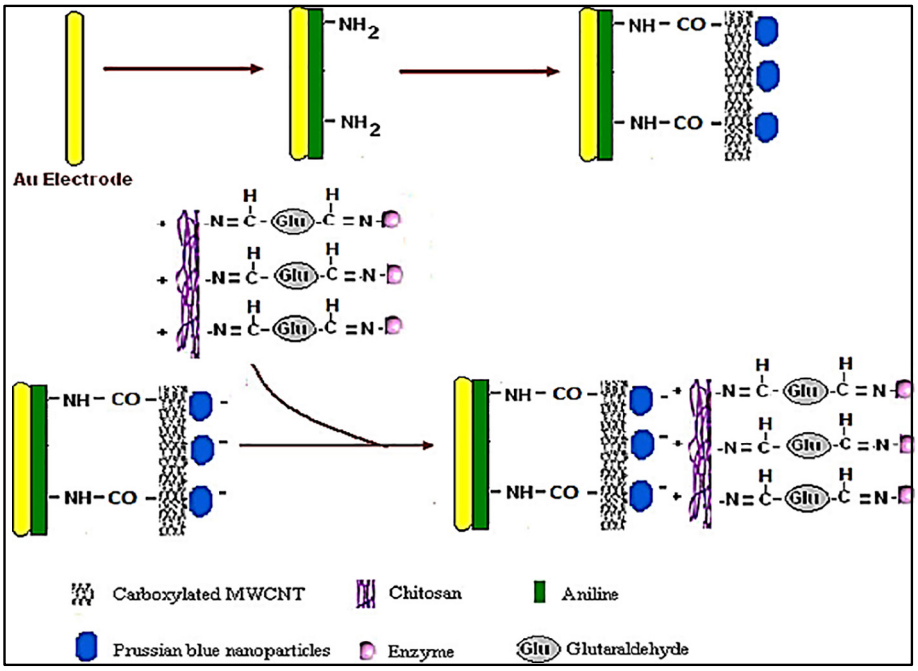

Scheme 15. Preparation of Uric acid biosensor based on immobilization of uricase enzyme.

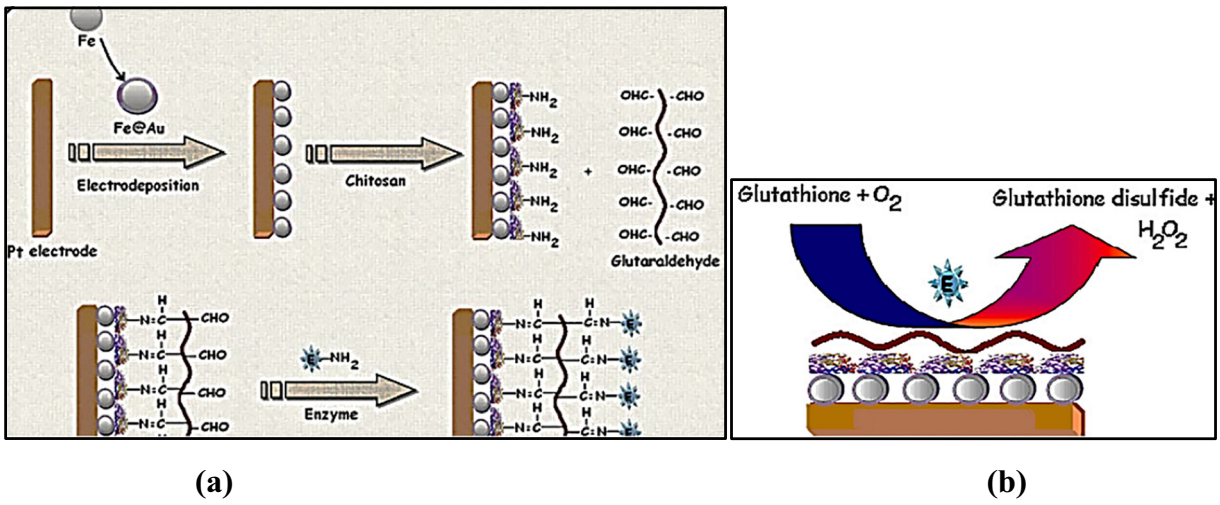

Scheme 16. (a) Assembling of Glutathione biosensor, (b) the mechanism of glutathione measurement by $GSHO_x$/CHIT/Fe@Au modified Pt electrode.

nucleic acid bases can be effective in tumor development [106]. In addition, the oxidation of unsaturated fatty acids may contribute as a secondary source in the production of MDA [107]. Chitosan (CH) was electrodeposited on the surface of polydopamine (PDA) modified glassy carbon electrode (GCE) [100–102]. With aid of CH and polydopamine properties such as the presence of abundant catechol and amine groups, uniform deposition of Ag NPs onto the POLY(DA-CH) is achieved (Scheme 22). The dispersibility of AgNPs on POLY(DA-CH) prevents electron-hole pairs recombination that produced from photo-electrocatalysis as well as directed the captured electrons to participate in the photo-electrocatalytic reaction process (Scheme 23). POLY(DA-CH)-AgNPs showed good excellent durability and electrochemical sensitivity for detecting MDA, a linear dynamic range, and a low limit of 1.45–7.9 μM and 1.45 μM, respectively.

Changes in the level of choline are associated with the appearance of several diseases such as Alzheimer's, Huntington, fatty liver, Parkinson's, interstitial lung deformities, and autism. From here, the specific identification of choline is important in both biological and clinical analysis. There are many methods that have been discovered to measure choline in body fluids, but they have some disadvantages, such as high cost, complexity, and specialized ability.

Nikzad and Karami [108] reported the colorimetric detection of choline (Fig. 38) based on DNAzyme-choline oxidase coupling. The choline oxidase produces hydrogen peroxide (H_2O_2) and betaine (zwitterionic quaternary ammonium compound) in the presence of choline and oxygen; then, the DNAzyme converts colorless 2,2′-azino-bis(3-ethylbenzothiazoline-6-sulfonic acid) diammonium salt (ABTS) into green $ABTS^{2-}$ radicals. Compared to conventional choline detection methods, the DNAzyme-choline oxidase coupling sensor showed excellent

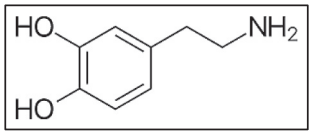

Fig. 32. Chemical structure of dopamine.

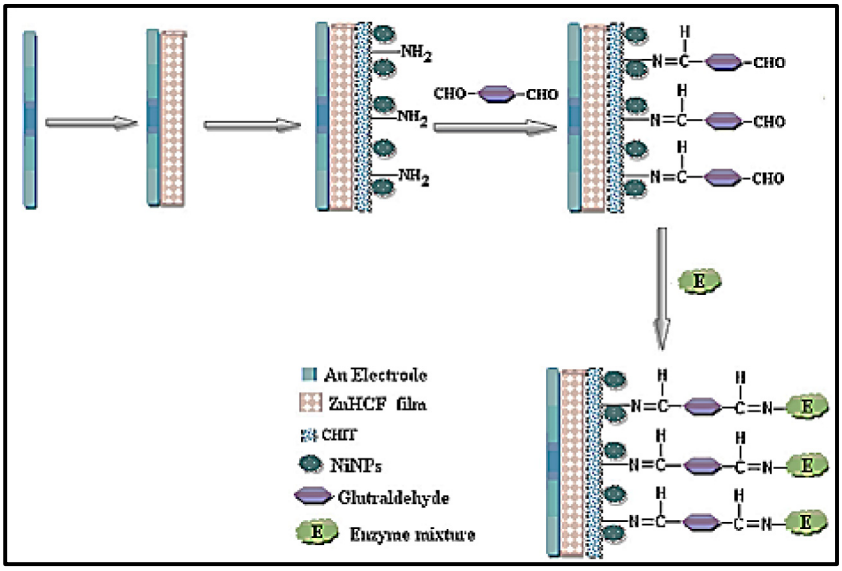

Fig. 31. Schematic representation of enzymes-nickel oxide nanoparticles-CH/zinc oxide/zinc hexacyanoferrate nanocomposite biosensor.

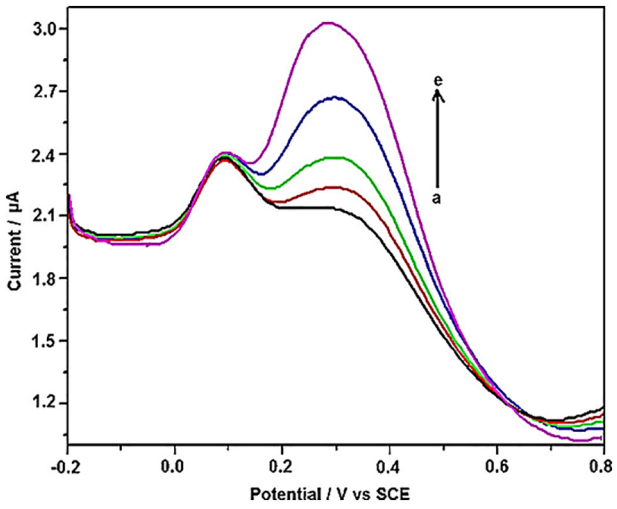

Fig. 33. Differential pulse voltammograms of 0.1 mM ASA, glucose and different concentrations of DA (a–d: 0.001–0.005 mM) in pH 7 solution at $CH_{0.12}$-$ZC_{2.5}$/PANI.

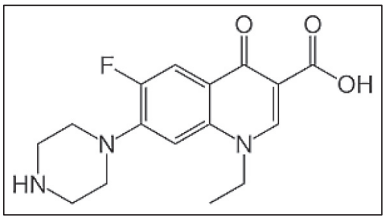

Fig. 34. Chemical structure of Norfloxacin.

selectivity towards choline concentration, linear range (0.1–25 μM) with a LOD of 22 nM (Fig. 39).

Cephalexin (CEX, Fig. 40) is one of the chemical compounds that inhibit bacterial activity and belongs to the cephalosporin family. The mechanism of action of this generation is by inhibition of the bacterial cell wall during bacterial division, and therefore the bacteria die by the effect of external osmotic pressure. Cephalexin is distinguished from its counterparts in its family by its easy oral absorption and its cheapness. Therefore, it is widely used in veterinary clinics as a treatment for urinary tract infection, skin infections, and mastitis in dairy cows [109]. Yu et al. [110] reported sensitive and selective electrochemical immunosensor for CEX determination using GCE modified with carboxylated single-walled carbon nanotube (SWNTs)/CH composite (SWNTs-COOH/CH) (Scheme 24). The role of SWNTs-COOH/CS was to enhance sensor performance and expand the electrochemical response to CEX. The free CEX in the solution can be well measured based on the competitive immunoreaction between the CEX and CEX antibodies. The developed approach exemplifies reproducibility and a high level of specificity and sensitivity for CEX detection at 1–800 μg/mL. This approach was used to determine CEX in 6th samples and obtained a recovery range of 80.15–94.04% (Fig. 41).

Tryptophan (Trp, Fig. 42) is one of the important amino-acids for the human body and low concentrations of it are necessary to perform many physiological functions, as well as it is considered as a component of protein and had the ability to create and maintain a positive nitrogen balance [111]. It is also a precursor to Serotonin and Melatonin, which plays an important role in improving mood and maintaining mental health. Since tryptophan is rarely found in plant products, the Tryptophan compound is sometimes added to diets, nutrients, and pharmaceutical formulations.

Tian et al. [112] reported an electrochemical sensor to combine black acetylene with molecular printing technology with high selectivity and sensitivity to estimate the metric voltmeter of Trp, using CH and Trp as a template molecule (Scheme 25). The molecularly printed CH-film was deposited on the surface of the ABPE electrode (black acetylene paste electrode). The ABPE was applied to Trp quantitative analysis in the field of pharmaceuticals, and human serum samples, with a LOD of 8 nM.

The rapid and sensitive identification of riboflavin (RF) compound is important in the treatment of seborrheic and glossitis dermatitis and the sensitivity to the sun's rays and skin disorders and mucosal (Fig. 43). Hassanpour et al. [4] developed an electrochemical sensor modified electrode for sensitive detection of RF in commercial multivitamin using CH film electrodeposited on the surface of GCE (Scheme 26). The modified electrode was used as an effective electrical interface to detect RF using cyclic, differential pulse, and square wave voltammetry techniques. The formation of hydrogen bonding leads to an increase in the absorption of RF on the surface of the modified electrode and subsequently increased the redox peak currents. Therefore, the kinetics of the redox reaction is enhanced, and the voltammetric responses of RF are significantly increased [113,114].

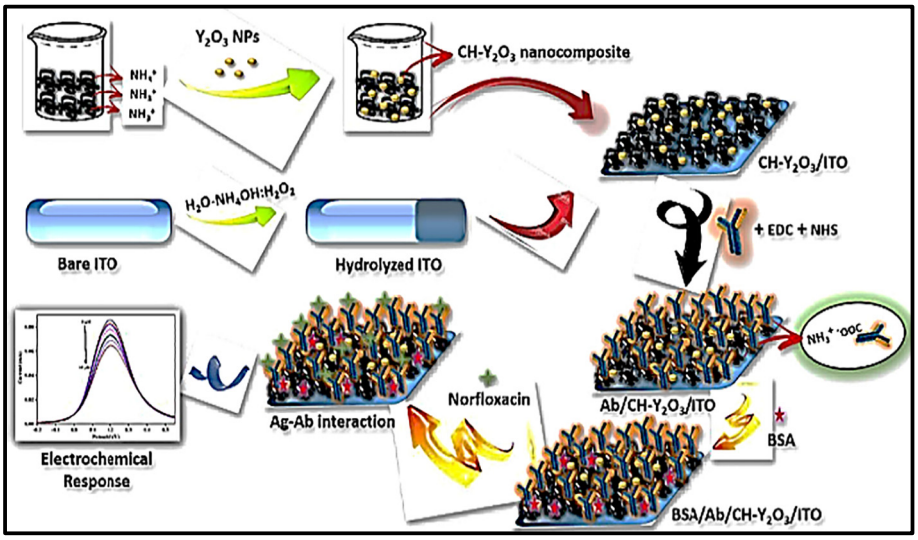

Scheme 17. Synthesis of BSA/anti-FQ/CH-Y_2O_3/ITO electrode.

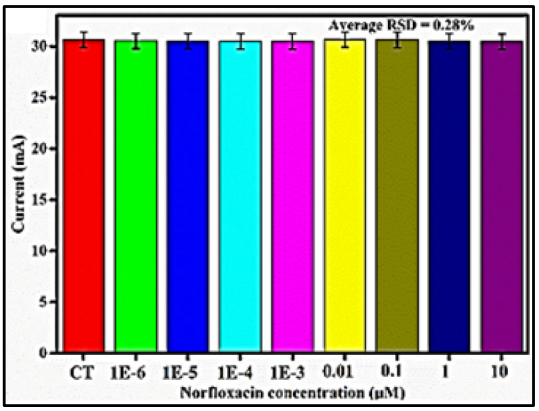

Fig. 35. Current response of NF at different concentration.

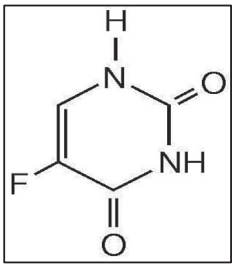

Fig. 36. Structure of 5-fluorouracil (5-FU).

Body fluids, including blood, sweat, tears, and the like, are important for monitoring the general health of people, as they carry vital signs (biomarkers) that indicate some diseases in a significant way. Besides, blood tests becoming clinically acceptable, sweat, tears, and urine fluids have recently attracted increased attention that can provide some solutions in health monitoring [115]. One downside is the poor clinical relationship between body fluids and blood; for this reason, these solutions are likely to take more time before being widely used.

Serotonin (5-HT, 5-hydroxytryptamine) (Fig. 44) a primary amino compound that is the 5-hydroxy derivative of tryptamine and is the production of chemical neurons, and it sends signals between nerve cells, and serotonin is often found in the digestive system, although it is also present in the blood platelets and the central nervous system [116]. It has a role as human, mouse metabolite, and neurotransmitter. It is a monoamine molecular messenger, a primary amino compound, a member of phenols, a member of hydroxyl indoles, and a member of tryptamines. Often low levels of 5-HT are correlated with diseases such as migraine headaches or depression, insomnia, anxiety, or obesity. A high level of 5-HT in the blood can lead to carcinoid syndrome in people with cancerous tumors [117].

Vilouras et al. [118] reported a GO-CH based chemiresistor for in-situ label-free electrochemical detections of 5-HT (Scheme 27). The sensor fabricated from Pt-electrodes patterned on GO-CH film with 2.5 μm thick. Cyclic voltammogram is used to determine 5-HT with different concentrations (0.2 μM to 2 mM) in Dulbecco's modified Eagle medium (DMEM), which showed a quasi-reversible redox with cathodic (I_{pc}) and anodic (I_{pa}) peak current at +400 mV and −300 mV, respectively.

9. Sensing of glucose as bioactive compound in serum

One of the main goals of sensors is to monitor the response of cells to different therapeutics and antibiotics drugs. It has been reported that glucose sensitivity of a glucose-oxidase hydrogel which is a catabolic enzyme with weak stability to reduce the substrate level, thus affecting cell metabolism [119,120]. Therefore, the ability of phenyl boronic acid (PBA, $C_6H_5B(OH)_2$) as a synthetic ligand to bond glucose in an aqueous medium with better recognition of its counterpart in small-scale bioreactors, has proven its application as a piece in glucose sensor technology. The main problem with using PBA to detect glucose is the necessity of measuring in the alkaline medium (pKa ~ 8.8). Hence, the combination of PBA with a definite functional grouping to work in physiological pH is one of the major successes of future development [121]. One expectation is the promotion of PBA by amino-group may lead to working at physiological pH. Hence the challenge has become to find a hydrogel system that responds only to changes in glucose concentration in physiological pH, pharmacokinetics is very similar to normal pancreatic activity, and without long-term toxic side effect.

New CH-based nano-hydrogel approaches have been used to design multifunctional biosensors with the purpose of determining glucose in physiological pH [122]. This approach includes the binding of 3-aminophenyl boronic acid onto CH-based nano-hydrogel using 3-aminopropyltriethoxy silane (3-APTES) or N-ethyl-carbodiimide

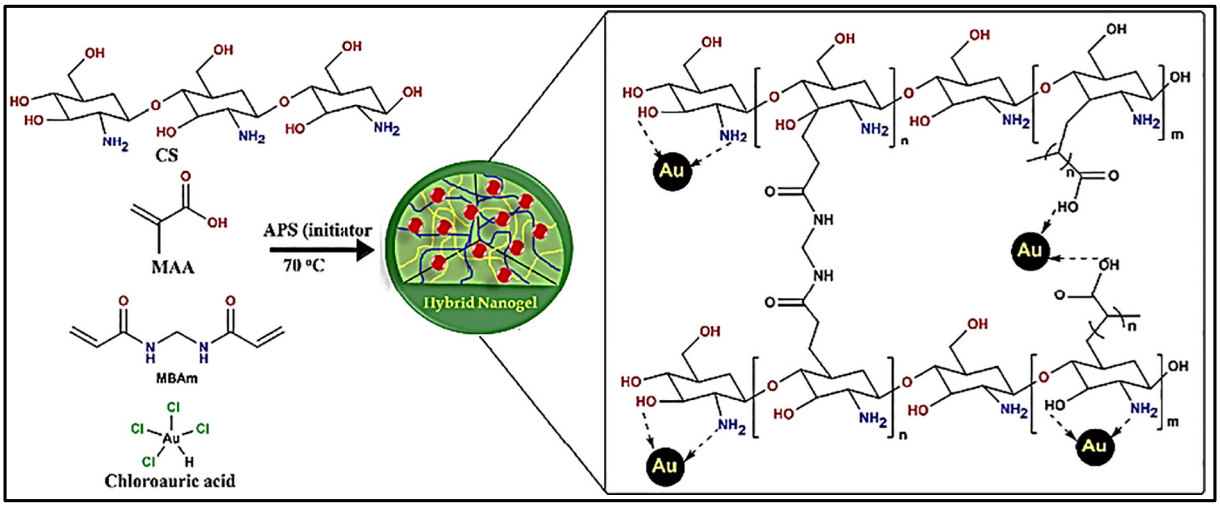

Scheme 18. Preparation of Au@CS-PMMA nanohydrogel.

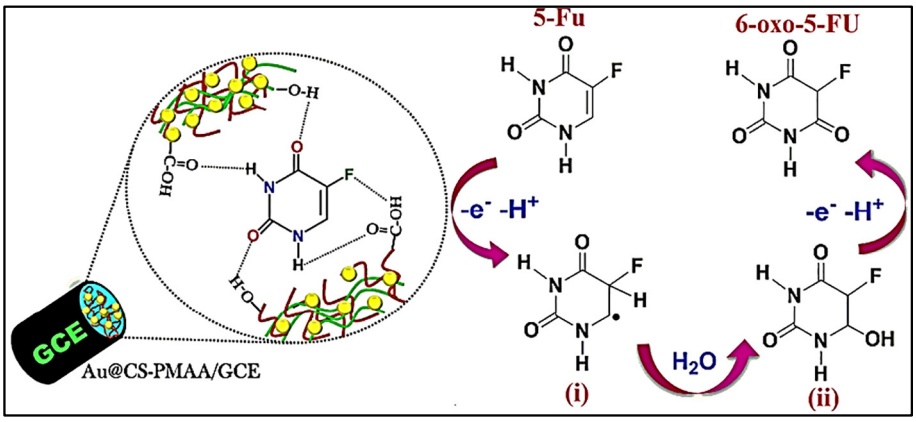

Scheme 19. Electrochemical oxidation mechanism of 5-FU at Au@CS-PMMA nanohydrogel surface.

hydrochloride (EDC) as a coupling agent (Scheme 28). Alizarin red (Fig. 45) ($C_{14}H_8O_4$, as a model drug) loading and release profile exhibited that the release of Alizarin red was faster in the presence of glucose, as a result of glucose competition for binding sites. The authors have believed, based on their findings, that the bioseparation of dyes containing Diols compositions, especially insulin-glycosylate drugs, may be linked to and released from the nanohydrogel in a manner similar to red alizarin.

Novel nanocomposite, AgNPs/NSC, that has a porous framework is fabricated by nitrogen- and sulfur-doped graphite carbon matrix (Scheme 29) [123]. The fabricated nanocomposite (AgNPs/NSC) was used as a non-enzymatic electrochemical sensor for glucose detection. The developed electrochemical sensor (AgNPs/NSC) showed an outstanding response towards glucose sensing as a result of the good conductivity, high surface area, and catalytic tendency. The fabricated glucose sensor is exhibited an excellent sensitivity ($35.2\ mA \cdot mM^{-1} \cdot cm^{-2}$) with a LOD of 0.046 mM, and 30 days durability. The presence of the nitrogen and sulfur heteroatoms alongside AgNPs in the carbon matrix enhanced the glucose selectivity (0.01 mM) in the presence of several interferences such as NaCl, dopamine (DA), ascorbic acid (AA), uric acid (UA), urea (UR) and other carbohydrate compounds.

Table 1
Optical density obtained by the SWTA using pAnti-stx2B-Ab and samples from 24 h culture of different strains in TSB culture medium.

Organisms	Optical density (450 nm)
E. coli O157:H7 EDL 933	0.436 ± 0.032
E. coli 8739 (non-pathogen)	0.036 ± 0.010
Pseudomonas putida CRDA V376	0.001 ± 0.029
Pseudomonas aeruginosa ATCC 15442	0.003 ± 0.025
Pseudomonas fluorescens CRDA V49	0.020 ± 0.012
Salmonella enterica serovar Typhi (ATCC® 19430)	0.133 ± 0.015
Salmonella Typhimurium SL 1344	0.098 ± 0.06
Salmonella enterica serovar Hadar (ATCC®51956™)	0.008 ± 0.007

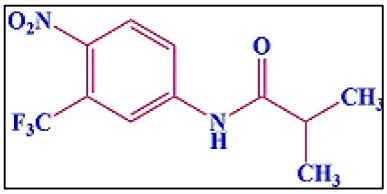

Fig. 37. Chemical structure of flutamide (FLU).

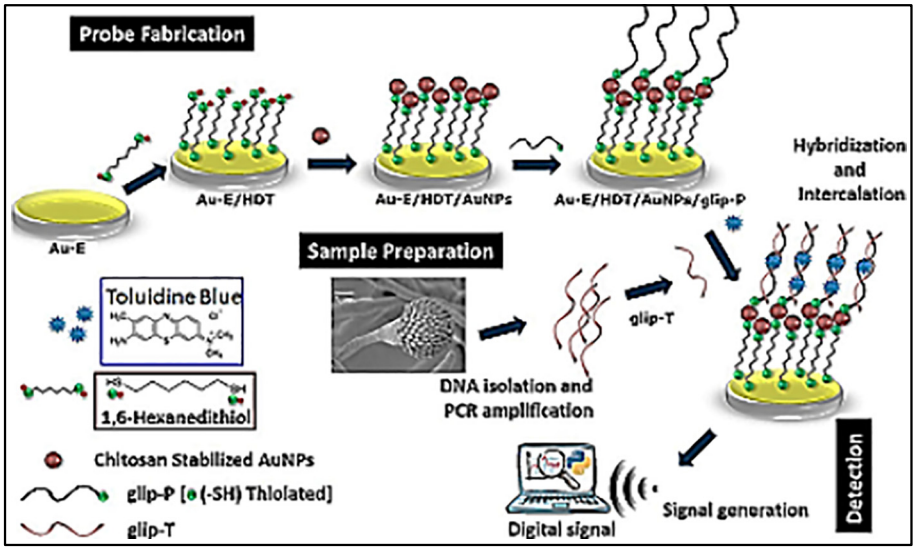

Scheme 20. Fabrication and detection process of glip-T biosensor.

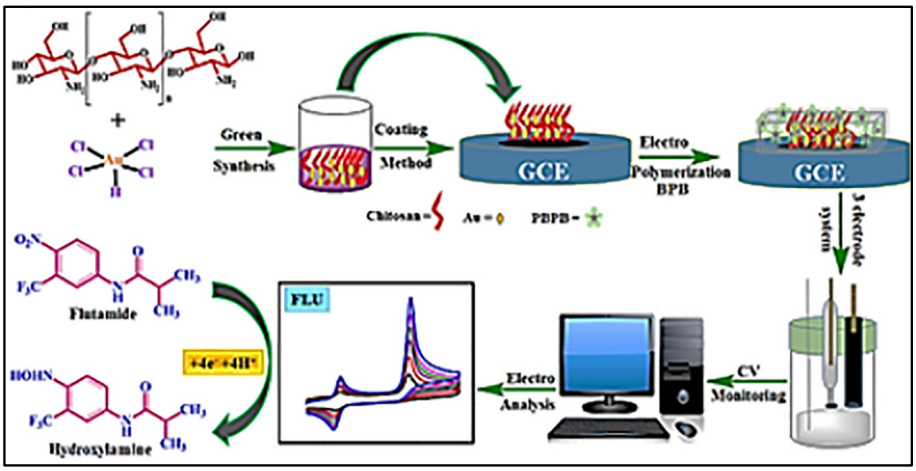

Scheme 21. Synthetic procedure of CS-AuCG/PBPB for the detection of FLU drug.

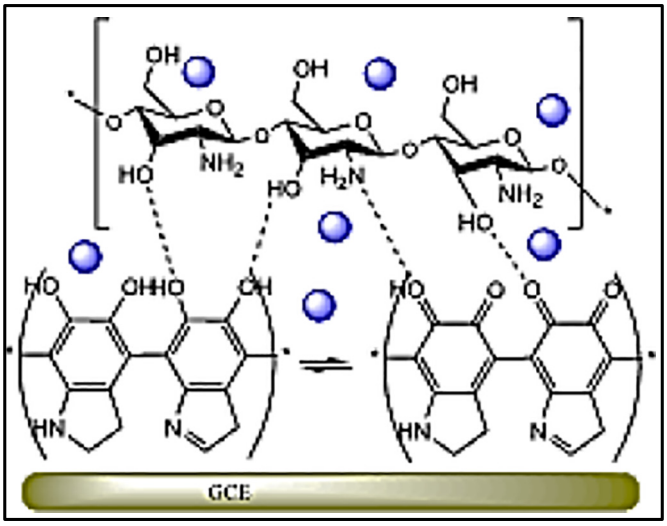

Scheme 22. Formation of POLY(DA-CS)/AgNPs.

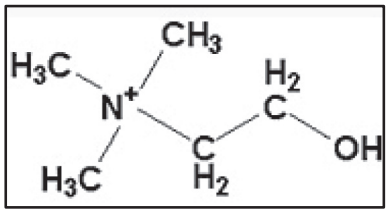

Fig. 38. Chemical structure of choline.

Alim et al. [124] designed selective enzymatic biosensor for glucose based on a polymerized-multiporous SnO_2 nanofibers/HRP (horse-radish peroxidase)/GO_x (glucose oxidase) onto glassy carbon electrode using CH. Electrospinning technique is used to synthesize SnO_2-multiporous nano-fibers (SnO_2-NFs) to obtain good electrical conductivity and considerable surface area. The SnO_2-NFs and polyaniline (PANI) is polymerized on SnO_2 using a chemical oxidation polymerization technique to obtain PANI-SnO_2-NF composite. Co-immobilization of GO_x and HRP on PANI-SnO_2-NF to modify the surface of the glassy carbon electrode using CH. The polymerized PANI-SnO_2-NF played a key role in facilitating the direct electron transfer between the electroactive center of the immobilized enzyme and the electrode surface. The PANI/SnO_2-NF/GO_x-HRP/CH/GC biosensor displayed a linear amperometric response (Fig. 46) towards the glucose concentration range from 5 to 100 μM with a LOD of 1.8 μM.

Fast optical and colorimetric sensor for the detection of glucose in aqueous solution is fabricated by [125]. Silver nanoparticles are dispersed on the surface of CH (CS/AgNCs) (Scheme 30). The surface plasmon resonance band at 429 nm is observed for CS/AgNCs, and this band began to disappear by the successive concentrations addition of glucose (the color changed from yellow to colorless). The most important benefits of this sensor are that it can be realized with the naked eye as well as UV–Vis spectrophotometer In the range of concentrations of 0–100 μM (Fig. 47), with LOD at 5 μM.

Asram et al. [126] constructed a novel impedimetric glucose biosensor based immobilization of glucose oxidase on CH modified nanostructured copper oxide (Nano-CuO) sputtered thin film on conductive fluorinated-tin oxide (FTO) layer (Scheme 31). Multi-layered FTO/Nano-CuO/CH/glucose oxidase biosensor provided excellent microenvironment for fast biocatalytic reaction to glucose. Surface morphology and CuO thin film roughness reveal nanocavities formation on the surface as a potent site for biosensitivity and a binding site for enzyme. FTO/Nano-CuO/CH/glucose oxidase was applied in glucose determination using the impedimetric technique, which displays high sensitivity for glucose (0.261 $k\Omega \cdot mM^{-1}$) with a LOD of 27 μM (Fig. 48).

GO_x-coated electrodes afford a suitable platform for enzymatic glucose sensing, induced by the presence of glucose oxidase and electrochemical transduction.

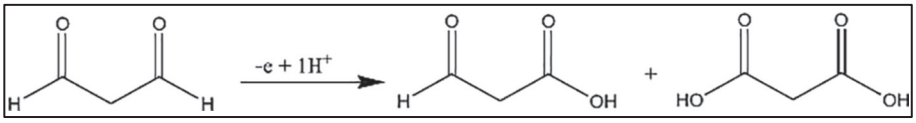

Scheme 23. Oxidation mechanism of MDA using poly(DA-CS)-AgNPs-GCE.

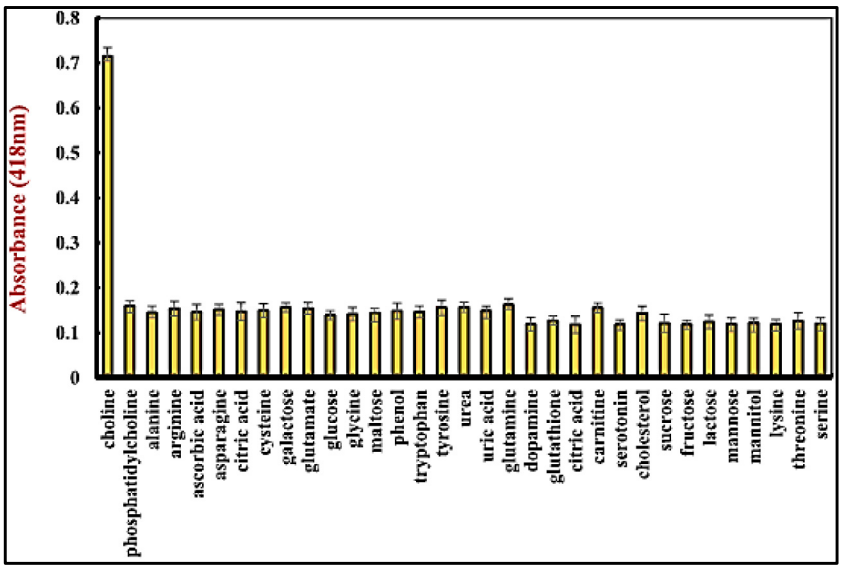

Fig. 39. Selectivity measurement of choline in the presence of interfering substances using the choline sensor.

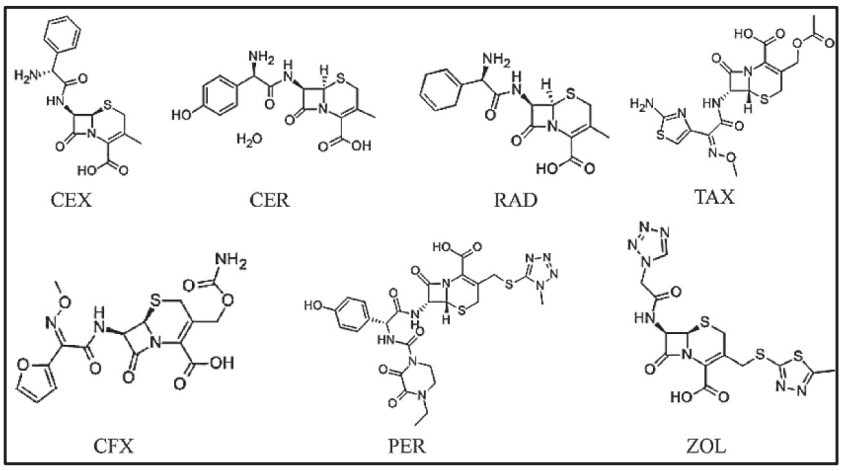

Fig. 40. Molecular structures of CEX, CER, RAD, TAX, CFX, PER, and ZOL.

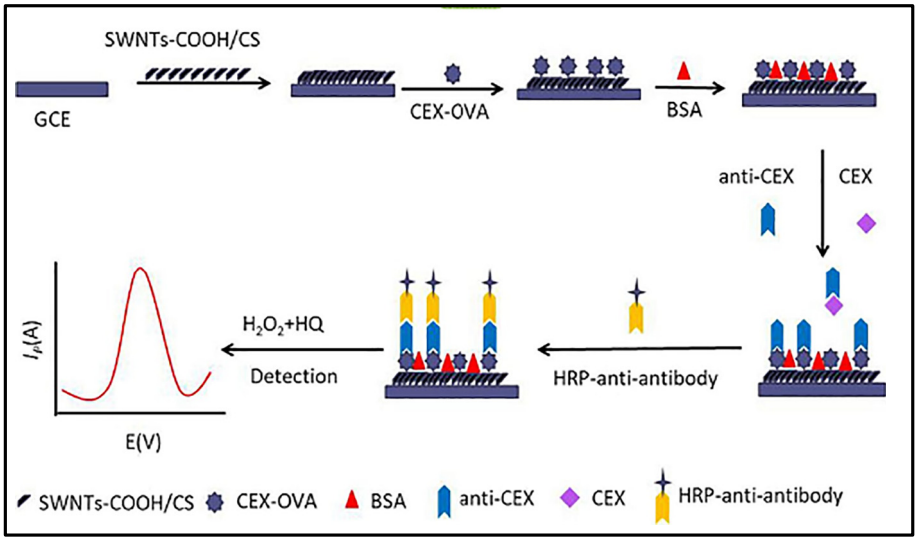

Scheme 24. Carboxylated single-walled carbon nanotube/chitosan (SWNTs-COOH/CS) composite modified on a glassy carbon electrode.

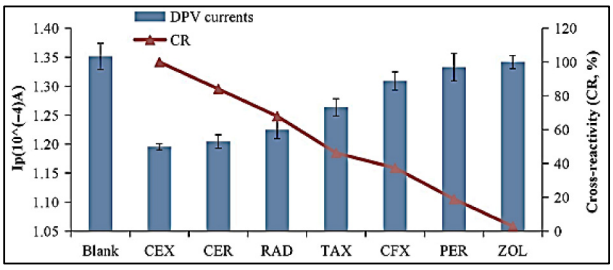

Fig. 41. Current response of the immunosensor to CEX, CER, RAD, TAX, CFX, PER, and ZOL at 200 μL, and the cross-reactivity (CR) of CEX to the six other cephalosporins.

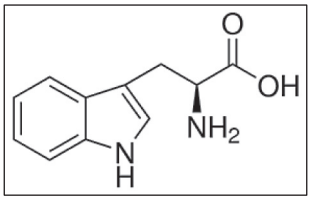

Fig. 42. Chemical structure of tryptophan.

Poletti et al. [127] showed high sensitivity of GO_x layers towards glucose detection when GO_x is blended with CH (GO_x + CH). Also, the sensitivity was increased eight times when GO_x is covalently bonded to chitosan (GO_x + CH). GO_x, in this case, can be used in its oxidized form, and no need to form reduced GO_x, as generally required for GO_x based coatings. GO_x + CH covalently bonded was achieved by carboxylic activation/amidation reaction of amino and carboxylic groups (Scheme 32). The GO-CH composite was deposited on standard screen-printed electrodes by a drop-casting approach. A comparison of chitosan-graphene and graphene alone showed the efficacy of the electrochemical response to glucose as there are a large number of enzyme binding sites as well as partial reduction of GO_x during the carboxylation step. Electrochemical measurements and comparisons were performed between GO_x + CH in each form of reduced GO_x, GO_x + CH in the blend, and covalently forms (Fig. 49a, b).

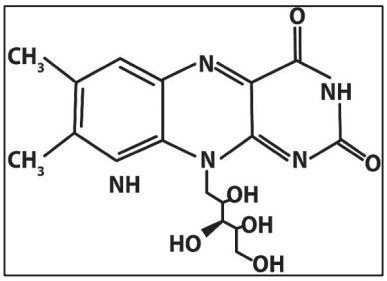

Fig. 43. Chemical structure of riboflavin.

Zhang et al. [128] provided an easy and effective way to prepare water-dispersible nitrogen-containing graphene-modifying CH materials using a one-step ball milling technology. The CH-graphene sensor showed a single-layer to the multilayered thickness and high catalytic activity for biosensors. In addition, the incorporate of Fe_3O_4 (magnetic nanoparticles) is also enhanced enzyme immobilization, electrochemical activity, additional to magnetic properties (Scheme 33). The presence of amino groups on the surface of graphene leads to an exceptional catalyst effect for the prepared electrochemical biosensors. The carboxylic group on the graphene surface enhanced the direct immobilization of glucose oxidase though covalent linkage while the

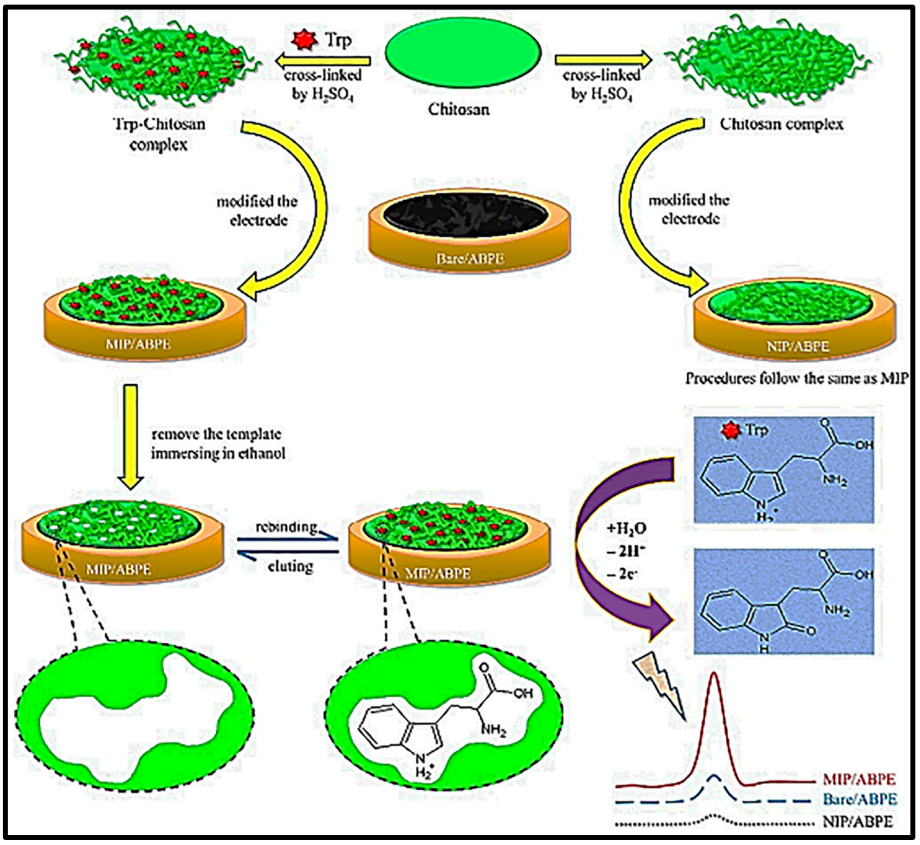

Scheme 25. Fabrication of molecularly imprinted polymers/acetylene black paste electrode.

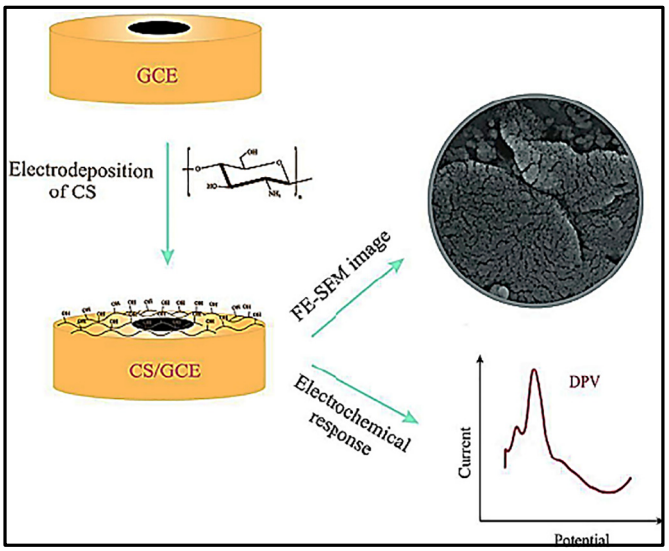

Scheme 26. Electro-deposition of chitosan on GCE surface using cyclic voltammetry technique.

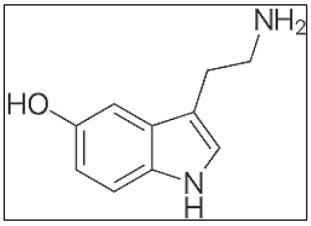

Fig. 44. Chemical structure of serotonin.

incorporation of Fe_3O_4 further facilitated enzyme loading and other properties. The resulting biosensor exhibits a glucose LOD of 16 μM. Formation of the multifunctional Fe_3O_4/CG nanocomposites provides additional advantages for applications in more clinical areas such as in-vivo biosensors.

10. Sensing of special medical compounds

Many analytical methods such as electrochemical [129], chemiluminescence [130], electro-chemiluminescence [131], fluorescence [132], field-effect transistor [133], surface plasmon resonance [134], enzyme-linked immunosorbent assays [135] and mass spectrometry [40,41] have been reported for PSA detection. These assays mostly depend on the use of antibodies as recognition elements. Despite the advantages of antibodies in the analysis of different proteins, modifying or preparing antibodies is still tricky, expensive, and time-consuming. It is an alternative and has some advantages is aptamers, which are oligonucleotide or peptide molecules that bind to a specific target molecule.

Jalalvand [136] designed a novel and efficient aptasensor based on immobilization of thiol terminated prostate-specific antigen (PSA) binding DNA aptamer onto AuNPs/fullerene C_{60}-CH-ionic liquid/MWCNTs/screen printed carbon electrode (Scheme 34) for ultrasensitive aptasensing of biomarker PSA. The formation of PSA-aptamer complex achieves a variation in EIS and DPV responses of the aptasensor, which enable to aptasensing of PSA by EIS and DPV methods. The designed aptasensor exhibited efficient anti-interference towards several biological compounds, sensitivity, and reproducibility.

The anticancer action of doxorubicin (DX) (Fig. 50) is associated with DNA damage by inhibition of topoisomerase II; however, the generation of free-radicals and quinone residue of DX undergo one-electron reduction at the *p*-quinone residue mediated by nicotinamide adenine dinucleotide phosphate (NADPH-CPR-CP450) where Cytochrome P450 reductase (CPR) causes one-electron transfer from NADPH to CP450. The semi-quinone radical generated by CPR reacts with O_2 to generate O_2^{-}• which is dissimulated to H_2O_2. The semi-quinone radical reacts with H_2O_2 to generate •OH that considered as DNA damage (Scheme 35).

Zangeneh et al. [137] developed a biosensor to monitor the DNA damage induced by DX but in the presence of Spinach extract as antioxidant. The authors modified GCE with MWCNTs, CH, followed by immobilization of Cytochrome P450 reductase (CPR) using glutaraldehyde as a crosslinker (CPRCP450/CH/MWCNTs/GCE). After that, DNA was gathered to the CPRCP450/CH/MWCNTs/GCE to fabricate the biosensor

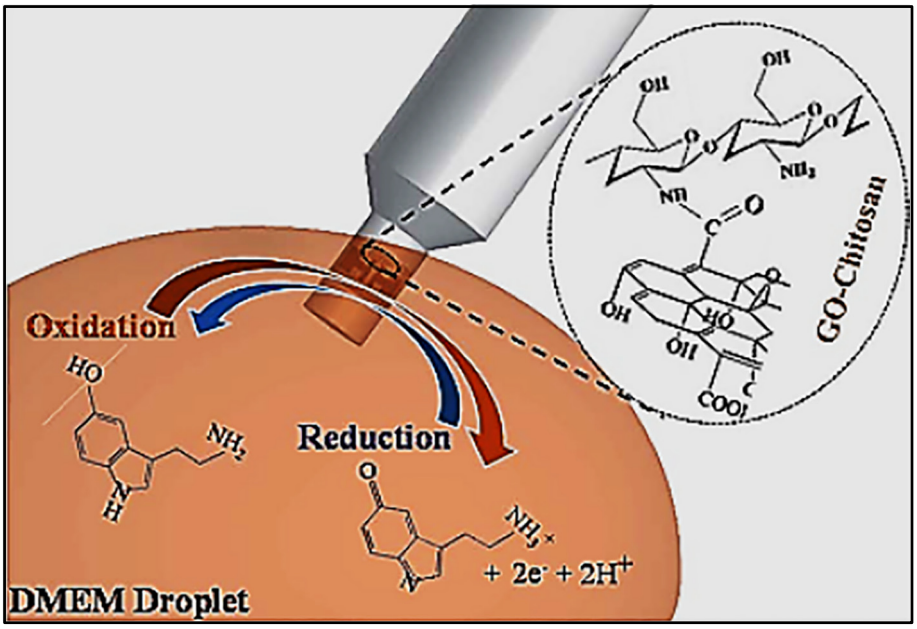

Scheme 27. GO-chitosan chemiresistor mounted on probe and redox reactions undergoing in a DMEM droplet.

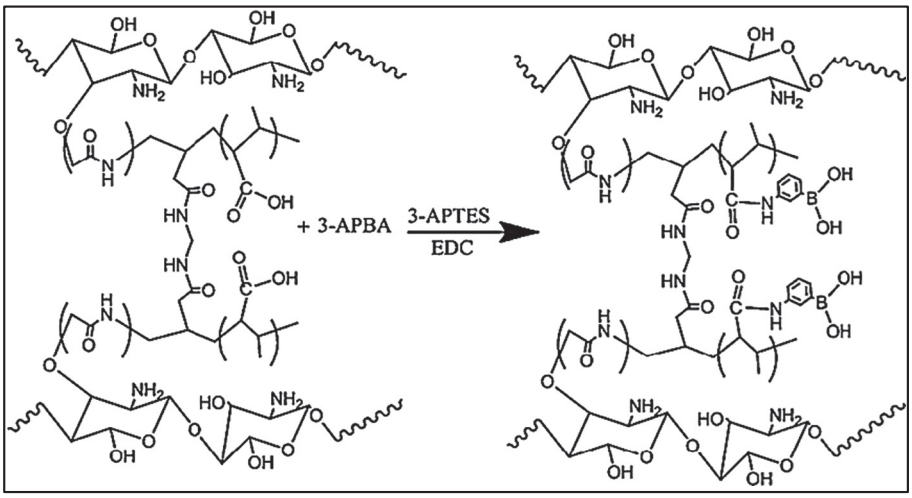

Scheme 28. Assembling of chitosan based nanohydrogel with 3-aminophenyl boronic acid (3-APBA).

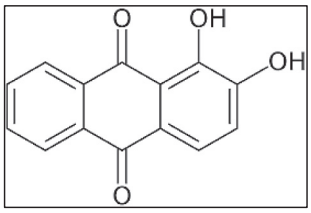

Fig. 45. Chemical structure of Alizarin dye.

(DNA/CPRCP450/CH/MWCNTs/GCE). DNA damage induced by DX is impedimetrically detected where the damaged DNA reduced the electrostatic repulsion of the negatively charged redox probe leading to decreasing the Rct (Fig. 51), as well as, an indirect determination of DX over a concentration range of 0.1–150 μM with a LOD of 0.05 μM is reported.

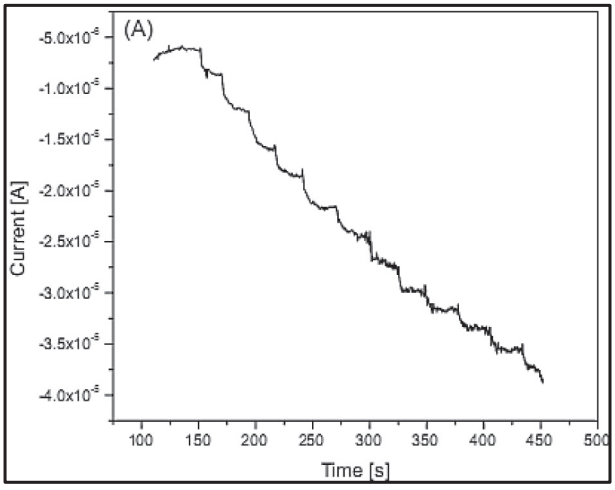

Fig. 46. Amperometric response of PANI/SnO_2-NF/GO_x-HRP/CH/GC glucose biosensor.

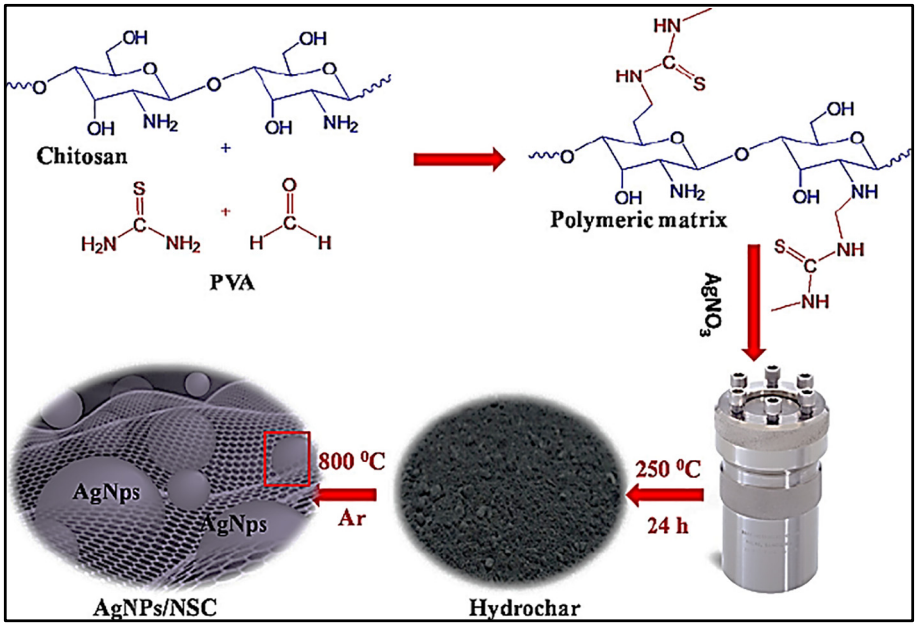

Scheme 29. Development of AgNPs/NSC glucose biosensor.

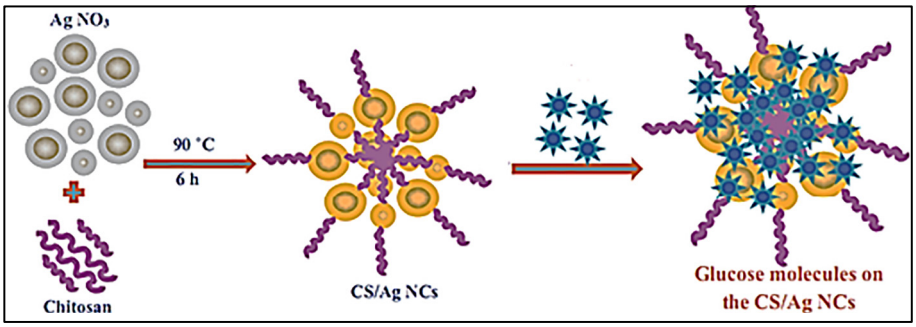

Scheme 30. Schematic representation for the synthesis of chitosan/silver nanocomposites and the addition of glucose molecules on CS/AgNCs.

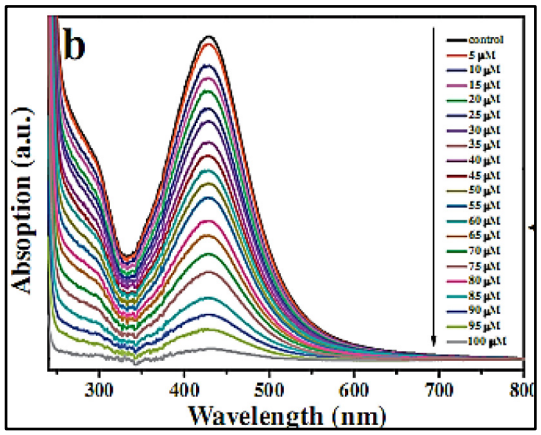

Fig. 47. UV–Vis spectrophotometric determination of glucose using CH/silver nanocomposites biosensor.

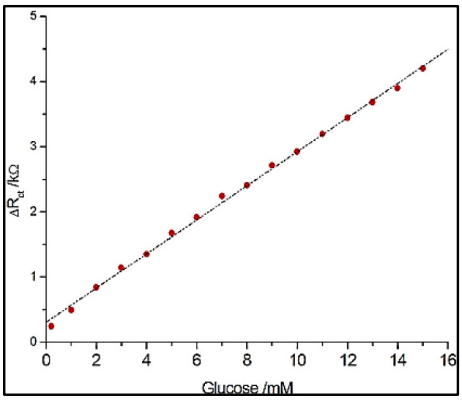

Fig. 48. The impedimetric determination of glucose using FTO/Nano-CuO/CH/glucose oxidase biosensor.

Carbohydrate antigen 15-3 (CA15-3) is a tumor marker that plays an important role in the diagnosis and screening for breast cancer. The serum CA15-3 level is below 30 U/mL for healthy individuals.

Hasanzadeh et al. [100–102] designed a new platform based on graphene quantum dots (GQD) GQD/Cys/AuNPs/CA15-3 antigen for detection of CA15-3 antibody in the human plasma sample. The sensitive label-free immunoassay based on gold nano-spear (AuNSs) electrochemically assembled onto cysteamine-graphene quantum dots (CysA/GQDs) (Scheme 36) to detect CA15-3 antibodies. CysA/AuNSs/GQDs hybrid provides a high surface area that enables the effective CA15-3 antigens immobilization, and enhance its bioactivity. Square wave voltammetry was employed to investigate the immunosensor and to monitor the binding of CA15-3 antigens-antibodies. The immunosensor showed a linear dynamic range of 0.16–125 U/mL and a LOD of 0.11 U/mL. The immunosensor was applied to analyze CA15-3 antibodies cell line lysates (breast adenocarcinoma cell line-MCF-7).

11. Mechanism of organic and inorganic analytes detection

The mechanism of the detection process of organic and inorganic compounds using chitosan or chemically modified chitosan as sensors is based mainly on the change in the optical or electrical properties of

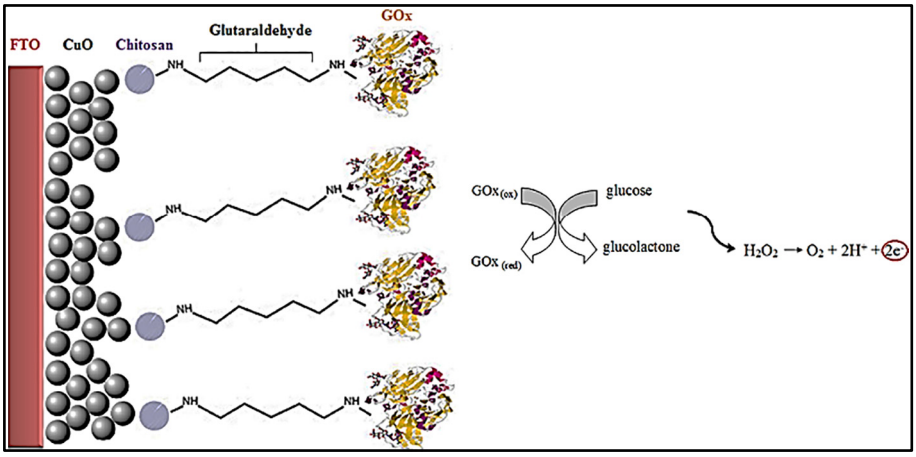

Scheme 31. Construction and glucose determination mechanism of FTO/Nano-CuO/CH/glucose oxidase biosensor.

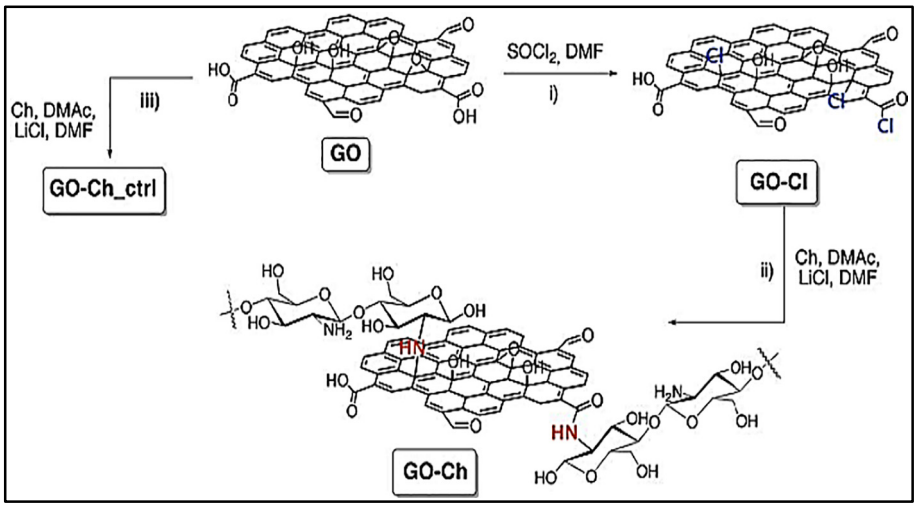

Scheme 32. Synthesis of GO—CH: (i) activation of carboxylic groups; (ii) coupling with the amine groups of CH; (iii) mix of CH and GO in DMF.

the chitosan. In electrochemical detection, electron transfer to or from the chitosan surface occurs. The transfer of electrons is mainly due to the oxidation-reduction reaction occurred on its surface. Electrochemically, the sensing process based on electric current exerted on the surface, and the response of the chitosan surface by the organic or inorganic compounds recorded. To explain the organic compounds sensing using a chitosan modified polymer, the detection of acetone illustrated. This illustration provides the fundamental description which explains the sensing mechanism of chitosan modified polymer towards acetone vapor. The oxygen is chemisorbed onto the surface of the chitosan particles when the sensor is exposed to air, Eq. (1). Under controlled input voltage, the number of free electrons moving randomly in the conduction band reduced as the chemisorbed oxygen traps them and transfers them from one particle to another. This results in an increase in the resistance and a decrease in the output voltage of the chitosan film until the saturation of oxygen species, as a result of no oxygen species will be formed again according to Eqs. (2), (3).

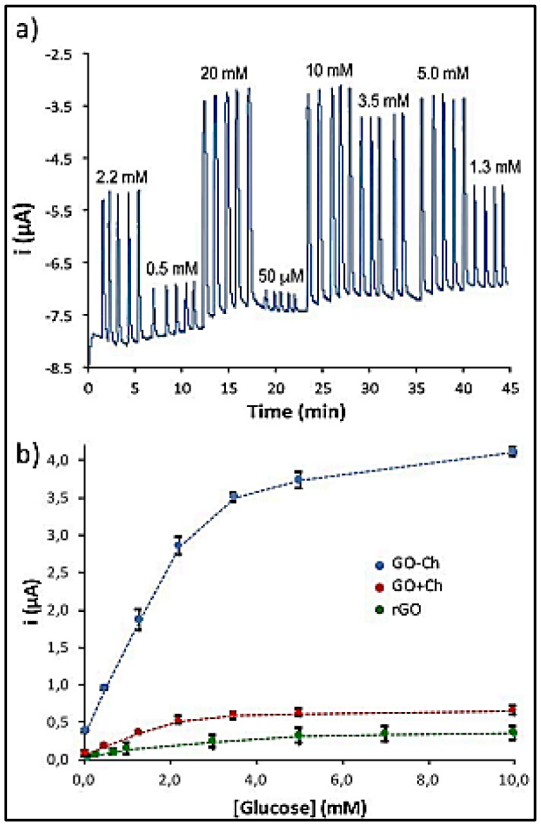

Fig. 49. (a) Amperometric response of GO-CH modified sensor at −0.4 V, (b) calibration plot of GO-CH modified sensor.

$$O_2\ (gas) \leftrightarrow O_2\ (absorbed) \quad (1)$$

$$O_2\ (absorbed) + e^- \leftrightarrow O_2^- \quad (2)$$

$$O_2^- + e^- \leftrightarrow 2O^- \quad (3)$$

This mechanism is generally describing the principles of organic compounds detection on the chitosan surface.

For inorganic (metal ions) detection by chitosan sensors, the detection mechanism mainly based on the oxidation-reduction of metal ions, and the output current is considered as an indication for the quantity or quality of the compounds under detection, as illustrated in Eqs. (4)–(6). At open circuit potential, adsorption of metal ions to chitosan surface occurs, Eq. (4).

$$Pb^{2+}{}_{(aq)} + CHN_{(surface)} \rightarrow Pb^{2+}{-}CHN_{(surface)} \quad (4)$$

The reduction of metal ions occurred at the chitosan surface at the potential of −1.0 V, Eq. (5).

$$Pb^{2+}{-}CHN_{(surface)} + 2e^- \rightarrow Pb^{o}{}_{(surface)} + CHN_{(surface)} \quad (5)$$

At electrical scanning of the chitosan sensor surface using potential range from −1.0 to 0.0 V, electric current is released, Eq. (6).

$$M^{o}{}_{(surface)} + CHN_{(surface)} \rightarrow M^{2+}{}_{(aq)} + CHN_{(surface)} + 2e^- \quad (6)$$

The quantity of released electrons (current density) is a useful indication for the concentration of the metal ion in the medium. While the potential of the reduction-oxidation process of the metal ion is a good detection for the type of this metal ion.

In the case of optical detection of contaminants (analytes), the change in the color of the sensor surface is a sufficient indicator for

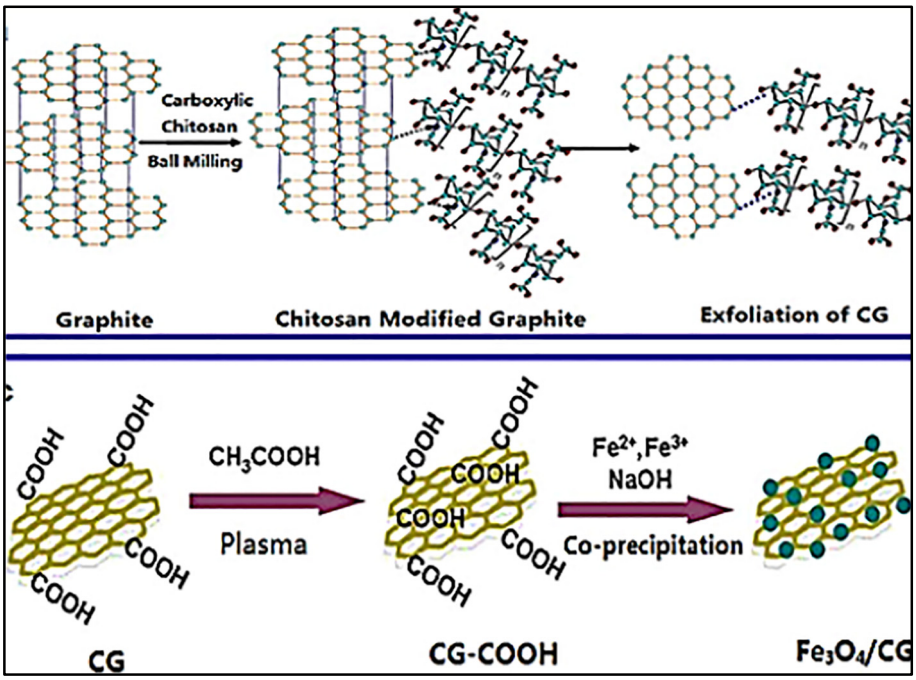

Scheme 33. Preparation of Fe_3O_4/CG nanocomposites.

the type of analytes in the medium. The nature of coordination between chitosan or modified chitosan sensors and the analytes in the medium is changed by changing the functional groups of each analyte. Furthermore, during the quantitative determination of the analytes, the color intensity is increased by increasing their concentration in the medium. The concentration of the analytes can be extracted from the formerly made calibration curve for each analyte.

The versatile applicability of chitosan polymer or its chemically modified forms came from the presence of numerous electron-donating functional groups within its segments. Furthermore, the introduction of electron-donating and electron-withdrawing groups to the chemical segments provides different centers for oxidation-reduction reactions with the easily adsorbed analytes on its surface.

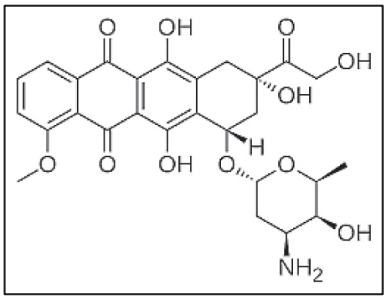

Fig. 50. Chemical structure of doxorubicin.

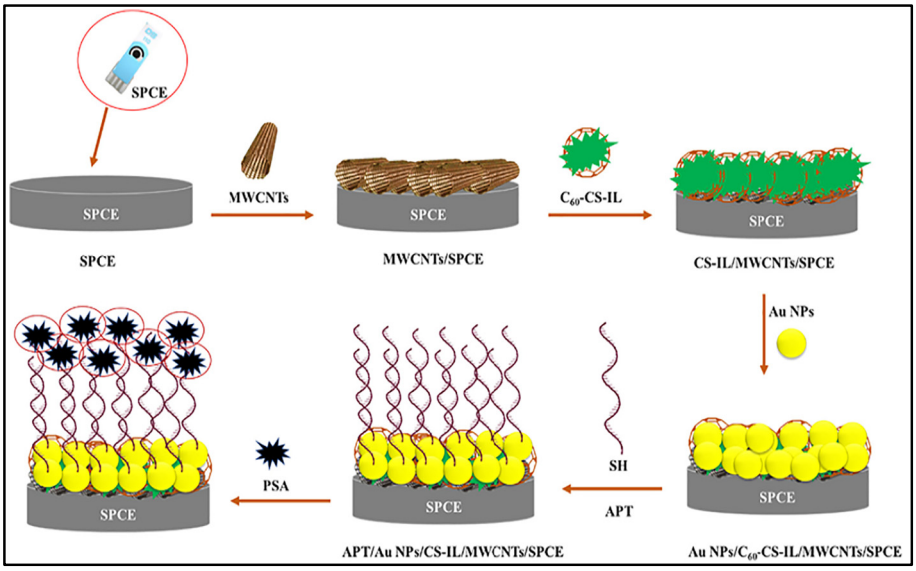

Scheme 34. Development of APT/AuNPs/C_{60}-CS-IL/MWCNTs/SPCE aptasensor.

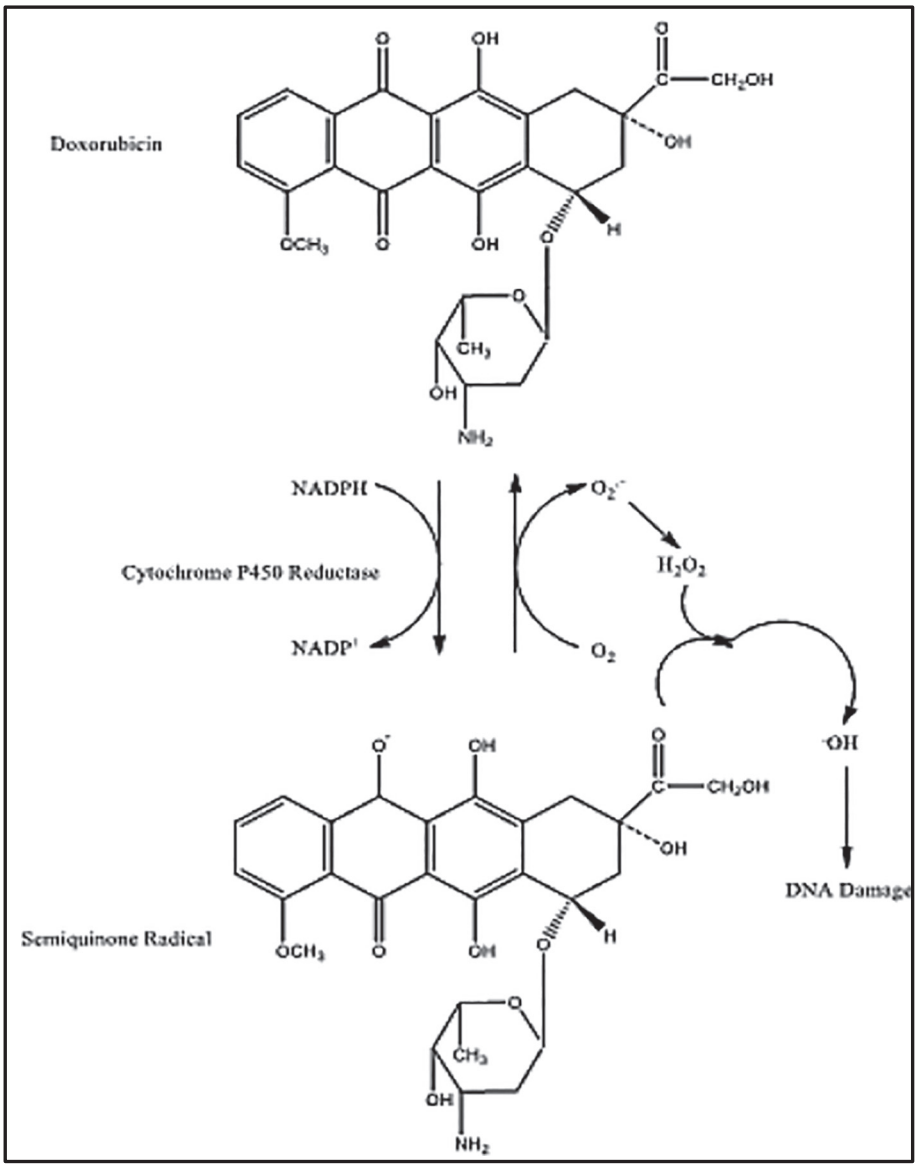

Scheme 35. Mechanism of induced damage of DNA by doxorubicin (DX).

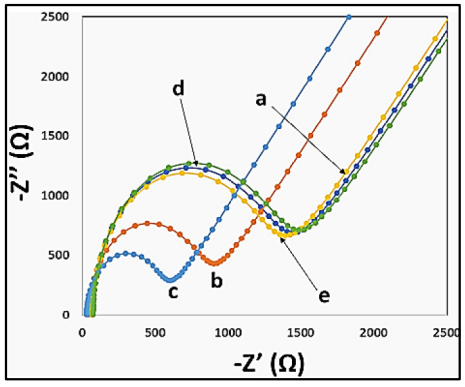

Fig. 51. EIS of DNA/CPRCP4-50/CH/MWCNTs/GCE in 5 mM $[Fe(CN)_6]^{3-/4-}$ immersed in (NADPH (2.0×10^{-3} M) + DX) solution and incubation for 8 min, a–c: 0.1×10^{-6} M, 5.0×10^{-6} M and 5.0×10^{-6} M DX, d–e: in 5, 10 ppm spinach extract.

CRediT authorship contribution statement

Nabel A. Negm: Conceptualization, Methodology, Writing - review & editing, Project administration.
Mohamed M. Betiha, **Ahmed Sadek**: Conceptualization, Methodology, Writing.
Ali A. Abd-Elaal: Validation and Investigation

Declaration of competing interest

Authors confirm that there is no conflict of interests in this work.

Acknowledgments

The work supported by Science, Technology & Innovation Funding Authority (ASRT) under a grant (ID: 6896).

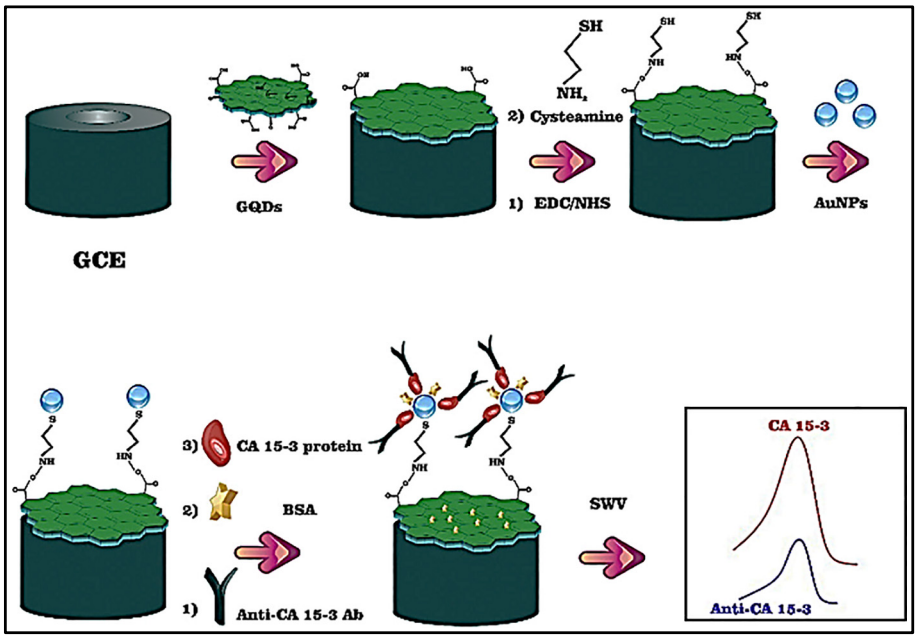

Scheme 36. Assembling of gold nanospear (AuNSs) on thiolated graphene quantum dots (CysA/GQDs).

References

[1] A. Baraketi, S. Auria, S. Shankar, C. Fraschini, S. Salmieri, J. Menissier, M. Lacroix, Novel spider web trap approach based on chitosan/cellulose nanocrystals/glycerol membrane for the detection of *Escherichia coli* O157:H7 on food surfaces, Int. J. Biol. Macromol. 146 (2020) 1009–1014.

[2] S. Chakraborty, A.P. Ilagan, Chitosan curcumin film as a sensor for detection of O-nitrophenol and fluoride ion using fluoresce quenching technique, Philippine Journal of Science 149 (2020) 27–33.

[3] C.S. Comino, I. Rassas, S. Minot, F. Bessueille, M.L.R. Mendez, A. Errachid, N.G. Renault, Voltammetric sensor based on electrodeposited molecularly imprinted chitosan f lm on BDD electrodes for catechol detection in buffer and in wine samples, Mater. Sci. Eng. C 110 (2020), 110667, .

[4] S. Hassanpour, A. Saadati, M. Hasanzadeh, Sensitive monitoring of riboflavin in commercial multivitamins using poly (chitosan)-based nanocomposite, J. Mol. Recognit. 33 (2020), e2817, .

[5] M.S. Alaejos, F.J.G. Montelongo, Chem. Rev. 104 (2004) 3239–3265.

[6] J. Li, J. Wang, L.G. Bachas, Anal. Chem. 74 (2002) 3336–3341.

[7] Y. Zou, C. Xiang, L.X. Sun, F. Xu, Biosens. Bioelectron. 23 (2008) 1010–1016.

[8] B. Krajewska, Application of chitin-and chitosan-based materials for enzyme immobilizations: a review, Enzym. Microb. Technol. 35 (2004) 126–139.

[9] S.K. Shukla, A.K. Mishra, in: S.B. Mishra (Ed.), Amorphous Materials: New Research, Nova Science Publishers, USA 2013, pp. 83–94.

[10] P. Linderholm, A. Bertsch, P. Renaud, Physiol. Meas. 23 (2004) 645–651.

[11] T. Godjevargova, K. Gabrovska, Macromol. Biosci. 5 (2005) 459–465.

[12] P.R. Leriao, L.J. Fonseca, M.A. Taipa, J.M. Cabral, M. Mateus, Appl. Biochem. Biotechnol. 110 (2003) 1–9.

[13] I. Yulianti, Detection of cadmium ion by evanescent wave based chitosan coated optical fiber sensor, 3rd International Conference on Mathematics, Science and Education, 2017.

[14] V.T. Tran, Liquid cladding mediated optical fiber sensors for copper ion detection, Micromachines (Basel) 9 (2018) 471–477.

[15] K. Bhavsar, Fiber optic sensor to detect heavy metal pollutants in water environments, OCEANS 2017, Aberdeen, 2017.

[16] N.M. Razali, Etched fiber Bragg grating sensor for nitrate sensing application, IEEE 7th International Conference on Photonics (ICP), 2018.

[17] M.S. Jadhav, Fluoride contamination sensor based on optical fiber grating technology, Opt. Fiber Technol. 38 (2017) 136–141.

[18] P. Chandra, W.C. Koh, H.B. Noh, Y.B. Shim, *In-vitro* monitoring of i-NOS concentrations with an immunosensor: the inhibitory effect of endocrine disruptors on i-NOS release, Biosens. Bioelectron. 32 (2012) 278–282.

[19] P. Chandra, P. Suman, H. Airon, M. Mukherjee, P. Kumar, Prospects and advancements in C-reactive protein detection, World J. Method 4 (2014) 1.

[20] R. Pallela, J. Venkatesan, I. Bhatnagar, Y. Shim, S. Kim, Applications of Marine Collagen-based Scaffolds in Bone Tissue Engineering, CRC Press, Boca Raton, FL, USA, 2013 519–528.

[21] S.K. Shukla, A.K. Mishra, O.A. Arotiba, B.B. Mamba, Chitosan-based nanomaterials: a state of the art review, Int. J. Biol. Macromol. 59 (2013) 46–58.

[22] P. Chandra, H.B. Noh, R. Pallela, Y.B. Shim, Ultrasensitive detection of drug resistant cancer cells in biological matrixes using an amperometric nanobiosensor, Biosens. Bioelectron. 70 (2015) 418–425.

[23] W.C. Koh, P. Chandra, D.M. Kim, Y.B. Shim, Electropolymerized self-assembled layer on gold nanoparticles: detection of inducible nitric oxide synthase in neuronal cell culture, Anal. Chem. 83 (2011) 6177–6183.

[24] W. Suginta, P. Khunkaewla, A. Schulte, Electrochemical biosensor applications of polysaccharides chitin and chitosan, Chem. Rev. 113 (2013) 5458–5479.

[25] S.K. Yadav, P. Chandra, R.N. Goyal, Y.B. Shim, A review on determination of steroids in biological samples exploiting nanobio-electroanalytical methods, Anal. Chim. Acta 762 (2013) 14–24.

[26] Y. Zhu, P. Chandra, Y.B. Shim, Ultrasensitive and selective electrochemical diagnosis of breast cancer based on a hydrazine-Au nanoparticle-aptamer bioconjugate, Anal. Chem. 85 (2012) 1058–1064.

[27] P. Chandra, J. Singh, A. Singh, A. Srivastava, R.N. Goyal, Y.B. Shim, Gold nanoparticles and nanocomposites in clinical diagnostics using electrochemical methods, J. Nanoparticles 2013 (2013).

[28] F. Lima, B.G. Lucca, A.M. Barbosa, V.S. Ferreira, S.K. Moccelini, A.C. Franzoi, I.C. Vieira, Biosensor based on pequi polyphenol oxidase immobilized on chitosan crosslinked with cyanuric chloride for thiodicarb determination, Enzym. Microb. Technol. 47 (2010) 153–158.

[29] S.C. Fernandes, I.R. Oliveira, O.F. Filho, A. Spinelli, I.C. Vieira, Biosensor based on laccase immobilized on microspheres of chitosan crosslinked with tripolyphosphate, Sens. Actuators B: Chem. 133 (2008) 202–207.

[30] R. Pauliukaite, M.E. Ghica, O.F. Filho, C.M. Brett, Electrochemical impedance studies of chitosan-modified electrodes for application in electrochemical sensors and biosensors, Electrochim. Acta 55 (2010) 6239–6247.

[31] C. Lao, Z. Zeledon, X. Gamisans, M. Sole, Sorption of Cd(II) and Pb(II) from aqueous by a low-rank coal (leonardite), Separat. Purificat. Technol. 45 (2005) 79–85.

[32] R.W. Rousseau, Handbook of Separation Process Technology, Wiley, New York, 1987.

[33] N.M. Razali, N.F.A. Zaidi, P.N. Jaafar, A. Hamzah, F. Ahmad, S. Ambran, AIP Conference Proceedings 2203 (2020), 020035, .

[34] N. Kocak, M. Sahin, S. Kücükkolbasi, Z. Erdogan, Synthesis and characterization of novel nano-chitosan Schiff base and use of Pb(II) sensor, Int. J. Biol. Macromol. 51 (2012) 1159–1166.

[35] E.A.K. Nivethaa, S. Dhanavel, V. Narayanan, A. Stephen, Chitosan stabilized Ag-Au nano-alloy for colorimetric sensing and 5-fluorouracil delivery, Int. J. Biol. Macromol. 95 (2017) 862–872.

[36] T. Priya, N. Dhanalakshmi, N. Thinakaran, Electrochemical behavior of Pb(II) on a heparin modified chitosan/graphene nanocomposite film coated glassy carbon electrode and its sensitive detection, Int. J. Biol. Macromol. 104 ((2017) 672–680.

[37] S. Kucukkolbasi, Z.O. Erdogan, J. Barek, M. Sahin, N. Kocak, A novel chitosan nanoparticle-Schiff base modified carbon paste electrode as a sensor for the determination of Pb(II) in waste water, Int. J. Electrochem. Sci. 8 (2013) 2164–2181.

[38] M.M. Abdi, L.C. Abdullah, A.R. Sadrolhosseini, W.M. Yunus, M.M. Moksin, P.M. Tahir, Surface plasmon resonance sensing detection of mercury and lead ions based on conducting polymer composite, PLoS One 6 (2011), e24578, .

[39] L.H. Junior, B.C. Janegitz, B.C. Lourencao, O.F. Filho, Anodic stripping voltammetric determination of mercury in water using a chitosan-modified carbon paste electrode, Anal. Lett. 40 (2007) 3119–3128.

[40] Y.T. Chen, L.P. Tuan, H.W. Chen, I.A. Wei, M.Y. Chou, H.M. Chen, Y.C. Tyan, S.F. Chen, Quantitative analysis of prostate specific antigen isoforms using

immunoprecipitation and stable ih sotope labeling mass spectrometry, Anal. Chem. 87 (2015) 545–553.
[41] Z. Chen, C. Zhang, Y. Tan, T. Zhou, H. Ma, C. Wan, Y. Lin, K. Li, Chitosan-functionalized gold nanoparticles for colorimetric detection of mercury ions based on chelation-induced aggregation, Microchim. Acta 182 (2015) 611–616.
[42] S. Liu, M. Kang, F. Yan, D. Peng, Y. Yang, L. He, M. Wang, S. Fang, Z. Zhang, Electrochemical DNA biosensor based on microspheres of cuprous oxide and nanochitosan for Hg(II) detection, Electrochim. Acta 160 (2015) 64–73.
[43] B.C. Janegitz, L.C. Filho, L.H. Marcolino, S.P. Souza, E.R. Pereira, O.F. Filho, Development of a carbon nanotubes paste electrode modified with crosslinked chitosan for cadmium(II) and mercury(II) determination, J. Electroanal. Chem. 660 (2011) 209–216.
[44] H.M. Lee, M.H. Kim, Y. Yoon, W.H. Park, Fluorescent property of chitosan oligomer and its application as a metal ion sensor, Marine Drugs 15 (2017) 105–123.
[45] V.K. Singh, C.S. Kushwaha, S.K. Shukla, Potentiometric detection of copper ion using chitin grafted poly aniline electrode, Int. J. Biol. Macromol. 147 (2020) 250–257.
[46] T.V. Duncan, Applications of nanotechnology in food packaging and food safety: barrier materials, antimicrobials and sensors, J. Colloid Interface Sci. 363 (2011) 1–24.
[47] H.S. Mader, O.S. Wolfbeis, Optical ammonia sensor based on up converting luminescent nanoparticles, Anal. Chem. 82 (2010) 5002–5004.
[48] I.M. El-Sherbiny, A. Hefnawy, E. Salih, New core-shell hyperbranched chitosan-based nanoparticles as optical sensor for ammonia detection, Int. J. Biol. Macromol. 86 (2016) 782–788.
[49] F.E. Tirtashi, M. Moradi, H. Tajik, M. Forough, P. Ezati, B. Kuswandi, Cellulose/chitosan pH-responsive indicator incorporated with carrot anthocyanins for intelligent food packaging, Int. J. Biol. Macromol. 136 (2019) 920–926.
[50] A.B. Abou Hammad, A.M. Elnahrawy, A.M. Youssef, A.M. Youssef, Sol-gel synthesis of hybrid chitosan/calcium aluminosilicate nanocomposite membranes and its application as support for CO_2 sensor, Int. J. Biol. Macromol. 125 (2019) 503–509.
[51] E. Pashai, G.N. Darzi, M. Jahanshahi, F. Yazdian, M. Rahimnejad, An electrochemical nitric oxide biosensor based on immobilized cytochrome-c on chitosan-gold nanocomposite modified gold electrode, Int. J. Biol. Macromol. 108 (2018) 250–258.
[52] O. Sisman, N. Kaur, G. Sberveglieri, E.N. Carmona, V. Sberveglieri, E. Comini, UV-enhanced humidity sensing of chitosan-SnO_2 hybrid nanowires, Nanomaterials 10 (2020) 329–339.
[53] A. Bouvree, J.F. Feller, M. Castro, Y. Grohens, M. Rinaudo, Conductive polymer nano-biocomposites (CPC): chitosan-carbon nanoparticle a good candidate to design polar vapor sensors, Sens. Actuators B Chem. 138 (2009) 138–147.
[54] J. Zou, K. Zhang, Q. Zhang, Giant humidity response using a chitosan-based protonic conductive sensor, IEEE Sensors J. 16 (2016) 8884–8889.
[55] K. Gabrovska, J. Ivanov, I. Vasileva, N. Dimova, T. Godjevargova, Immobilization of urease on nanostructured polymer membrane and preparation of urea amperometric biosensor, Int. J. Biol. Macromol. 48 (2011) 620–626.
[56] A. Mulyasuryani, A. Roosdiana, A. Srihardyastutie, The potentiometric urea biosensor using chitosan membrane, Indonesian Journal Chemistry 10 (2010) 162–166.
[57] T. Tang, S. Cao, C. Xi, X. Li, L. Zhang, G. Wang, Z. Chen, Chitosan functionalized magnetic graphene oxide nanocomposite for the sensitive and effective determination of alkaloids in hotpot, Int. J. Biol. Macromol. 146 (2020) 343–352.
[58] A.K. Sharma, B.S. Kaith, I. Priya, Chemically modified chitosan-sodium alginate as chemosensor adsorbent for the detection of picric acid and removal of biebrich scarlet, Int. J. Biol. Macromol. 147 (2020) 582–594.
[59] E.M. Bakhsh, F. Ali, S.B. Khan, H. Marwani, E.Y. Danish, A.M. Asiri, Copper nanoparticles embedded chitosan for efficient detection and reduction of nitroaniline, Int. J. Biol. Macromol. 131 (2019) 666–675.
[60] C.T. Wang, W.L. Chou, Y.M. Kuo, F.L. Chang, Paired removal of color and COD from textile dyeing wastewater by simultaneous anodic and indirect cathodic oxidation, J. Hazard. Mater. 169 (2009) 16–22.
[61] P.A. Soloman, C.A. Basha, M. Velan, B. Subramania, Electro oxidation of malachite green and modeling using ANN, Chem. Biochem. Eng. Q. 24 (2010) 445–452.
[62] S. Srivastava, R. Sinha, D. Roy, Toxicological effects of malachite green, Aquat. Toxicol. 66 (2004) 319–329.
[63] Y.A. Evcimen, W.S. Breitbart, Ifosfamide neuropsy-chiatric toxicity in patients with cancer, Psycho. Oncology 16 (2007) 956–960.
[64] A.R. Sadrolhosseini, M.A. Mahdi, P.M. Nia, S. Shafie, K. Shameli, Polypyrrole-chitosan-$CaFe_2O_4$ layer sensor for detection of anionic and cationic dye using surface plasmon resonance, International Journal of Polymer Science (2020), 3489509, https://doi.org/10.1155/2020/3489509.
[65] A.Y. Mironenko, A.A. Sergeev, A.E. Nazirov, S.S. Voznesenskiy, S.Y. Bratskaya, A.G. Mirochnik, Highly sensitive chitosan-based optical fluorescent sensor for gaseous methyl amine detection, Progress on Chemistry and Application of Chitin and its Derivatives 22 (2017) 159–165.
[66] R. Kato, H. Akamatsu, T. Hattori, Preparation of chitosan derivatives with chromophores for optically sensing inorganic anions and carboxylates, Anal. Lett. 49 (2016) 744–752.
[67] Y. Li, X. Zhai, X. Liu, L. Wang, H. Liu, H. Wang, Electrochemical determination of bisphenol-A at ordered mesoporous carbon modified nano-carbon ionic liquid paste electrode, Talanta 148 (2016) 362–369.
[68] B. Su, H. Shao, N. Li, X. Chen, Z. Cai, X. Chen, A sensitive bisphenol A voltammetric sensor relying on AuPd nanoparticles/graphene composites modified glassy carbon electrode, Talanta 166 (2017) 126–132.
[69] P. Jing, X. Zhang, Z. Wu, L. Bao, Y. Xu, C. Liang, W. Cao, Electrochemical sensing of bisphenol-A by graphene-1-butyl-3-methyl imidazolium hexafluorophosphate modified electrode, Talanta 141 (2015) 41–46.
[70] K. Huang, Y. Liu, Y. Liu, L. Wang, Molybdenum disulfide nanoflower-chitosan-Au nanoparticles composites based electrochemical sensing platform for bisphenol-A determination, J. Hazard. Mater. 276 (2014) 207–215.
[71] S.H. Huang, Y.C. Shih, C.Y. Wu, C.J. Yuan, Y.S. Yang, Y.K. Li, T.K. Wu, Biosens. Bioelectron. 19 (2004) 1627–1633.
[72] R.L. Wortmann, E. Braunwald, A.S. Fauci, D.L. Kasper, S.L. Hauser, D.L. Longo, J.L. Jameson, Development and analytical application uric acid biosensor, Harrison's Principles of Internal Medicine, 15th edn McGraw-Hill, New York, 2001.
[73] U.M. Khosla, S. Zharikov, J.L. Finch, T. Nakagawa, C. Roncal, W. Mu, J.F. Baker, E. Krishnan, L. Chen, H.R. Schumacher, Am. J. Med. 118 (2005) 816–826.
[74] H.J. Moallem, G. Taningo, C.K. Jiang, R. Hishhorn, S. Fikrig, Clin. Immunol. 105 (2002) 75–80.
[75] A. Meister, D. Dolphin, R. Poulson, O. Avramovic, Glutathione: Chemical, Biochemical and Medical Aspects, Part A, Wiley-Interscience Publication, New York, 1989 367–434.
[76] T. Ohkuwa, Y. Sata, M. Naoi, J. Chromatogr. B 705 (1998) 23–28.
[77] A. Meister, M.E. Anderson, Annu. Rev. Biochem. 52 (1983) 711–760.
[78] E. Obrador, J. Carretero, A. Ortega, I. Medina, V. Rodilla, J.A. Pellicer, J.M. Strela, Hepatology 35 (2002) 74–81.
[79] P.K. Sudeep, S.T.S. Joseph, K.G. Thomas, J. Am. Chem. Soc. 127 (2005) 6516–6517.
[80] N. Chauhan, J. Narang, C.S. Pundir, An amperometric glutathione biosensor based on chitosan-iron coated gold nanoparticles modified Pt-electrode, Int. J. Biol. Macromol. 51 (2012) 879–886.
[81] L. Sibulesky, K.C. Hayes, A. Pronczuk, C.W. DiFranco, B. Rosner, E.L. Berson, Safety of vitamin-A daily in adults with retinitis pigmentosa, Am. J. Clin. Nutr. 69 (1999) 656–663.
[82] B.G. Nordestgaard, M. Benn, P. Schnohr, A. Tybjaerg-Hansen, Non-fasting triglycerides and risk of myocardial infarction, ischemic heart disease, and death in men and women, J. Am. Med. Assoc. 298 (2007) 299–308.
[83] J. Narang, N. Chauhan, C.S. Pundir, Construction of triglyceride biosensor based on nickel oxide-chitosan/zinc oxide/zinc hexacyanoferrate film, Int. J. Biol. Macromol. 60 (2013) 45–51.
[84] S.S. Kumar, J. Mathiyarasu, K. Lakshminaraha Phani, J. Electroanal. Chem. 578 (2005) 95–103.
[85] T. Luczak, Electrochim. Acta 53 (2008) 5725–5731.
[86] X. Zhou, N. Zheng, S.H. Hou, X.J. Li, Z.B. Yuan, J. Electroanal. Chem. 642 (2010) 31–34.
[87] Q. Liu, X. Zhu, Z. Huo, X. He, Y. Liang, M. Xu, Talanta 97 (2012) 557–562.
[88] M.H. Mashhadizadeh, T. Yousefia, A.N. Golikand, Electrochim. Acta 59 (2012) 321–328.
[89] K. Pandiselvi, S. Thambidurai, Chitosan-ZnO/polyanilne nanocomposite modified glassy carbon electrode for selective detection of dopamine, Int. J. Biol. Macromol. 67 (2014) 270–278.
[90] C. Tong, G. Xiang, Sensitive determination of norfloxacin by the fluorescence probe of terbium (III)-sodium dodecyl benzene sulfonate and its luminescence mechanism, J. Fluoresc. 16 (2006) 831–837.
[91] Y. Ni, Y. Wang, S. Kokot, Multicomponent kinetic spectrophotometric determination of pefloxacin and norfloxacin in pharmaceutical preparations and human plasma samples with the aid of chemometrics, Spectrochim. Acta A Mol. Biomol. Spectrosc. 70 (2008) 1049–1059.
[92] G.H. Wan, H. Cui, Y.L. Pan, P. Zheng, L.J. Liu, Determination of quinolones residues in prawn using high-performance liquid chromatography with Ce(IV)-Ru (bpy^{32+})-HNO_3 chemiluminescence detection, J. Chromatogr. B843 (2006) 1–9.
[93] A.K. Yadav, T.K. Dhiman, G.B. Lakshmi, A.N. Berlina, P.R. Solanki, A highly sensitive label-free amperometric biosensor for norfloxacin detection based on chitosan-yttria nanocomposite, Int. J. Biol. Macromol. 151 (2020) 566–575.
[94] S.K. Vishnu, P. Ranganathan, S.P. Rwei, C. Pattamaprom, T. Kavitha, P. Sarojini, New reductant free synthesis of gold nanoparticles doped chitosan-based semi-IPN nanogel: a robust nanoreactor for exclusively sensitive 5-fluoro uracil sensor, Int. J. Biol. Macromol. 148 (2020) 79–88.
[95] I. Bhatnagar, K. Mahato, K.K.R. Ealla, A. Asthana, P. Chandra, Chitosan stabilized gold nanoparticle mediated self-assembled gliP nanobiosensor for diagnosis of invasive Aspergillosis, Int. J. Biol. Macromol. 110 (2018) 449–456.
[96] Z. Rezaeifar, G.H. Rounaghi, Z. Eshaghi, M. Chamsaz, Electrochemical determination of anticancer drug, flutamide in human plasma sample using a microfabricated sensor based on hyperbranched polyglycerol modified graphene oxide reinforced hollow fiber graphite electrode, Mater. Sci. Eng. C 91 (2018) 10–18.
[97] S.S. Viera, S.M. Esponda, Z.S. Ferrera, J.J. Rodriguez, Cytostatic drugs in environmental samples: an update on the extraction and determination procedures, Trends Anal. Chem. 80 (2016) 373–386.
[98] L. Svorc, K. Borovska, K. Cinkova, D.M. Stankovic, A. Plankova, Advanced electrochemical platform for determination of cytostatic drug flutamide in various matrices using a boron-doped diamond electrode, Electrochim. Acta 251 (2017) 621–630.
[99] B. Mutharani, P. Ranganathan, S.M. Chen, Chitosan-gold collapse gel/poly (bromophenol blue) redox-active film. A perspective for selective electrochemical sensing of flutamide, Int. J. Biol. Macromol. 124 (2019) 759–770.
[100] M. Hasanzadeh, P. Babaie, V. Gharamaleki, A. Jouyban, The use of chitosan as a bioactive polysaccharide in non-invasive detection of malondialdehyde biomarker in human exhaled breath condensate: a new platform towards diagnosis of some lung disease, Int. J. Biol. Macromol. 120 ((2018) 2482–2492.
[101] M. Hasanzadeh, A. Mohammadzadeh, M. Jafari, B. Habibi, Ultrasensitive immunoassay of glycoprotein 125 (CA125) in untreated human plasma samples using poly(CTAB-chitosan) doped with silver nanoparticles, Int. J. Biol. Macromol. 120 (2018) 2048–2064.

[102] M. Hasanzadeh, S. Tagi, E. Solhi, A. Mokhtarzadeh, N. Shadjou, A. Eftekhari, S. Mahboob, An innovative immunosensor for ultrasensitive detection of breast cancer specific carbohydrate (CA15-3) in unprocessed human plasma and MCF-7 breast cancer cell lysates using gold nanospear electrochemically assembled onto thiolated graphene quantum dots, Int. J. Biol. Macromol. 114 (2018) 1008–1017.
[103] E. Fogarasi, M.D. Croitoru, L. Fulop, Malondialdehyde levels can be measured in serum and saliva by using a fast HPLC method with visible detection/Determinarea printrometoda HPLC-VIS rapid aconcentratiilor serice si salivare ale malondialdehidei, Rev. Romana Med. Lab. (2016) 319–324.
[104] M. Khoubnasabjafari, K. Ansarin, A. Jouyban, Reliability of malondialdehyde as a biomarker of oxidative stress in psychological disorders, Bioimpacts 5 (2015) 123–127.
[105] S.R. Shetty, S. Babu, S. Kumari, Status of salivary lipid peroxidation in oral cancer and precancer, Indian J. Med. Paediatr. Oncol. 35 (2014) 156–158.
[106] A. Gonenc, Y. Ozkan, M. Torun, Plasma malondialdehyde (MDA) levels in breast and lung cancer patients, J. Clin. Pharm. Ther. 26 (2001) 141–144.
[107] A.S. Atiba, F.M. Abbiyesuku, D.A. Oparinde, Plasma malondialdehyde (MDA): an indication of liver damage in women with pre-eclamsia, Ethiop. J. Health Sci. 26 (2016) 479–486.
[108] N. Nikzad, Z. Karami, Label-free colorimetric sensor for sensitive detection of choline based on DNAzyme-choline oxidase coupling, Int. J. Biol. Macromol. 115 (2018) 1241–1248.
[109] A.A. Sawant, L.M. Sordillo, B.M. Jayarao, A survey on antibiotic usage in dairy herds in Pennsylvania, J. Dairy Sci. 88 (2005) 2991–2999.
[110] W. Yu, Y. Sang, T. Wang, W. Liu, X. Wang, Electrochemical immunosensor based on carboxylated single-walled carbon nanotube-chitosan functional layer for the detection of cephalexin, Food Sci. Nutr. 8 (2020) 1001–1011.
[111] A.R. Fiorucci, E.T. Cavalheiro, The use of carbon paste electrode in the direct voltammetric determination of tryptophan in pharmaceutical formulations, J. Pharm. Biomed. Anal. 28 (2002) 909–915.
[112] Y. Tian, P. Deng, Q. He, Y. Wu, Z. Ding, G. Li, J. Liu, A simple and efficient molecularly imprinted electrochemical sensor for the selective determination of tryptophan, Biomolecules 9 (2019) 294–310.
[113] G. Muthusankar, C. Rajkumar, S.M. Chen, Sonochemical driven simple preparation of nitrogen-doped carbon quantum dots/SnO_2 nanocomposite: a novel electrocatalyst for sensitive voltammetric determination of riboflavin, Sensors Actuators B Chem. 281 (2019) 602–612.
[114] N. Shadjou, M. Hasanzadeh, A. Omari, Electrochemical quantification of some water soluble vitamins in commercial multivitamin using polyamino acid caped by graphene quantum dots nanocomposite as dual signal amplification elements, Anal. Biochem. 539 (2017) 70–80.
[115] W. Dang, Stretchable wireless system for sweat pH monitoring, Biosens. Bioelectron. 107 (2018) 192–202.
[116] P.A. Robiolio, Carcinoid heart disease: correlation of high serotonin levels with valvular abnormalities detected by cardiac catheterization and echocardiography, Circulation 92 (1995) 790–795.
[117] G.K. Dimitriadis, G. Kaltsas, Tumour detection in syndromic NET: carcinoid syndrome, Neuroendocrine Tumors in Real Life, Springer 2018, pp. 161–169 , Edn.
[118] A. Vilouras, A. Paul, M.A. Kafi, R. Dahiya, Graphene oxide-chitosan based ultraflexible electrochemical sensor for detection of serotonin, IEEE SENSORS (2018) https://doi.org/10.1109/ICSENS.2018.8589730.
[119] K. Chaturvedi, K. Ganguly, M.N. Nadagouda, T.M. Aminabhavi, Polymeric hydrogels for oral insulin delivery, J. Control. Release 165 (2013) 129–138.
[120] G. Zhen, T.T. Dang, M. Ma, B.C. Tang, H. Cheng, S. Jiang, Y. Dong, Y. Zhang, D.G. Anderson, Glucose-responsive microgels integrated with enzyme nano-capsules for closed-loop insulin delivery, ACS Nano 7 (2013) 6758–6766.
[121] Z.H. Farooqi, W. Wu, S. Zhou, M. Zhou, Engineering of phenylboronic acid based glucose-sensitive microgels with 4-vinylpyridine for working at physiological pH and temperature, Macromol. Chem. Phys. 212 (2011) 1510–1514.
[122] F. Ullah, M.B.H. Othman, F. Javed, Z. Ahmad, H.M. Akil, S.Z. Rasib, Functional properties of chitosan built nano-hydrogel with enhanced glucose-sensitivity, Int. J. Biol. Macromol. 83 (2016) 376–384.
[123] N. Khalaf, T. Ahamad, M. Naushad, N. Al-hokbany, S.I. Al-Saeedi, S. Almotairi, S.M. Alshehri, Chitosan polymer complex derived nanocomposite (AgNPs/NSC) for electrochemical non-enzymatic glucose sensor, Int. J. Biol. Macromol. 146 (2020) 763–772.
[124] S. Alim, A.K.M. Kafi, J. Rajan, M.M. Yusoff, Application of polymerized multiporous nanofiber of SnO_2 for design in abienzyme glucose biosensor based on HRP/GO_x, Int. J. Biol. Macromol. 123 (2019) 1028–1034.
[125] M. Maruthupandy, G. Rajivgandhi, T. Muneeswaran, T. Vennila, F. Quero, J.M. Song, Chitosan/silver nanocomposites for colorimetric detection of glucose molecules, Int. J. Biol. Macromol. 121 (2019) 822–828.
[126] P.N. Asram, S.A. Mozaffari, M.S. Tehrani, P.A. Azar, A novel impedimetric glucose biosensor based on immobilized glucose oxidase on a CuO-Chitosan nanobiocomposite modified FTO electrode, Int. J. Biol. Macromol. 118 ((2018) 649–660.
[127] F. Poletti, L. Favaretto, A. Kovtun, E. Treossi, F. Corticelli, M. Gazzano, V. Palermo, C. Zanardi, M. Melucci, Electrochemical sensing of glucose by chitosan modified graphene oxide, J. Phys. Mater. 3 (2020), 014011, .
[128] W. Zhang, Y. Liu, X. Li, R. Zou, H. Wu, H. Shi, S. Yu, Multifunctional glucose biosensors from Fe_3O_4 nanoparticles modified chitosan/graphene nanocomposites, Sci. Rep. 5 (2014), 11129, .
[129] D. Fan, N. Li, H. Ma, Y. Li, L. Hu, B. Du, Q. Wei, Electrochemical immunosensor for detection of prostate specific antigen based on an acid cleavable linker into MSN-based controlled release system, Biosens. Bioelectron. 85 (2016) 580–586.
[130] D. Liu, X. Huang, Z. Wang, A. Jin, X. Sun, L. Zhu, F. Wang, Y. Ma, G. Niu, A.R. Walker, X. Chen, Gold nanoparticle-based activatable probe for sensing ultralow levels of prostate-specific antigen, ACS Nano 7 (2013) 5568–5576.
[131] H. Ma, X. Li, T. Yan, Y. Li, Y. Zhang, D. Wu, Q. Wei, B. Du, Electrochemiluminescent immunosensing of prostate-specific antigen based on silver nanoparticles-doped Pb(II) metal-organic framework, Biosens. Bioelectron. 79 (2016) 379–385.
[132] T. Kaya, T. Kaneko, S. Kojima, Y. Nakamura, Y. Ide, K. Ishida, Y. Suda, K. Yamashita, High-sensitivity immunoassay with surface plasmon field-enhanced fluorescence spectroscopy using a plastic sensor chip: application to quantitative analysis of total prostate-specific antigen and GalNAcß1-4GlcNAc-linked prostate-specific antigen for prostate cancer diagnosis, Anal. Chem. 87 (2015) 1797–1803.
[133] Y.W. Huang, C.S. Wu, C.K. Chuang, S.T. Pang, T.M. Pan, Y.S. Yang, F.H. Ko, Real-time and label-free detection of the prostate-specific antigen in human serum by a polycrystalline silicon nanowire field-effect transistor biosensor, Anal. Chem. 85 (2013) 7912–7918.
[134] M. Alvarezicaza, U. Bilitewski, Mass production of biosensors, Anal. Chem. 65 (1999) 525–533.
[135] J. Liang, C. Yao, X. Li, Z. Wu, C. Huang, Q. Fu, C. Lan, D. Cao, Y. Tang, Silver nanoprism etching-based plasmonic ELISA for the high sensitive detection of prostate-specific antigen, Biosens. Bioelectron. 69 (2015) 128–134.
[136] A.R. Jalalvand, Fabrication of a novel and ultrasensitive label-free electrochemical aptasensor for detection of biomarker prostate specific antigen, Int. J. Biol. Macromol. 126 (2019) 1065–1073.
[137] M.M. Zangeneh, H. Norouzi, M. Mahmoudi, H.C. Goicoechea, A.R. Jalalvand, Fabrication of a novel impedimetric biosensor for label free detection of DNA damage induced by doxorubicin, Int. J. Biol. Macromol. 124 (2019) 963–971.